ITERATED EVOLUTOIDAL TRANSFORMATIONS

OLEG OGANDZHANYANTS

Iterated evolutoidal transformations

by

©Oleg Ogandzhanyants

A Thesis submitted to the School of Graduate Studies
in partial fulfillment of the requirements for the degree of

Master of Science

Department of Mathematics and Statistics

Memorial University of Newfoundland

October 2013

St. John's Newfoundland

Abstract

Evolutoids of a plane curve are a generalization of an evolute. They form a one-parameter family of curves whose tangents cut the given curve under a fixed angle, which in the case of the evolute is the right angle. The evolutoidal transformation is a point transformation determined by the inclination of the said tangents and the radius of curvature of the original curve at the given point. Iterated evolutoidal transformations depend on the derivatives of the radius of curvature.

The main results of this thesis concern the geometry and structure of the sets consisting of all images of a certain point on the original curve (image-sets) under iterated evolutoidal transformations with varying inclinations of tangents. To my knowledge, a systematic study of such sets has not been undertaken before and several results presented in this thesis are new. A number of special curves, such as sinusoidal spirals and epi- and hypocycloids, appear frequently in this study, in particular, as boundaries of the image-sets. A geometrical construction of the 2nd and 3rd iterations as well as some particular cases of iterations of higher orders reveal interesting connections to elegant theorems of Euclidean geometry. Some of them do appear in old literature, but here they are reinterpreted and proved in a different way.

Acknowledgements

I would like to thank my supervisor Dr. Margo Kondratieva and co-supervisor Dr. Sergey Sadov for their time and attention to my work.

I express my gratitude to Professors Marco Merkli, Yuri Bahturin, Zhuang Niu, Hong Wang for their inspiring teaching.

Also, I am grateful to Dr. J.C. Loredo-Osti for his support in the capacity of this Department's Graduate Officer.

Special thanks to the Department staff: Ms. Ros English, Ms. Wanda Heath, Ms. Leonce Morrissey, Ms. Jennifer Bishop and Ms. C.J. Buglar for their continuing assistance.

This Master of Science program has been financially supported by the Memorial University School of Graduate Studies scholarship, the NSERC grants to Dr. M. Kondratieva and to Dr. S. Sadov as well as Teaching Assistantship and a special scholarship provided by the Department of Mathematics and Statistics.

Table of Contents

List of Tables

List of Figures

Chapter 1

Overview

Let a smooth plane curve γ be given. At each point of γ, draw a line forming angle θ with the oriented tangent to γ. The envelope of such lines is a curve called the *θ-evolutoid* of γ and denoted by γ_θ. In the case $\theta = \frac{\pi}{2}$, the θ-evolutoid of a curve is its evolute, that is, the locus of all centers of curvature of γ.

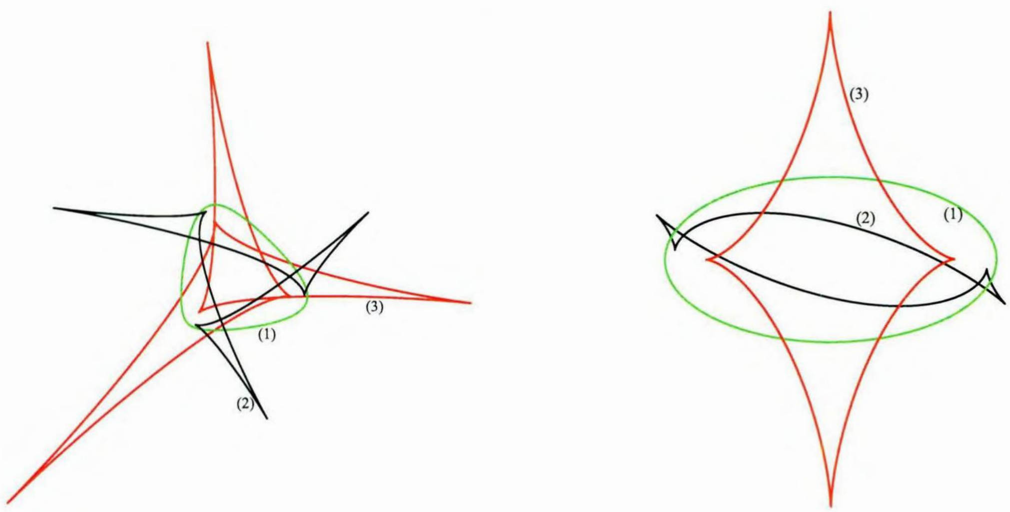

(a) (b)

Figure 1.1: Two examples of a curve(1), its $\frac{\pi}{5}$-evolutoid(2) and evolute(3).

Two examples of evolutoids for curves given by parametric equations: (a) $(e^{\cos\varphi}, e^{\sin\varphi})$;

(b) $(2\cos\varphi, \sin\varphi)$ are shown in Figure 1.1.

The family of evolutoids realizes two homotopies from a curve to its evolute as the parameter θ runs from 0 to $\frac{\pi}{2}$ and from π to $\frac{\pi}{2}$.

Study of evolutoids (développoïdes, the original French term) has a long history that goes back to Réaumur (1709) and Lancret (1811). Higher order evolutoids (evolutoids of evolutoids and so on) were studied by Haton de la Goupillière and Aoust [18]. However, these two authors constructed evolutoids and iterated evolutoids as curves determined by radius of curvature as a known function of a parameter. In contrast, we define evolutoidal transformation as a point transformation in the plane. Although evolutoids have never been an object of mainstream research in geometry, they have never been abandoned altogether. For example, [1] is a doctoral dissertation defended in France in 1938. Later, starting in the 1960s, evolutoids appear from time to time in literature on theory of singularities. Some properties of evolutoids and their applications in mechanics and optics are given in [17, pp. 148–166] (Gravitational catastrophe machines) and in very recent papers [9], [16].

The motivation, which brought us to the evolutoids, is different from a generalization of evolute. We consider an oriented *oval* γ, that is, a smooth oriented closed plane curve bounding a convex region D, a point $P \in D$ and the *pencil of secants* to γ through P, that is of $\{\overrightarrow{PX} \mid X \in \gamma\}$. Consider a problem of finding the minimal angle formed by the tangent to γ at X and $\overrightarrow{PX}$ as X runs over γ. It appears as part of a problem about asymptotics of a certain integral arising in diffraction theory (Section 2.1). For a given θ, the set of points in D for which $\theta^* = \theta$ is called the θ*-level* and denoted $\hat{\gamma}_\theta$. We prove that the θ-level is a subset of the θ-evolutoid (Theorem 2.4.3). Thus, we consider the θ-evolutoid as a generalization of the θ-level: for the latter θ is the global minimum whereas for the former θ is the local minimum. Note that points of the θ-evolutoid may lay outside of D (see Figure 1.1). Some basic theorems on geometry of evolutoids are presented in Chapter 2.

The transformation that produces the θ-evolutoid from the original curve γ point-wise is called *the θ-evolutoidal transformation.* The main subject of our study is compositions of evolutoidal transformations.

Denote by X_θ the image of a point $X \in \gamma$ under the θ-evolutoidal transformation. By the definition of the transformation, the line XX_θ is tangent to γ_θ at X_θ and forms angle θ with the tangent to γ at X. The evolutoidal transformation is local: X_θ is determined by the point X, the direction of tangent to γ at X, and the radius of curvature of γ at X, $R(X)$. The radius of curvature of a curve can be endowed with the sign so that the theory of evolutoidal transformation is linear. In Chapter 3, we define *orientation* of a curve and its evolutoids (with possible cusps), and define the signed radius of curvature. We prove that the so defined orientation is preserved by evolutoidal transformations (Theorem 3.2.14).

Let $X_{\theta_1\theta_2}$ be the image of the point $X_{\theta_1} \in \gamma_{\theta_1}$ under the θ_2-evolutoidal transformation of γ_{θ_1}. A fundamental property is *commutativity of evolutoidal transformations*: $X_{\theta_1\theta_2} = X_{\theta_2\theta_1}$ for any θ_1, θ_2. This property was probably discovered by Haton de la Goupillière [18]. We prove it analitically in a different way in Theorem 3.3.1, and give a geometrical interpretation of a composition of two evolutoidal transformations, which is believed to be new, in Theorem 3.3.3.

Different sets $\{\theta_1, ..., \theta_N\}$ and $\{\theta'_1, ..., \theta'_N\}$ define, in general, different compositions of N evolutoidal transformations, and may yield different images, but their geometry exhibits similar pattern. This geometric pattern prompts us to refer to a composition of N evolutoidal transformations as *the Nth iteration*, $N = 1, 2, ...$, emphasising the number of transformations, even if $\theta_1, ..., \theta_N$ are not all equal. Chapter 4 is devoted to the construction and some general properties of the Nth iteration.

The image of the Nth iteration of a point $X \in \gamma$ is denoted by $X_{\theta_1...\theta_N}$. Iterated evolutoidal transformations of X are determined by the *germ* of γ at X. More precisely, the Nth iteration $X_{\theta_1 \dots \theta_N}$ is determined by the $(N+1)$*th jet* of γ at X, $j_{N+1}(\gamma, X)$. Equivalently, $X_{\theta_1 \dots \theta_N}$ is determined by X and the derivatives $R(X), R'(X), \dots, R^{(N-1)}(X)$ of the radius of curvature of γ at X with respect to a Gaussian parameter.

From now on, let us fix the curve γ and a point $X \in \gamma$. We study the ranges of the iterations $X_{\theta_1 \dots \theta_N}$, $N \geq 1$, as the angles θ_i vary. The set of $X_{\theta_1 \dots \theta_N}$ for all values of $\theta_i \in [0, \pi]$, that is, the range of the map $(\theta_1, \dots, \theta_N) \to X_{\theta_1 \dots \theta_N}$, will be called the *image-set* and denoted by Ω_X^N.

Our study concerns shapes of such image-sets Ω_X^N. In the case $N = 1$, the set Ω_X^1 is a circle C_X of radius $R(X)/2$, tangent to γ at X. For $N > 1$, Ω_X^N is generally a closed 2-dimensional region.

The boundary of Ω_X^2 is the parametric curve $\{X_{\theta\theta}, \ 0 \leq \theta \leq \pi\}$ and can be identified as a *cardioid*. Geometric and analytic proofs of this remarkable fact are presented in Chapter 3 (Theorem 3.4.7).

A cardioid can be viewed as either an epicycloid with one cusp[1] or as a sinusoidal spiral of order $n = 1/2$ with polar equation $r^n(\varphi) = a^n \sin(n\varphi)$ [14].

The image-set Ω_X^3 of the third iteration in general is bounded by arcs of one of involutes of a nephroid [2]. The proof of this statement (Theorem 6.1.13) is based on a sequence of elegant and interesting theorems of Euclidean geometry proved synthetically and analytically in Chapters 5 and 6. We also established algebraic relations for $R(X), R'(X), R''(X)$ that determine different types of a nephroidal involute. For example, if $R(X) + R''(X) = 0$, then Ω_X^3 is bounded by that involute which is itself a nephroid.

---

[1]Epicycloid is a curve produced by tracing a given point on a circle of radius r, which rolls around a fixed circle of radius R. The ratio R/r is called *the ratio of epicycloid.* [14, p. 168]. Up until Chapter 8, we will consider only cases with integer ratio, which is equal to the number of cusps of epicycloids. A cardioid occurs when the radii of the two circles coincide.

[2]A nephroid is an epicycloid with two cusps [14, p. 171].

Another distinguished nephroidal involute, a sinusoidal spiral of order $1/3$ called *the Cayley sextic* [14, p. 178], corresponds to the case where $R(X), R'(X), R''(X)$ form a geometric sequence. This fact admits a nice generalization for all $N \geq 1$. The image-set of X under the N-th iteration is bounded by arcs of a sinusoidal spiral of order $1/N$ if the sequence $R(X), R'(X), ..., R^{(N-1)}(X)$ is geometric. This is the Sinusoidal Spiral Theorem (7.2.6) proved in Chapter 7.

In order to get insight about a more general situation (for an arbitrary germ γ at X) in case of $N \geq 3$ iterations, we pay close attention to the *α-constant sum image-sets*, that is, we will require that $\theta_1 + \theta_2 + ... + \theta_N = \alpha \bmod \pi$, where α is some constant.

In the case of the 3rd iteration, a constant sum image-set is bounded by either a *deltoid* (which is *a three-cusped hypocycloid*) [3] or an affine image of a deltoid, which is treated as a parallel projection in $\mathbb{R}^3$ of a deltoid in Theorem 6.2.24. Note that constant-sum image-sets overlap and do not tile the whole image-set. Interestingly, the areas of all these image-sets are equal (Lemmas 6.2.19 and 6.2.23). It turns out that the envelope (in the usual sense, "*tangent envelope*") of the family of the deltoid's projections is a circle or a circular arc connecting the cusps of a curve bounding the image-set of X (Theorem 6.4.5). The latter curve is the *cuspidal envelope* of the deltoid's projections (Figure 1.2).

The radius of the circle or of the arc depends on $R(X), R'(X), R''(X)$ and could be infinite as it is in Figure 1.2(c). The latter happens precisely when $R(X) + R''(X) = 0$, that is, the boundary of Ω^3_X is a nephroid (Theorem 6.1.13). In this important particular case, the constant sum image-sets are bounded by proper (as opposed to projected) deltoids.

The observation that the locus of cusps of all deltoids from this family is the two-

[3]Hypocycloid is a curve produced by tracing a given point on a circle, which rolls inside a fixed circle. The ratio of a hypocycloid and its equality to the number of cusps of a hypocycloid is defined as in the case of an epicycloid.

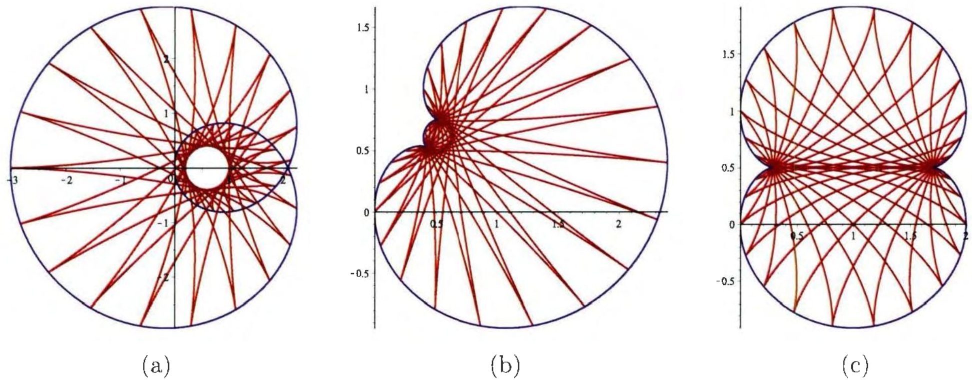

Figure 1.2: The tangent envelopes (a circle or an arc) and the cuspidal envelopes of the deltoid's projections.

cusped epicycloid is generalized in the Epicycloid Envelope Theorem (Theorem 7.1.16) that pertains to the case of general N. For instance, as shown in Figure 1.3(a), the cuspidal and tangent envelopes of the family of 4-cusped hypocycloids are the 3-cusped epicycloid and the 3-cusped hypocycloid respectively. Another part of the Theorem is illustrated by Figure 1.3(c): the cuspidal and tangent envelopes of the family of 2-cusped epicloids are the 3-cusped hypocycloid and the 3-cusped epicycloid respectively. Finally, looking at the deltoids on Figure 1.2(c), we see that the centers of these deltoids lie on a circle centered at the center of the large nephroid (Figure 1.4). A generalization of this fact is the third part of Theorem 7.1.16.

This result is known in the literature [15]. However, in our work it appears in a different context and has a different proof based on the Triple Envelope Theorem (Theorem 6.3.2), which is outlined below.

Denote $X_{\theta^N} = X_{\theta_1\theta_2\ldots\theta_N}$, if $\theta_1 = \theta_2 = \ldots = \theta_N = \theta$. Then denote $\Gamma_N = \{X_{\theta^N}\}_{\theta=0}^{\pi}$. Incidentally Γ_N contains the boundary of Ω_X^N (Theorem 6.4.9). For example, the boundary of Ω_X^2 is the cardioid $\{X_{\theta^2}\}_{\theta=0}^{\pi}$, as mentioned earlier.

Next, we introduce three family of curves, each formed by points $X_{\theta_1\theta_2\ldots\theta_N}$ where all but one θ_i are equal. Namely,

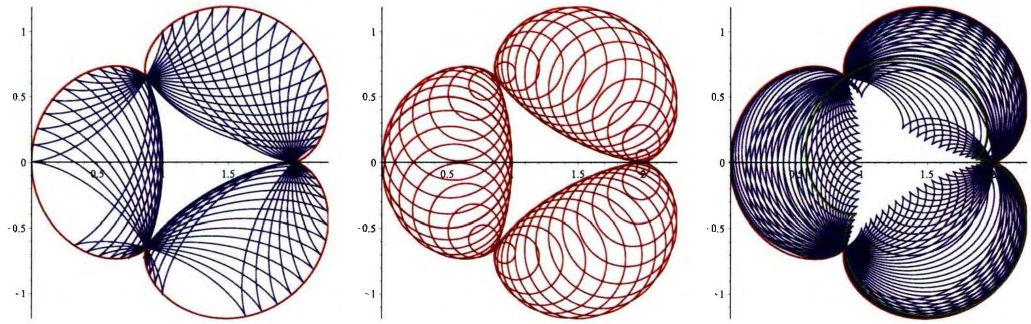

(a) (b) (c)

Figure 1.3: An illustration to the Epicycloid Envelope Theorem and The Triple Envelope Theorem.

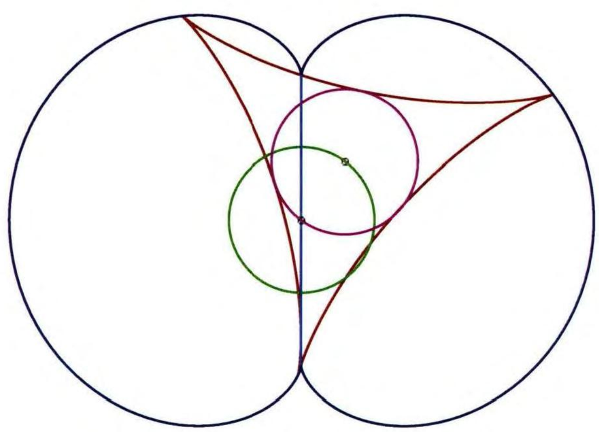

Figure 1.4: An illustration to the centroid part of Epicycloid Envelope Theorem.

– family (A) consists of curves $\tilde{\Gamma}_N^\alpha = \{X_{\theta^{N-1}(\alpha-(N-1)\theta)}\}_{\theta=0}^{\pi}$;

– family (B) consists of the circular image-sets of the first iteration of the evolutoidal transformations of all points $X_{\alpha^{N-1}} \in \Gamma_{N-1}$, i.e. $\hat{\Gamma}_N^\alpha = \{X_{\theta\alpha^{N-1}}\}_{\theta=0}^{\pi}$;

– family (C) consists of the curves $\Gamma_N^\alpha = \{X_{\alpha\theta^{N-1}}\}_{\theta=0}^{\pi}$.

The Triple Envelope Theorem states: *The envelopes of the three families of curves (A), (B) and (C) coincide for all $N \geq 2$.* The illustration on this theorem is presented in Figures 1.3 and 1.5.

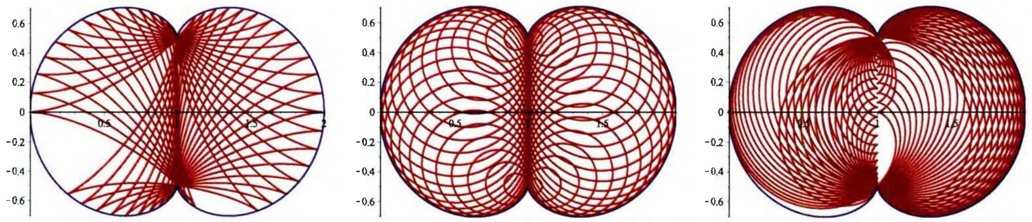

(a) (b) (c)

Figure 1.5: Another illustration to The Triple Envelope Theorem, $(R, R', R'') = (1, 0, -1)$. (a) The family (A) of deltoids; (b) The family (B) of circles; (c) The family (C) of cardioids.

This theorem is a key point for understanding many aspects related to the evolutoidal transformation and its iterations. As well, it provides new approaches to proofs of already known facts from geometry of planar curves, in particular, of epi- and hypocycloids.

In Chapter 8 the reader will find a brief discussion of statements which could be proven based on the results and methods developed in this Thesis, as well as an overview of future possible research directions.

Chapter 2

Envelopes of θ-secants

2.1 Motivation: Asymptotics of a contour integral

The origin of this thesis is related to the study of asymptotics as $\lambda \to \infty$ of an integral from diffraction theory [11], [12]

$$I(\lambda, t) = \int_\gamma e^{i\lambda\Phi_t(s)}\, ds.$$

Here $\gamma : I \to \mathbb{R}^2,\ s \to X(s)$, is a convex smooth curve parametrized by arclength s, X_0 is a fixed point inside γ, and the phase factor $\Phi_t(s)$ is given by

$$\Phi_t(s) = \|X(s) - X_0\| + ts.$$

The stationary phase method leads to the equation

$$\cos\theta(s_*) = t$$

for the critical points of the phase, where $\theta(s_*)$ is the angle[1] between the tangent to γ at $X(s_*)$ and vector $\overrightarrow{X_0X}(s_*)$. It turns out that a real critical point exists if and only if there is a point $X \in \gamma$ such that the angle between $\overrightarrow{X_0X}$ and the tangent to γ at X is less than θ. For points close to boundary, a solution is more likely to exist than for points deep inside.[2] The rest of this Chapter is devoted to a way to describe geometric conditions assuring existence of the special points.

While this research was initially prompted by an asymptotic problem in diffraction theory, this line will not be pursued in the thesis.

[1]Here $\theta(s_*)$ has the same meaning as $\theta(X)$ in (2.2.1).

[2]In terms of Definition 2.2.2, the critical points exist iff X_0 lies outside the curve $\hat{\gamma}_\theta$.

2.2 Extremal problem for a pencil of secants

In this Section, we consider some properties of a special class of curves, called ovals.

A *region* is an open connected set [19, Ch. 10.1].

A curve bounding a convex region in $\mathbb{R}^2$ is called a convex curve, although it may not be a convex set.

Definition 2.2.1. *An oval is a smooth closed plane curve*[3]*, bounding a convex region.*

Let γ be an oriented oval, that is, an oval such that when travelling on it one always has the curve interior to the left (or to the right). Denote the interior of γ by D.

Take a point $P \notin \gamma$. For each point $X \in \gamma$, the angle $\theta = \theta(X, P)$ between $\overrightarrow{PX}$ and a tangent vector $\vec{v}(X) = \vec{v}$ to γ at X is determined by

$$\cos\theta = \frac{\overrightarrow{PX} \cdot \vec{v}}{\| \overrightarrow{PX} \| \cdot \| \vec{v} \|}. \tag{2.2.1}$$

The direction of $\vec{v}$ must agree with orientation of γ.

By *the pencil of secants* to γ through the point P, we understand the family of rays $\{\overrightarrow{PX} \mid X \in \gamma\}$.

Let us consider the following question: *What is the range of all possible values of θ as X runs over γ?* We assume that $0 \le \theta \le \pi$ throughout. There are two possible cases:

(1) The point $P \notin \overline{D}$, i.e. P lies outside γ, as in Figure 2.1(a). Then there are two tangents from P to γ. We have:

$$\min_{X\in\gamma} \theta = 0, \ \max_{X\in\gamma} \theta = \pi,$$

and $\cos\theta$ can take any value in $[-1, 1]$.

[3] A curve has two meanings: (1) a map $I \to \mathbb{R}^2$ (a parametrized curve); (2) the range of this map (a geometric curve). Before we introduce parametrization, we will treat a curve as a geometric object.

(2) The point $P \in D$, i.e. P lies inside γ, as in Figure 2.1(b). Then the map $X \to \cos\theta$ is a continuous function from the compact set γ to $\mathbb{R}$. Therefore, it must attain its minimum and maximum. Denote

$$\theta_{\min}(P,\gamma) = \min_{X\in\gamma} \theta(X,P),$$

$$\theta_{\max}(P,\gamma) = \max_{X\in\gamma} \theta(X,P).$$

If in a given context, the curve γ is fixed, we simply write $\theta_{\min}(P)$ and $\theta_{\max}(P)$. There are points $X_* = X_*(P), X_{**} = X_{**}(P) \in \gamma$ corresponding to the minimal and maximal angles respectively. These points X_* and X_{**} are not necessarily unique.

Remark. For any P there exist a point $X_1 \in \gamma$ that minimizes and a point $X_2 \in \gamma$ that maximizes the distance from P to $X \in \gamma$ respectively. These points X_1 and X_2 are not necessarily unique. The lines PX_1 and PX_2 are perpendicular to the tangents to γ at X_1 and X_2 respectively. Therefore, the value $\theta = \pi/2$ is always attainable. Consequently, $\theta_{\min}(P) \leq \pi/2 \leq \theta_{\max}(P)$.

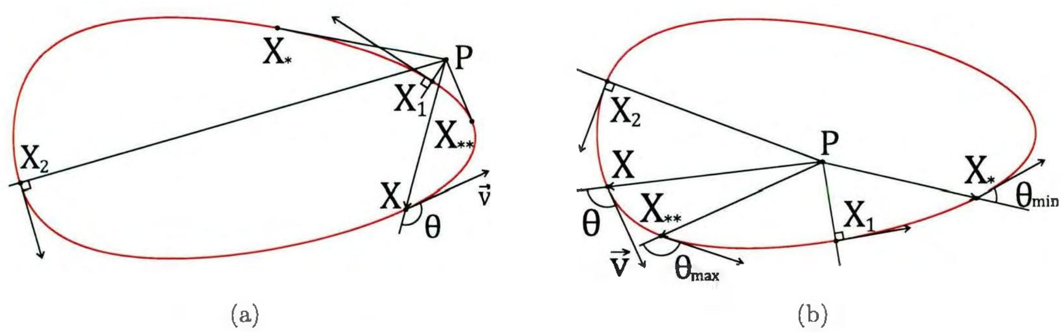

Figure 2.1: What is the range of all possible values of $\theta(P)$ as X runs over γ? (a) P lies outside of γ; (b) P lies inside γ.

We will now introduce a curve $\hat{\gamma}_\theta$, a part of the θ-evolutoid γ_θ to be defined in Section 2.4.

Definition 2.2.2. *Given $\theta \in [0, \pi/2]$, the set (possibly empty) of all points $P \in D$ for which $\theta_{\min}(P) = \theta$ will be called the θ-level set and denoted by $\hat{\gamma}_\theta$. That is, $\hat{\gamma}_\theta = \{P \in D \,|\, \theta_{\min}(P) = \theta\}$. Denote the set $\{P \in D \,|\, \theta_{min}(P) \geq \theta\}$ by $D(\theta)$.*

Remark. Let γ_- be the curve γ with reversed orientation. Then $\theta_{\min}(P, \gamma_-) = \pi - \theta_{\max}(P, \gamma)$. For this reason, we do not introduce a curve analogous to $\hat{\gamma}_\theta$ by the condition $\theta_{\max}(P) = \theta$.

As an example, let us compute $\theta_{\min}$ and $\theta_{\max}$ in two elementary cases.

Example 1. Let γ be the circle

$$\begin{cases} x = \cos\varphi \\ y = \sin\varphi \end{cases}, \quad 0 \leq \varphi < 2\pi.$$

At a point $X = (x, y)$ on γ, the tangent vector to γ is given by $\overrightarrow{v} = (dx/d\varphi, dy/d\varphi) = (-\sin\varphi, \cos\varphi)$. Let O be the center of γ and a point P be such that $|OP| < 1$. We may assume that $P = (\rho, 0)$, $0 \leq \rho < 1$. Then $\overrightarrow{PX} = \overrightarrow{OX} - \overrightarrow{OP} = (\cos\varphi - \rho, \sin\varphi)$. (see Figure 2.2(a)).

Let $\cos\theta$ be defined as in (2.2.1).

Proposition 2.2.3. *For all φ, we have $-\rho \leq \cos\theta \leq \rho$. The extremal values $\theta_{min} = \arccos\rho$ and $\theta_{max} = \pi - \arccos\rho$ are attained at the points $X_* = (\rho, \sqrt{1-\rho^2})$ and $X_{**} = (\rho, -\sqrt{1-\rho^2})$, where $\varphi = \rho$ and $\varphi = -\rho$ respectively.* (See Figure 2.2(b)).

Proof. If $\rho = 0$, i.e. $P = O$, then $\theta(X, P) = \text{const} = \frac{\pi}{2}$.

If $\rho > 0$, then by (2.2.1), the angle θ between $\overrightarrow{PX}$ and $\vec{v}$, can be expressed in terms of ρ and φ:

$$\cos\theta = \frac{\rho\sin\varphi}{\sqrt{\rho^2 - 2\rho\cos\varphi + 1}}.$$

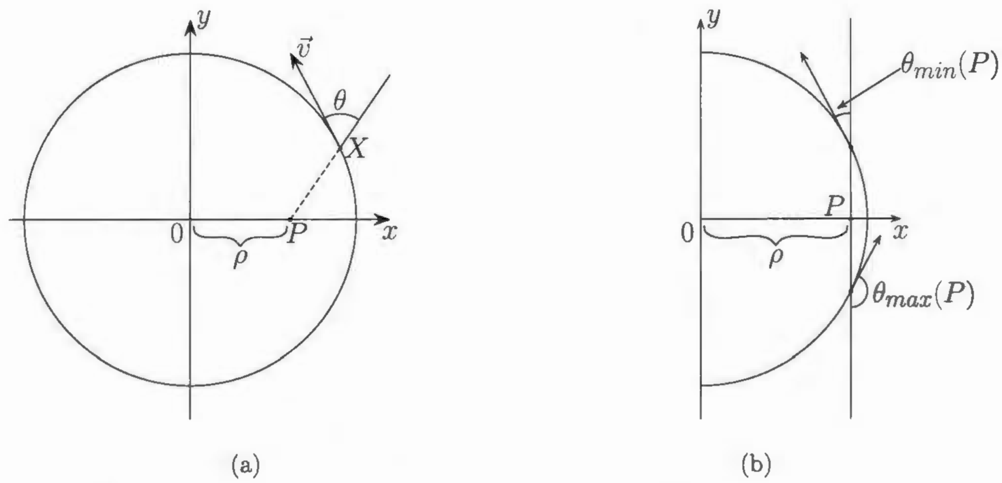

Figure 2.2: Circular case: (a) Point X in general position; (b) Extremal angles.

The condition for extremum $d\cos\theta(\varphi)/d\varphi = 0$ yields the equation

$$\rho^2\cos^2\varphi - (\rho+\rho^3)\cos\varphi + \rho^2 = 0, \tag{2.2.2}$$

whose solutions are $\cos\varphi = \rho$ or $1/\rho$. The only[4] relevant value $\cos\theta = \rho$ corresponds to $x = \rho,\ y = \pm\sqrt{1-\rho^2}$. □

Corollary 2.2.4. [5] *If γ is a unit circle and $\theta \in [0, \pi/2]$, then $\hat{\gamma}_\theta$ is the concentric circle of radius $\cos\theta$.*

□

Example 2. Let γ be the ellipse with semiaxes $a > b$, given by parametric equations[6] $X = (x(\varphi), y(\varphi))$,

$$\begin{cases} x = a\cos\varphi \\ y = b\sin\varphi \end{cases}, \quad 0 \le \varphi < 2\pi.$$

[4] Because $\frac{1}{\rho} > 1$ lies outside of the range of $\cos\varphi$.
[5] This is, although in a different context, a particular case of Réaumur's Theorem 2.4.6.
[6] That is, a parametrization by a trammel (ellipsograph) of Archimedes, see [10].

Consider the case $P = (0,0)$. Determine the range of $\theta(X(\varphi), P)$ as φ varies from 0 to 2π.

Proposition 2.2.5. *For all φ, we have*

$$\frac{b^2 - a^2}{a^2 + b^2} \leq \cos\theta \leq \frac{a^2 - b^2}{a^2 + b^2}. \tag{2.2.3}$$

The extremal values $\theta_{min} = \arccos\frac{a^2-b^2}{a^2+b^2}$ and $\theta_{max} = \arccos\frac{b^2-a^2}{a^2+b^2}$ are attained at the points corresponding to $\varphi \in \{\frac{\pi}{4}, \frac{5\pi}{4}\}$ and $\varphi \in \{\frac{3\pi}{4}, \frac{7\pi}{4}\}$ respectively, regardless of the values a and b.

Proof. We have $\overrightarrow{OX} = (a\cos\varphi, b\sin\varphi)$, $\overrightarrow{v} = (-a\sin\varphi, \cos\varphi)$. Hence

$$\begin{aligned}\cos\theta(\varphi) = \frac{\overrightarrow{OX} \cdot \overrightarrow{v}}{\|\overrightarrow{OX}\| \cdot \|\overrightarrow{v}\|} &= \frac{(b^2 - a^2)\sin\varphi\cos\varphi}{\sqrt{(a^2\cos^2\varphi + b^2\sin^2\varphi)(a^2\sin^2\varphi + b^2\cos^2\varphi)}} \\ &= \frac{(b^2 - a^2)\sin\varphi\cos\varphi}{\sqrt{(a^2 + b^2)^2 - (a^2 - b^2)^2\cos^2 2\varphi}}.\end{aligned}$$

Differentiating, we get

$$\frac{d\cos\theta(\varphi)}{d\varphi} = \frac{2(b^2 - a^2)\cos 2\varphi(4a^2b^2 + 3(a^2 - b^2)^2\sin^2 2\varphi)}{((a^2 + b^2)^2 - (a^2 - b^2)^2\cos^2 2\varphi)^{\frac{3}{2}}}.$$

Since $b^2 - a^2 < 0$ and $4a^2b^2 + 3(a^2 - b^2)^2\sin^2 2\varphi > 0$, the extrema of $\cos\theta(\varphi)$ coincide with zeros of $\cos 2\varphi$. Therefore $\cos\theta$ attains its minimum at $\varphi = \frac{\pi}{4}, \frac{5\pi}{4}$ and its maximum at $\varphi = \frac{3\pi}{4}, \frac{7\pi}{4}$. □

Remark. If P is not the center of the ellipse, then the condition of extremum leads to an equation $P_6(\varphi) = 0$, where P_6 is a trigonometrical polynomial of degree 6.

2.3 Properties of θ-level sets

Let γ be an oriented oval and vector $\vec{v}$ be the tangent vector to γ at $X \in \gamma$.

Definition 2.3.1. *The line that crosses γ at X and forms the exterior angle θ with $\vec{v}$ is called the θ-secant to γ at X and denoted by $l_X(\theta)$.*

Denote by $\pi_X(\theta)$ the open half-plane bounded by $l_X(\theta)$ and containing the tangent vector $\vec{v}$ to γ at X and by $D_X(\theta)$ the part of D, the region bounded by γ, lying in $\pi_X(\theta)$. Denote also by $\overline{\pi}_X(\theta)$ and by $\overline{D}_X(\theta)$ the closures of $\pi_X(\theta)$ and $D_X(\theta)$ respectively. The boundary of the closure of any region Q will be denoted by ∂Q. Denote $D(\theta) = \bigcup\limits_{\theta' > \theta} \hat{\gamma}_{\theta'}$.

Lemma 2.3.2. *If $D(\theta) \neq \varnothing$ then a curve $\hat{\gamma}_\theta$ of an oval is a convex closed curve.*

Proof. Let us take an oval γ. Fix a θ such that $D(\theta)$ is nonempty. Then the line $l_X(\theta)$ partitions D into two convex parts, as in Figure 2.3.

A vector $\overrightarrow{PX}$ from a point $P \in D \setminus \overline{\pi}_X(\theta)$ forms with $\vec{v}$ at X an angle which is less

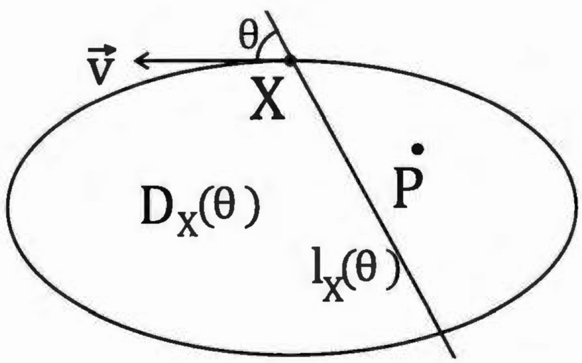

Figure 2.3: Partitioning of an oval by a θ-secant.

then θ. So, $D(\theta) \subset \overline{D}_X(\theta)$.

Therefore, if a point $P \in \hat{\gamma}_\theta$, then $P \in \bigcap\limits_X \overline{D}_X(\theta)$. Since any $D_X(\theta)$ is convex, $\bigcap\limits_X \overline{D}_X(\theta)$ is convex, too.

Note that if a point $P \in D_X(\theta)$ then $\overrightarrow{PX}$ forms with $\vec{v}$ at X an angle greater than θ, therefore $\hat{\gamma}_\theta \not\subset \bigcap\limits_X D_X$. Consequently $\hat{\gamma}_\theta \subset \partial \bigcap\limits_X D_X(\theta)$.

On the other hand, any point $\tilde{P} \in \partial \bigcap\limits_X D_X(\theta)$ lies on the chord $l_{\tilde{X}} \bigcap D$ for some $\tilde{X} \in \gamma$, i.e. $\widehat{\overrightarrow{\tilde{P}\tilde{X}}, \vec{v}(\tilde{X})} = \theta$, and if we take any $X' \in \gamma$ such that $X' \neq \tilde{X}$, then $\widehat{\overrightarrow{\tilde{P}\tilde{X}}, \vec{v}(X')} \geq \theta$, otherwise $\tilde{P} \in D \setminus \overline{D}_{X'}(\theta)$. Hence $\partial \bigcap\limits_X D_X(\theta) \subset \hat{\gamma}_\theta$.

Therefore $\partial \bigcap\limits_X D_X(\theta) = \hat{\gamma}_\theta$. □

Definition 2.3.3. *A curve that is tangent to each member of a family of curves is called an envelope*[7] *of a family of curves* [2, §5.12].

Lemma 2.3.2 gives a good insight on the relationship between the $\hat{\gamma}_\theta$ and the envelope of the family of lines $\{l_X(\theta)\}_{X \in \gamma}$, that is, the envelope of θ-secants[8]. The latter is a convenient object to observe since its equations can be easily obtained from the equations of γ [2, §5.3].

If γ contains a rectilinear segment $X'X''$, then θ-secants are parallel for all points of γ lying between X' and X'', hence there are smooth curves for which envelopes of θ-secants do not exist. To guarantee the existence of an envelope, we will introduce the restricted class of ovals called strict ovals.

An oval with no linear segments and points of hyperosculation, that is points where the curvature is zero, is called a *strict oval.*

Lemma 2.3.4. *If γ is a strict oval, then $\hat{\gamma}_\theta$ does not contain a rectilinear arc.*[9]

Proof. Suppose there is a θ such that $\hat{\gamma}_\theta$ contains an arc PP', which is straight. Then this arc is a part of some chord of γ, XX'. Set $\overline{P} = \partial D_X(\theta) \bigcap XX'$ and $\overline{P'} = \partial D_{X'}(\theta) \bigcap XX'$.

[7]There are many alternative definitions of envelope, but for the current purposes this one matches best. More detailed definition will be presented later in this Chapter.

[8]A more detailed relationship will be established in Section 2.4.

[9]This statement is valid even if we allow γ to have points of hyperosculation.

Now, take any point $P_0 \in [P, P']$, $P_0 \notin \{P, P'\}$. Then there will be $X_0 \notin \{X, X'\}$ such that $\partial D_{X_0}(\theta) \ni P_0$. Note that $P_0 = \partial D_{X_0}(\theta) \bigcap XX'$. Then either $P' \notin D_{X_0}(\theta)$ or $P \notin D_{X_0}(\theta)$. The one which does not belong to $D_{X_0}(\theta)$ can not belong to $\hat{\gamma}_\theta$. Contradiction. $\square$

Lemma 2.3.5. *If $\theta_1 > \theta_2$, then $D(\theta_1) \subset D(\theta_2)$ and $\hat{\gamma}_{\theta_1}$ lies inside $\hat{\gamma}_{\theta_2}$.*

Proof. If $\theta_1 \neq \theta_2$, then $\hat{\gamma}_{\theta_1} \cap \hat{\gamma}_{\theta_2} = \varnothing$, because a point $P \in D$ belongs to only one $\hat{\gamma}_\theta$, namely, $P \in \hat{\gamma}_{\theta_{\min(P)}}$. $\square$

The following Lemma introduces a special point of an strictly convex oval, which will be used to characterize $\hat{\gamma}_\theta$ as a distinguished part of the envelope of the θ-secants at the end of this Chapter.

Lemma 2.3.6. (Existence of the special point for a strict oval) *For any oriented strict oval γ, there exists a unique value θ^* such that $\hat{\gamma}_{\theta^*}$ is a point.*

Proof. Consider the family of $\hat{\gamma}_\theta$ of a given γ. By Lemma 2.3.5, $\hat{\gamma}_{\theta_1} \cap \hat{\gamma}_{\theta_2} = \varnothing$, if $\theta_1 \neq \theta_2$, so the curves are nested. Note that for $\theta = \frac{\pi}{2}$, $D(\theta) = \varnothing$, because we can always drop perpendicular to γ from any point $P \in D$, connecting P to the most and the least distant points of γ, as $\overline{D}$ is compact.

On the other hand, if $D(\theta) \neq \varnothing$, then there is a point $P \in D(\theta)$ such that $\tilde{\theta} = \theta_{\min}(P) > \theta$. Hence $P \in \hat{\gamma}_{\tilde{\theta}}$, which lies inside $\hat{\gamma}_\theta$. Thus, having a sequence $0 < \theta_1 < \theta_2 < ... \leq \frac{\pi}{2}$, the corresponding sequence $D(\theta_1) \supset D(\theta_2) \supset ... \supseteq \varnothing$. By the Bolzano-Weierstrass theorem, there must be $\theta^* \leq \pi/2$, where $D(\theta^*) = \varnothing$ and for any $\theta < \theta^*$ the corresponding $D(\theta^*)$ is not empty.

Further, by Lemma 2.3.2, $\hat{\gamma}_{\theta^*}$ can not consist of two coinciding arcs $\overset{\frown}{ab}$ and $\overset{\frown}{ba}$, since all chords of $\hat{\gamma}_{\theta^*}$ must lie entirely inside it, nor can $\overset{\frown}{ab}$ and $\overset{\frown}{ba}$ be line segments, since $\hat{\gamma}_{\theta^*}$ must not contain any straight arc by Lemma 2.3.4.

Hence, $\hat{\gamma}_{\theta^*}$ is just a point, P^*. The uniqueness of θ^* implies the uniqueness of P^*. $\square$

Remark. If we need to find the locus of points in D for which given θ is the global maximum on γ instead of the minimum, we may simply change the orientation of γ and consider the θ-level family in that case. We will again end up with some critical point, P^{**}, which will represent the member of the family, corresponding to the critical value of θ denoted by θ^{**}, i.e. $\hat{\gamma}_{\theta^{**}} = \{P^{**}\}$.

If γ has an axis of symmetry, the points P^* and P^{**} lie on the axis. Hence if γ has more than one axes of symmetry, the points coincide, and $\theta^* + \theta^{**} = \pi$. But in general, $P^* \neq P^{**}$ and the sum of two critical angles is not necessarily π.

One may give the following description of the $\hat{\gamma}_\theta$-family. Suppose a train goes

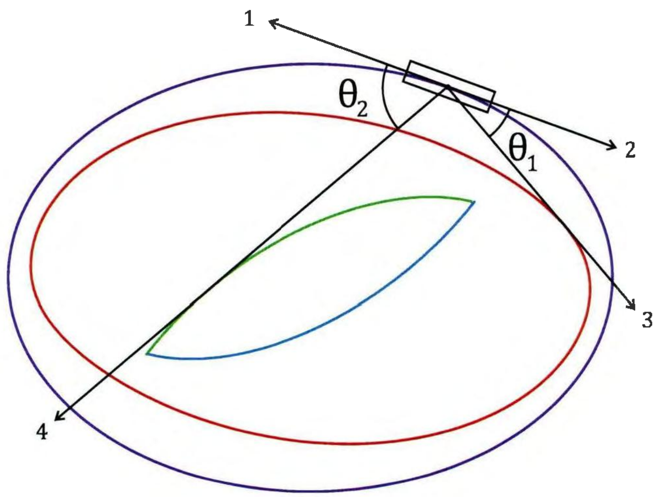

Figure 2.4: Train model.

around a rail-road loop of the shape of our γ in counter-clockwise direction. Let us fix 4 searchlights on the train: the first sends its light-beam forward, the second – backwards, the third and the fourth point inside D and form angles $\theta_1 \leq \theta^*$ and $\theta_2 \leq \pi - \theta^{**}$ with the light-beams pointing backwards and forward, respectively, as shown in Figure 2.4. Then the boundaries of the regions unlit by the third and the fourth searchlights will have the shapes of $\hat{\gamma}_{\theta_1}$ for γ oriented counter-clockwise and $\hat{\gamma}_{\theta_2}$ for γ oriented clockwise respectively.

2.4 Evolutoids

Let γ be a strict oriented oval whose radius of curvature is a continuous function of the parameter. Then γ can be locally represented (up to the 2nd derivative of its parametric representation) by its osculating circle[10]. This fact allows us to take advantage of the results obtained in the circular case (Proposition 2.2.3 and Figure 2.2(b)). Given $\theta \in [0, \pi]$, let us define the θ-evolutoid of γ by explicit construction.

Definition 2.4.1. *Let a point $X \in \gamma$. Let E be the corresponding center of curvature of γ. Draw the θ-secant to γ at X, $l_X(\theta)$. Let P be the foot of the perpendicular EP dropped from E to $l_X(\theta)$,* (see Figure 2.5(a)). *The locus of all such points P for all $X \in \gamma$ is called the θ-evolutoid of γ and denoted by γ_θ.*

Note that P may be inside or outside of the region bounded by γ or it may lie on γ, since it is determined by local properties of γ in a neighbourhood of X.

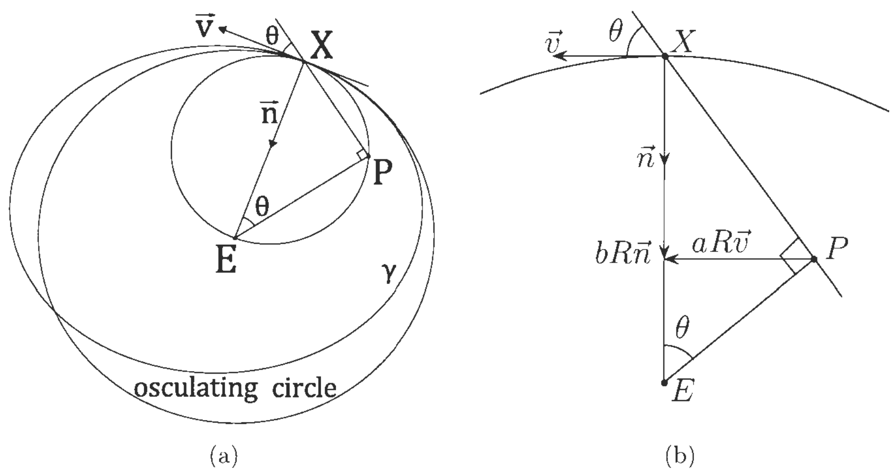

Figure 2.5: Construction of a point P on γ_θ, corresponding to a point $X \in \gamma$.

[10]A curve γ is the envelope of its osculating circles [2, Ch. 5]

Lemma 2.4.2. *Let R be the radius of curvature and $\vec{n}$ be the unit normal vector to γ at X pointing inward the region bounded by γ. Then*

$$R\sin^2\theta = \vec{n}\cdot\overrightarrow{XP}, \tag{2.4.1}$$

Proof. Look at Figure 2.5(b). (Here b is for $\sin^2\theta$). The scalar product $\vec{n}\cdot\overrightarrow{XP}$ is the orthogonal projection of vector $\overrightarrow{XP}$ onto $\vec{n}$, which is $|EX|\sin^2\theta = R\sin^2\theta$. $\square$

We will now establish a relation between the curves $\hat{\gamma}_\theta$ and γ_θ.

Theorem 2.4.3. *The set $\hat{\gamma}_\theta$ is a subset of γ_θ.*

Proof. Let an oval γ be parametrized by its arclength, s, and let $\vec{v}(s)$ be a tangent to γ at $X(s)$. Let a point P be such that $\overrightarrow{PX}(s_0)$ and $\vec{v}(s_0)$ form angle θ. Let also R be defined as in Lemma 2.4.2. The statement of the theorem is equivalent to the assertion: if $P\in\hat{\gamma}_\theta$, then equation (2.4.1) holds. We have, $\|\vec{v}\| = 1$, and

$$\cos\theta = \frac{\overrightarrow{PX}\cdot\vec{v}}{\|\overrightarrow{PX}\|}. \tag{2.4.2}$$

If $\theta_{\min}(P, X(s_0)) = \theta$ then $\theta(s)$ has a global minimum at $s = s_0$. Hence, it must have a local minimum at this point. That implies $\frac{d\cos\theta(s)}{ds}|_{s=s_0} = 0$.

Differentiating the components of (2.4.2)

$$\frac{d\vec{v}}{ds} = \frac{\vec{n}}{R},\ \frac{d\overrightarrow{PX}}{ds} = \vec{v},\ \frac{d\|\overrightarrow{PX}\|}{ds} = \overrightarrow{PX}\cdot\vec{v}\cdot\frac{1}{\|\overrightarrow{PX}\|},$$

we have:

$$\|\overrightarrow{PX}\|^2(\cos\theta)'_s = \|\overrightarrow{PX}\|(\frac{dP\vec{X}}{ds}\cdot\vec{v} + \frac{\vec{n}}{R}\cdot\overrightarrow{PX}) - P\vec{X}\cdot\vec{v}\cdot\frac{d\|\overrightarrow{PX}\|}{ds} =$$

$$= (1 + \frac{\vec{n}}{R}\cdot\overrightarrow{PX})\|\overrightarrow{PX}\| - (\overrightarrow{PX}\cdot\vec{v})^2\cdot\frac{1}{\|\overrightarrow{PX}\|} = 0.$$

From here, we obtain:

$$1 + \frac{\vec{n}}{R} \cdot \overrightarrow{PX} = \frac{(\overrightarrow{PX} \cdot \vec{v})^2}{\|\overrightarrow{PX}\|^2} = \cos^2\theta,$$

and the equation (2.4.1) follows. $\square$

Thus, a necessary condition for a point $P \in D$ to lie on $\hat{\gamma}_\theta$ is $P \in \gamma_\theta$. To determine a condition for a point $P \in \gamma_\theta$ to lie on $\hat{\gamma}_\theta$, let us focus our attention on the family $\{\gamma_\theta\}_{\theta=0}^{\pi}$.

Let a curve γ be given by the parametric equations $X = (x, y) = (x(\varphi), y(\varphi))$, where φ is some parameter. Denote $\dot{x} = dx/d\varphi$, $\dot{y} = dy/d\varphi$, and let $\vec{v}(\varphi)$ and $R(\varphi)$ be the tangent vector to γ and the radius of curvature of γ at the point X respectively.

Lemma 2.4.4. *Let $\theta \in [0, \pi]$ be fixed. The parametric equations of the θ-evolutoid are*

$$\gamma_\theta = \begin{cases} x_\theta = x - g\sin\theta(\dot{x}\cos\theta + \dot{y}\sin\theta) \\ \\ y_\theta = y + g\sin\theta(\dot{x}\sin\theta - \dot{y}\cos\theta) \end{cases}, \quad g = \frac{R}{\|\vec{v}\|}. \tag{2.4.3}$$

Proof. We have $\vec{v} = (\dot{x}, \dot{y})$, $\vec{n} = (-\dot{y}, \dot{x})$.

If we consider the radius of curvature R from the geometrical point of view, it is a positive number

$$R = \frac{(\dot{x}^2 + \dot{y}^2)^{\frac{3}{2}}}{|\dot{x}\ddot{y} - \ddot{x}\dot{y}|}. \tag{2.4.4}$$

However, for a closed convex oriented curve the expression $(\dot{x}\ddot{y} - \ddot{x}\dot{y})$ is always of the same sign, so the absolute value symbol may be dropped[11].

According to our construction presented in Definition 2.4.1, the equation of γ_θ has

[11]In our definition of normal vectors, the choice of sign is consistent with the formula for the evolute: $\vec{E} = \vec{X} + R\vec{n}^*$, where $\vec{n}^* = \vec{n}/\|\vec{n}\|$ is a normal unit vector. Thus we will take that $R \leq 0$ for a clockwise oriented oval, i.e. the unit normals are exterioir. Hence, local minima of R on γ oriented clockwise will coincide with local maxima of R on the same curve oriented counter-clockwise, and visa versa. For more details, see Section 3.2.

the following vector form (see Figure 2.5(b)):

$$\vec{P} = \vec{X} + R\sin\theta(-(\cos\theta)\vec{v} + (\sin\theta)\vec{n}). \tag{2.4.5}$$

From (2.4.5), we can immediately obtain the parametric equation for γ_θ. □

Before we prove the next statement, we introduce the precise definition of the envelope. Let each curve C_φ in the family $\mathcal{F}$ be given as the solution of an equation $f_\varphi(x, y) = 0$, where $\varphi \in [a, b]$ is a parameter. Write $F(\varphi, x, y) = f_\varphi(x, y)$ and assume F is differentiable.

Definition 2.4.5. *The set of points $\mathcal{D}$, for which $F(\varphi, x, y) = \frac{\partial F}{\partial \varphi}(\varphi, x, y) = 0$ for some value of $\varphi \in [a, b]$, is the envelope of the family $\mathcal{F}$.*

There are alternative definitions:

(1) *The envelope $\mathcal{D}_1$ is the limit of intersections of nearby curves C_φ;* (2) *The envelope $\mathcal{D}_2$ is a curve tangent to all of C_φ;* (3) *The envelope $\mathcal{D}_3$ is the boundary of the region filled by the curves C_φ. Then $\mathcal{D}_1 \subset \mathcal{D}$, $\mathcal{D}_2 \subset \mathcal{D}$ and $\mathcal{D}_3 \subset \mathcal{D}$* [2, §§5.3-5.18].

A curve $\mathcal{D}_1$, which is an envelope in the sense of Definition 2.3.3, is called a *tangential envelope*. By Definition 2.4.5, it is a subset of the envelope in general.

Theorem 2.4.6. (Theorem of Réaumur). *The envelope of the θ-secants to γ is the θ-evolutoid.*

Proof.[12] Let a point $P = (x_p, y_p)$ lie on the θ-isocline passing through a point $X = (x, y) = (x(\varphi), y(\varphi)) \in \gamma$.

Denote $\cos\theta = c$, $\sin\theta = s$. Then

$$\cos\theta = \frac{\overrightarrow{PX} \cdot \overrightarrow{v}}{\| \overrightarrow{PX} \| \cdot \| \overrightarrow{v} \|}, \quad \sin\theta = -\frac{\overrightarrow{PX} \cdot \overrightarrow{n}}{\| \overrightarrow{PX} \| \cdot \| \overrightarrow{n} \|}. \tag{2.4.6}$$

[12]We do not know the original proof and present our own. Réaumur defined the θ-evolutoid as the envelope of θ-secants and then showed its equivalence to the locus described in Definition 2.4.1.

Expanding equations (2.4.6), we get

$$s(\dot{x}(x-x_p)+\dot{y}(y-y_p))=c(\dot{y}(x-x_p)-\dot{x}(y-y_p)). \tag{2.4.7}$$

Define the function

$$f(x_p,y_p,\varphi,\theta)=x_p(-\dot{x}s+\dot{y}c)+y_p(-\dot{y}s-\dot{x}c)+s(x\dot{x}+y\dot{y})+c(-\dot{y}x+\dot{x}y)=0. \tag{2.4.8}$$

By Definition 2.4.5, the condition for envelope is

$$\frac{df(x_p,y_p,\varphi,\theta)}{d\varphi}=f(x_p,y_p,\varphi,\theta)=0. \tag{2.4.9}$$

We have

$$\frac{df(x_p,y_p,\varphi,\theta)}{d\varphi}=x_p(-\ddot{x}s+\ddot{y}c)+y_p(-\ddot{y}s-\ddot{x}c)+s(\dot{x}^2+\dot{y}^2+x\dot{x}+y\dot{y})+c(\ddot{x}y-\ddot{y}x)=0. \tag{2.4.10}$$

Equations (2.4.8) and (2.4.10) form a system of two linear equation with respect two variables, x_p and y_p. The solution of the system matches (2.4.3). □

As an example, several evolutoids for the case of an ellipse are shown in Figure 2.6. We can see that even for such elementary case, evolutoids may have singularities and self-intersections. A necessary condition for singularities of an evolutiod is established in Chapter 3.

According to Theorem of Réaumur, each point on θ-evolutoid corresponds to a point on the original curve. So there is a point-wise map $\mathcal{E}_\theta:\ \gamma\to\gamma_\theta$.

Definition 2.4.7. *The point-wise map $\mathcal{E}_\theta:\ \gamma\to\gamma_\theta$, such that the line passing through $X\in\gamma$ and $\mathcal{E}_\theta(X)\in\gamma_\theta$ is the θ-secant to γ at X, is called the θ-evolutoidal transformation.*

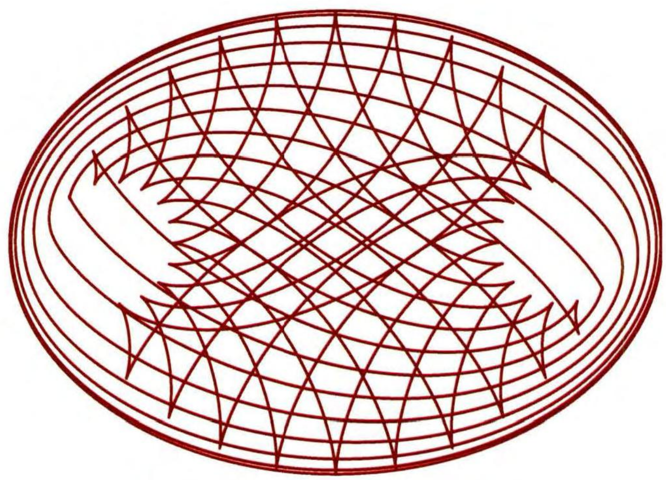

Figure 2.6: Some evolutoids of an ellipse with semiaxes $\sqrt{2}a$ and a.

Lemma 2.4.8. *For any strict oval, γ, if $\theta \leq \theta^*$ and the map $\mathcal{E}_\theta$ is invertible, then γ_θ coincides with $\hat{\gamma}_\theta$.*

Proof. By Lemma 2.3.4, $\hat{\gamma}_\theta$ is a strictly convex closed curve, and by Theorem 2.4.3, it is a subset of γ_θ.
Invertibility of $\mathcal{E}_\theta$ implies that γ_θ has no self-intersection point[13]. So, γ_θ is a closed simple curve, whose subset, $\hat{\gamma}_\theta$, is a strictly convex curve. Any proper subset of such curve is not a closed curve, hence $\hat{\gamma}_\theta$ and γ_θ coincide. □

The inverse statement is not always true, for instance, the evolute of a circle γ, that is, the circle's central point, is both $\gamma_{\frac{\pi}{2}}$ and $\hat{\gamma}_{\frac{\pi}{2}}$, meanwhile $\mathcal{E}_{\frac{\pi}{2}}$ is not invertible in that case. A less trivial counterexample is when γ contains an arc of a logarithmic spiral[14]. As one can easily show, there is a θ' such that $\mathcal{E}_{\theta'}$ maps the whole arc into a point, the pole of the spiral. Then it is possible to construct the rest of γ such that the pole of the spiral is inside the region bounded by γ and belongs to both $\hat{\gamma}_{\theta'}$ and $\gamma_{\theta'}$.
However, the key point to distinguish between the two curves is convexity of $\hat{\gamma}_\theta$.

[13] self-intersection of a closed curve $\gamma(\varphi)$, $\varphi \in [a, b] \in \mathbb{R}$, $\gamma(a) = \gamma(b)$, means, that there are $\varphi_1 \neq \varphi_2 \in (a, b)$ such that $\gamma(\varphi_1) = \gamma(\varphi_2)$

[14] that is, a curve, whose equation in polar coordinates is $r = a^\varphi$, [21, p. 300].

Proposition 2.4.9. *For any strict oval γ, and $\theta \leq \theta^*$, the curves $\hat{\gamma}_\theta$ and γ_θ coincide if and only if the latter is not self-intersecting.*

Proof. If γ_θ is not self-intersecting, it is strictly convex by the reasons presented in Lemma 2.4.8. Then the curves coincide since $\hat{\gamma}_\theta$ is enveloped by θ-secants to γ, and γ_θ is the envelope of them. The converse is obvious. $\square$

Lemma 2.4.8 and Proposition 2.4.9 give insight on sufficient conditions of a point to lie on $\hat{\gamma}_\theta$ (details are shown in Figure 2.7).

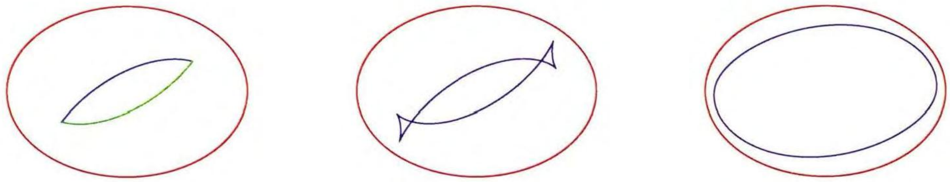

(a) (b) (c)

Figure 2.7: Difference between $\hat{\gamma}_\theta$ and γ_θ. In the picture, γ is an ellipse oriented clockwise: (a) γ and $\hat{\gamma}_{\frac{\pi}{3}}$; (b) γ and $\gamma_{\frac{\pi}{3}}$; (c) γ, $\gamma_{\frac{\pi}{6}}$ and $\hat{\gamma}_{\frac{\pi}{6}}$. In that case, $\gamma_{\frac{\pi}{6}}$ and $\hat{\gamma}_{\frac{\pi}{6}}$ coincide.

Suppose now that γ_θ is self-intersecting. Since it is a closed curve, the region it bounds can be broken into regions[15] bounded by simple curves, which are unions of arcs of γ_θ. Let us call such simple curves *constituents of* γ_θ and denote by ω_θ^k, $k = 1, 2, \ldots$. If we know the position of P^*, that is $\hat{\gamma}_{\theta^*}$, we can easily spot the proper constituent, which is $\hat{\gamma}_\theta$, since the region it bounds contains P^*. It is clear, due to nesting property of θ-levels established in Lemma 2.3.5.

From the analysis of properties of $\hat{\gamma}_\theta$, we move to that of evolutoids; the latter contain the former and can be conveniently parametrized. Starting from the next Chapter we focus our attention on local properties of evolutoids and of the map $\mathcal{E}_\theta$.

[15] It can be shown that the number of such regions is finite, if we do not allow γ to have infinitely many isolated vertices, that is the points of local extrema of the curvature of γ.

Chapter 3

Evolutoids of evolutoids

3.1 Radius of curvature of an evolutoid

We will denote by X_θ a point on θ-evolutoid of a curve γ, corresponding to a point $X \in \gamma$, and write $X_\theta \in \gamma_\theta$.

Definition 3.1.1. *For a fixed $\theta \in [0, \pi]$, the pointwise map of a parametrized curve γ into its θ-evolutoid is called the θ-evolutoidal transformation of the curve and denoted by $\mathcal{E}_\theta : \gamma \longmapsto \gamma_\theta,\ X \longmapsto X_\theta$.*

Consider a $\gamma_\theta,\ \theta \in [0, \pi]$ of a given $\gamma \in C^3$ with non-zero curvature, parametrized by an arclength parameter, φ.

We will use the following notations:

$\vec{v_\theta} = \vec{v_\theta}(\varphi) = (\dot{X}_\theta, \dot{Y}_\theta)$ the tangent vector to γ_θ at $X_\theta(\varphi)$;

$P = X_\theta(\varphi)$;

$E = X_{\frac{\pi}{2}}(\varphi)$;

$R_\theta = R_\theta(\varphi),\ R = R(\varphi)$ and $R_E = R_{\frac{\pi}{2}}(\varphi)$ - radii of curvature of γ_θ at $X_\theta(\varphi)$, γ at $X(\varphi)$, and $\gamma_{\frac{\pi}{2}}$ at $X_{\frac{\pi}{2}}(\varphi)$ respectively;

$E_\theta = E_\theta(\varphi), E_e = E_e(\varphi)$- centers of curvature of γ_θ at $X_\theta(\varphi)$ and the evolute, $\gamma_{\frac{\pi}{2}}$, at

E respectively.

Lemma 3.1.2. *The center of curvature of γ_θ at $X_\theta(\varphi)$, E_θ, lies on the line PE.*

Proof. The statement follows from perpendicularity of PX and PE, by construction of γ_θ, since PX is tangent to θ-evolutoid at $P = X_\theta$. $\square$

Let us calculate $\vec{v_\theta}(\varphi)$, using the short notations s and c for $\sin\theta$ and $\cos\theta$ respectively:

$$\vec{v_\theta} = \dot{X_\theta} = \dot{X} + \dot{R}(-cs\vec{v} + s^2\vec{n}) + R(-cs\dot{\vec{v}} + s^2\dot{\vec{n}}) = \vec{v}c(c - \dot{R}s) + \vec{n}s(\dot{R}s - c). \quad (3.1.1)$$

Denote $c^2 - \dot{R}cs$ and $\dot{R}s^2 - cs$ by A_θ and B_θ respectively. Then $\vec{v_\theta} = A_\theta(\dot{x}, \dot{y}) + B_\theta(-\dot{y}, \dot{x})$. Then we get

$$\begin{cases} \dot{X_\theta} = \dot{x}A_\theta - \dot{y}B_\theta \\ \dot{Y_\theta} = \dot{y}A_\theta + \dot{x}B_\theta. \end{cases} \quad (3.1.2)$$

Since $A_\theta^2 + B_\theta^2 = (c - \dot{R}s)^2$, calculating $\|\vec{v_\theta}\|^2$ yields:

$$\|\vec{v_\theta}\|^2 = \dot{X_\theta}^2 + \dot{Y_\theta}^2 = (A_\theta^2 + B_\theta^2)\underbrace{(\dot{x}^2 + \dot{y}^2)}_{=\|\vec{v}\|^2=1} = (c - \dot{R}s)^2. \quad (3.1.3)$$

The formula for the radius of curvature of an evolutoid of a curve, parametrized by some parameter φ, not necessarily the arclength parameter, is given in the following proposition, which was offered as an exercise in [6, p. 47].

Proposition 3.1.3. *The radius of curvature*[1] *of γ_θ can be expressed via R and $\dot{R}$:*

$$|R_\theta| = |(c - \dot{R}s)R|. \quad (3.1.4)$$

[1]For now, we do not focus on sign of radius of curvature and looking for its absolute value.

Proof. To calculate R_θ, let us express all the constituents of the formula

$$|R_\theta| = \frac{(\dot{X}_\theta^2 + \dot{Y}_\theta^2)^{\frac{3}{2}}}{|\dot{X}_\theta \ddot{Y}_\theta - \dot{Y}_\theta \ddot{X}_\theta|} \tag{3.1.5}$$

in terms of $\dot{x}, \ddot{x}, \dot{y}, \ddot{y}$ and θ. We have:

$$\begin{cases} \ddot{X}_\theta = \ddot{x}A_\theta - \ddot{y}B_\theta + \dot{x}\dot{A}_\theta - \dot{y}\dot{B}_\theta \\ \ddot{Y}_\theta = \ddot{x}B_\theta + \ddot{y}A_\theta + \dot{x}\dot{B}_\theta + \dot{y}\dot{A}_\theta. \end{cases} \tag{3.1.6}$$

Note, that $\dot{B}_\theta A_\theta = \dot{A}_\theta B_\theta$. Then plugging the expressions 3.1.6 in the denominator of (3.1.5), we obtain:

$$\dot{X}_\theta \ddot{Y}_\theta - \dot{Y}_\theta \ddot{X}_\theta = (A_\theta^2 + B_\theta^2)(\dot{x}_\theta \ddot{y}_\theta - \dot{y}_\theta \ddot{x}_\theta). \tag{3.1.7}$$

From equation (3.1.7), we note that the signs of $\dot{X}_\theta \ddot{Y}_\theta - \dot{Y}_\theta \ddot{X}_\theta$ and $\dot{x}_\theta \ddot{y}_\theta - \dot{y}_\theta \ddot{x}_\theta$ coincide. Finally, using 3.1.3, we get the desired result:

$$|R_\theta| = \frac{(\dot{X_\theta}^2 + \dot{Y_\theta}^2)^{\frac{3}{2}}}{|\dot{X}_\theta \ddot{Y}_\theta - \dot{Y}_\theta \ddot{X}_\theta|} = \sqrt{A_\theta^2 + B_\theta^2} \frac{(\dot{x}^2 + \dot{y}^2)^{\frac{3}{2}}}{|\dot{x}_\theta \ddot{y}_\theta - \dot{y}_\theta \ddot{x}_\theta|} = |(c - \dot{R}s)R|. \tag{3.1.8}$$

□

Note that singularities of γ_θ correspond to $R_\theta = 0$. Equivalently, $\dot{R}\sin\theta - \cos\theta = 0$, i.e. $\dot{R} = \cot\theta$. Thus, we obtain the following statement.

Corollary 3.1.4. *If $\dot{R} = \cot\theta$ at some point of γ, then the corresponding point of θ-evolutoid is singular.*

From Proposition 3.1.3 follows a well-known [2, Ch. 2] identity for $R_{\frac{\pi}{2}}$, the radius of curvature of the evolute of γ.

$$|R_{\frac{\pi}{2}}| = |\dot{R}R|. \tag{3.1.9}$$

3.2 Invariance of the orientation.

Let us provide a brief background needed to give a justification for our choice of a sign for the radius of curvature of an evolutoid.

Definition 3.2.1. *An oriented pair is an ordered pair of orthogonal unit vectors* $\{\vec{v}, \vec{n}\}$, *i.e.* $\|\vec{v}\| = \|\vec{n}\| = 1,\ (\vec{v}, \vec{n}) = 0$.

For each direction of $\vec{v}$, *we have two choices for* $\vec{n}(s)$:

(a) Left orientation. The rotation of vector $\vec{v}$ *by* $\pi/2$ *counter-clockwise places it in the position of* $\vec{n}$.

(b) Right orientation. The rotation of vector $\vec{v}$ *by* $\pi/2$ *clockwise places it in the position of* $\vec{n}$.

Definition 3.2.2. *The* orientation *of the oriented pair* $\{\vec{v}, \vec{n}\}$ *is the number*

$$\varepsilon(\{\vec{v}, \vec{n}\}) := \begin{cases} 1, & \text{if } \{\vec{v}, \vec{n}\} \text{ is a left-oriented pair,} \\ -1, & \text{if } \{\vec{v}, \vec{n}\} \text{ is a right-oriented pair.} \end{cases} \tag{3.2.1}$$

Let $I \in \mathbb{R}$ be an interval.

Definition 3.2.3. *An oriented smooth curve parametrized by an arclength parameter, s, is a triple* $(\gamma = \vec{X}(s), \vec{v}(s), \vec{n}(s))$ *of vector functions* $I \to \mathbb{R}^2$, *where*

(1) γ *is a smooth curve parametrized by an arclength parameter;*

(2) $\vec{v}(s) = d\vec{X}(s)/ds$

(3) $\{\vec{v}, \vec{n}\}$ *is an oriented pair for each* $s \in I$ *continuously depending on s.*

The vector fields $\vec{v}(s)$, $\vec{n}(s)$ *are called the tangent and normal vectors respectively.*

(4) *The orientation* $\varepsilon(\gamma)$ *is defined as* $\varepsilon(\{\vec{v}, \vec{n}\})$, *which has the same value for any* $s \in I$.

Definition 3.2.4. *An* oriented *curve with a return point (in other words, a cusp*[2]*)* s_* *parametrized by an arclength parameter, s, is a triple* $(\gamma = \vec{X}(s), \vec{v}(s), \vec{n}(s))$, *where*

(1) $\gamma : I_- \cup s_* \cup I_+ \to \mathbb{R}^2$ *is a (non-oriented) curve with a returning point parametrized by an arclength parameter s;*

(2) $\vec{v}$ *and* $\vec{n}$ *are vector fields defined on* $I_- \cup I_+$ *such that* $(\gamma, \vec{v}, \vec{n})|_{I_\pm}$ *are oriented smooth curves, where* $I_- = \{s \in I \,|\, s < s_*\}$, $I_+ = \{s \in I \,|\, s > s_*\}$.

(3) $\vec{n}_\pm = \lim\limits_{s \to s_* \pm 0} \vec{n}(s)$. *We require* $\vec{n}_- = \vec{n}_+$, *i.e.* $\vec{n}(s_*)$ *can be defined as the* $\lim \vec{n}(s)$, *making* $\vec{n}(s)$ *a continuous vector function.*

Remark. If we define $\vec{v}_- = \lim\limits_{s \to s_* - 0} \vec{v}(s)$ and $\vec{v}_+ = \lim\limits_{s \to s_* + 0} \vec{v}(s)$, then the oriented pairs $\{\vec{v}_-, \vec{n}_-\}$ and $\{\vec{v}_+, \vec{n}_+\}$ are related by

$$\begin{cases} \vec{v}_+ = -\vec{v}_- \\ \vec{n}_+ = \vec{n}_- \ . \end{cases} \tag{3.2.2}$$

Definition 3.2.5. *The curvature of a smooth curve* $(x(s), y(s))$ *in the arclength parametrization s is given by the formula:*

$$\kappa(s) = \dot{x}\ddot{y} - \ddot{x}\dot{y}. \tag{3.2.3}$$

Remark. Let $\vec{n}(s)$ be the interior normal, i.e.[3] $\vec{n}(s) \uparrow\uparrow \dot{\vec{v}}(s)$. The pair $\{\vec{v}, \vec{n}\}$ may be either left- or right-oriented. Since the sign of the number $(\dot{x}\ddot{y} - \ddot{x}\dot{y})$ coincides with the sigh of $\vec{v} \times \dot{\vec{v}}$, in the left-oriented case $\kappa(s) > 0$, and in the right-oriented case $\kappa(s) < 0$, [2, Ch. 2].

Definition 3.2.6. *The radius of curvature* $R(s)$ *is defined as* $R(s) = \kappa^{-1}(s)$, *provided*

[2]Cusps are local singularities in that they are not formed by self intersection points of the curve. The plane curve cusps are all diffeomorphic to one of the following forms: $x^2 - y^{2k+1} = 0$, where $k \geq 1$ is an integer. [2]

[3]We will use the notation $\vec{a} \uparrow\uparrow \vec{b}$ if vectors $\vec{a}$ and $\vec{b}$ are codirectional.

$\kappa(s) \neq 0$.

If γ is a curve with a return point s_*, then generally we do not define $R(s_*)$ and $\kappa(s_*)$, although in many cases it turns out $\lim\limits_{s \to s_*} R(s_*) = 0$ exists, and in these cases we can define $R(s_*) = 0$.

Thus $R(s_*)$ and $\kappa(s_*)$ are signed numbers as defined by (3.2.3). If $\kappa(s) \neq 0$ for all s, then $\operatorname{sgn}(\kappa(s)) = \text{const}$.

Definition 3.2.7. *The tangent and normal unit vectors $\vec{v}$ and $\vec{n}$, called collectively the $Frenet - Serret$ frame [6] of a curve γ, form an orthonormal basis in $\mathbb{R}^2$:*
vector $\vec{v}$ is the unit vector tangent to the curve, defined earlier in 3.2.3,
vector $\vec{n}$ is the normal unit vector, the derivative of $\vec{v}$ with respect to the arclength parameter of the curve, divided by its length: $\vec{n} = \dot{\vec{v}}/\kappa$.

The definition 3.2.7 does not leave freedom for the curve orientation, since it allows only left-oriented pairs $\{\vec{v}, \vec{n}\}$. The following definition helps avoiding this disadvantage.

Definition 3.2.8. *The tangent and normal unit vectors $\vec{v}$ and $\vec{n}$, called collectively the VN frame of a curve γ, form an orthonormal basis in $\mathbb{R}^2$:*
vector $\vec{v}$ is the unit vector tangent to the curve, defined earlier in 3.2.3,
vector $\vec{n}$ is the normal unit vector, the derivative of $\vec{v}$ with respect to the arclength parameter of the curve, divided by its length and multiplied by $\varepsilon(\gamma)$: $\vec{n} = \varepsilon(\gamma)\dot{\vec{v}}/\kappa$.

Under such definition, vectors $\vec{v}$, $\dot{\vec{v}}$, $\vec{n}$ and $\dot{\vec{n}}$ are bound by the two equations:

$$\begin{cases} \dot{\vec{n}} = -\varepsilon(\gamma)\vec{v}\kappa \\ \dot{\vec{v}} = \varepsilon(\gamma)\vec{n}\kappa. \end{cases} \tag{3.2.4}$$

The consistency of formulas (3.2.4) with formula (3.2.5) is shown in Table 3.1.

The radius-vector of the center of curvature $\vec{E}(s)$ of γ at $X(s)$ is defined by

case	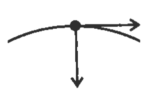	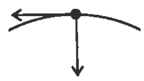	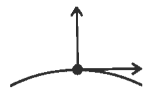	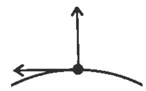	
ε	-1	1	1	-1	
$\kappa,\ R$	< 0	> 0	< 0	> 0	
$\dot{x}\ddot{y} - \ddot{x}\dot{y}$	< 0	> 0	< 0	> 0	
$\mathrm{sgn}(\vec{v}, \vec{n})$	+	+	-	-	$\Rightarrow \vec{v} = \kappa\vec{n}\varepsilon(\gamma)$
$\mathrm{sgn}(\vec{n}, \vec{v})$	-	-	+	+	$\Rightarrow \vec{n} = -\kappa\vec{v}\varepsilon(\gamma)$

Table 3.1: Table of signatures for different cases of oriented pairs $\{\vec{v}, \vec{n}\}$

$$\vec{E}(s) = \vec{X}(s) + R(s)\varepsilon(\gamma)\vec{n}(s). \tag{3.2.5}$$

Definition 3.2.9. *A curve γ is traced counterclockwise (clockwise) at a point $X \in \gamma$ if the pair $\{\vec{v}, \frac{\overrightarrow{XE}}{\|\overrightarrow{XE}\|}\}$ is left-oriented (right-oriented), where $\vec{v}$ and E are the tangent vector and the center of curvature of γ at X.*

Theorem 3.2.10. *Consider a smooth oriented curve $(\gamma = \vec{X}(s), \vec{v}(s), \vec{n}(s))$, where $\{\vec{v}(s), \vec{n}(s)\}$ is a VN frame. Let $\theta \in [0, \pi]$. Then vector*

$$\vec{X}(s) + R(s)\sin\theta(-(\cos\theta)\vec{v} + (\sin\theta)\varepsilon(\gamma)\vec{n}) \tag{3.2.6}$$

is $\vec{X}_\theta(s)$, if γ is traced counterclockwise at $X(s)$, or $\vec{X}_{\pi-\theta}(s)$, if γ is traced clockwise at $X(s)$.

Proof. Suppose γ is traced counterclockwise at $X(s)$. Then formula (2.4.5) is the left-oriented case, i.e. $\varepsilon(\gamma) = 1$. In the right-oriented case, a curve differs from its left-oriented counterpart, that is, from the curve with the same tangent and the same signed radius of curvature, only by the direction of the normal vector. Then the multiplication of the normal vector by $\varepsilon(\gamma)$ makes the formula (2.4.5) work. The proof of the case of γ traced clockwise at $X(s)$ is analogous. □

The definition of $R(s)$ makes (3.2.5) orientation-independent in the case of a smooth curve. On the other hand, the notions of curvature, radius and center of curvature in formula (3.2.5) remain valid for a curve with a return point s_*: excluding the value s_*, we apply the previous definition to the smooth components $\gamma|_{I_\pm}$ of γ. The formula (3.2.5) is still consistent if $\lim_{s\to s_*} R(s) = 0$. In that case we assign $R(s_*) = 0$.

Consider the family of evolutoids of a curve γ parametrized by an arclength parameter s and smooth at a point $X(s^*)$. By Corollary 3.1.4, a singularity appears at a point $X_{\theta_1}(s^*) \in \gamma_{\theta_1}$ if $\dot{R}(s^*) = \cot\theta$. Since the range of $\cot\theta$ is $(-\infty, +\infty)$, and it is one-to-one on $(0,\pi)$, there must be exactly one evolutoid out of the family, which has a singularity at $X_\theta(s^*)$.

Definition 3.2.11. *Let $X(s^*)$ be a point on a smooth oriented curve γ and denote the circle with $X(s^*)E(s^*)$ as its diameter by $\Gamma_1(s^*)$. Define on $\Gamma_1(s^*)$ the vector field of tangents to γ_θ, $\vec{v}_\theta(s^*) = \vec{X}_\theta(s)/ds\,|_{\,s=s^*}$, $0 \le \theta \le \pi$, as in* 3.1.1.

We require the corresponding normal vector field $\vec{n}_\theta(s^*)$ be continuous in θ on the interval $[0,\pi]$.

Theorem 3.2.12. *Fix a value s^* of the parameter of an oriented smooth curve γ and let $\theta_1 = \operatorname{arccot} dR/ds$. The orientations $\varepsilon(\{\vec{v}_\theta(s^*), \vec{n}_\theta(s^*)\})$ and $\varepsilon(\{\vec{v}(s^*), \vec{n}(s^*)\})$ coincide if $\theta \in [0,\theta_1)$, and are opposite if $\theta \in (\theta_1, \pi]$.*

Proof. We will consider only the case of a left-oriented γ with $\vec{n}(s^*)$ pointing toward the center of curvature of γ at $X(s^*)$, since the proof for the other cases is identical. Let $\theta \in [0,\theta_1)$. Then γ_θ at $X_\theta(s^*)$ is regular. By Lemma 3.1.2, normals to θ-evolutoids, $\vec{n}_\theta(s^*)$, are placed along corresponding lines $E(s^*)X_\theta(s^*)$ for $\theta \in [0,\pi]$. By continuity of the vector field of normals, $\vec{n}_\theta(s^*) \upuparrows \overrightarrow{X_\theta(s^*)E}(s^*)$, $\theta \in [0, \frac{\pi}{2})$ and $\vec{n}_\theta(s^*) \upuparrows \overrightarrow{E(s^*)X}_\theta(s^*)$, $\theta \in (\frac{\pi}{2}, \pi]$. For $\theta = \frac{\pi}{2}$, $\vec{n}_\theta(s^*) \upuparrows \vec{v}(s^*)$.

There are two possible cases:

(1) $\theta \in [0,\theta_1)$. In the formula (3.1.2), $A_\theta > 0$ and $B_\theta < 0$. That implies $\vec{v}_\theta(s^*) \upuparrows$

$\overrightarrow{X_\theta(s^*)X(s^*)}$ and the pair $(\vec{v}_\theta(s^*), \vec{n}_\theta(s^*))$ is left-oriented.

(2) $\theta \in (\theta_1, \pi]$. We have $A_\theta < 0$ and $B_\theta > 0$, hence $\vec{v}_\theta(s_*) \upuparrows \overrightarrow{X(s_*)X_\theta(s_*)}$, and the pair $(\vec{v}_\theta(s^*), \vec{n}_\theta(s^*))$ is right-oriented. $\square$

Definition 3.2.13. *The signed radius of curvature of the θ-evolutiod at a point $X_\theta(s)$ is*

$$R_\theta = (\cos\theta - \dot{R}\sin\theta)R. \tag{3.2.7}$$

Theorem 3.2.14. *The orientation $\varepsilon(\gamma)$ is invariant under evolutoidal transformation in the sense of formula* (3.2.5)*:*

$$\vec{E}_\theta(s) = \vec{X}_\theta(s) + R_\theta(s)\varepsilon(\gamma)\vec{n}_\theta(s). \tag{3.2.8}$$

Proof. Fix an $s^* \in I$. By Theorem 3.2.12, the signature of $R_\theta(s^*)$ changes simultaneously with the change of the orientation of the θ-evolutoid at $X_\theta(s^*)$. Therefore, the normal $n_\theta(s^*)$ becomes exterior if it was interior on γ, and visa versa. $\square$

Corollary 3.2.15. *Curves γ_θ at $X_\theta(s)$ and γ at $X(s)$ are traced in the same way.*[4]

Lemma 3.2.16. *Curves γ and γ_π coincide pointwise and have opposite orientation.*

Proof. Consider the behavior of the family of evolutoids of a curve γ, $\{\gamma_\theta\}_{\theta=0}^{\pi}$ at the points corresponding to a fixed value of the parameter $s^* \in I$. By Lemma 3.1.4, there is only one $\theta_1 \in [0, \pi]$ such that $\gamma_{\theta_1}(s^*)$ is singular, namely $\theta_1 = \operatorname{arccot}\dot{R}(s^*)$. Then we have:

(1) $\cos\theta - \dot{R}\sin\theta > 0,\ \theta \in [0, \theta_1)$,

(2) $\cos\theta - \dot{R}\sin\theta < 0,\ \theta \in (\theta_1, \pi]$.

That implies that R and R_θ have the same sign in the case (1) and different signs in the case (2). On the other hand, curves γ and γ_π coincide point-wise by formula

[4]Of course, if γ_θ is not singular at $X_\theta(s)$, i.e. $\theta \neq \operatorname{arccot}\dot{R}(s)$.

(2.4.3). By equation (3.2.7), $R_\pi(s^*) = -R(s^*)$ and hence γ and γ_π are oriented in an opposite way. $\square$

Lemma 3.2.16 implies that π-evolutoidal transformation, $\mathcal{E}_\pi$, maps a curve γ into the same curve but of opposite orientation. More precisely, the direction of the tangents is the same, but the direction of the normals is opposite. Denote such curve by $\overline{\gamma}$, so that $\overline{\gamma} = \gamma_\pi$. Since the evolutes of $\overline{\gamma}$ and γ coincide, the formula (3.2.5) holds provided $R(s) = -R_\pi(s)$ for all $s \in I$. Note also that $\overline{\overline{\gamma}} = \gamma$.

In order to avoid computational complications and extend the domain of parameter of the evolutoidal transformation $\mathcal{E}_\theta$ from 0 to 2π in a way consistent with its geometrical interpretation, we introduce the following object.

Definition 3.2.17. *Let $\theta \in [0, \pi]$. A curve $\gamma_{(\theta+\pi)}$ is defined as $\overline{\gamma}_\theta$.*

We always think of θ as of a value defined $\bmod 2\pi$. Thus if θ is a multiple of π, then $\mathcal{E}_\theta$ is an *involution*, that is, its square is the identity transformation.

Remark. The parametric equations of $\gamma_{(\theta+\pi)}$ and γ_θ are the same. It follows from equations (2.4.3).

The results of this Section allow us to bypass the discrepancy between the analytic expressions and the geometrical picture of the evolutoidal transformations. The presence of the orientation of γ in formula (3.2.6) could be removed. Indeed, the choice of the normals is optional because the evolutoidal transformation of γ is well defined by its tangents. Hence we can always stick to the left-oriented case.

If we have two curves passing through the same point X, whose tangents coincide and centers of curvature at X are symmetrical (with respect to X), then the point on the θ-evolutoid of one of the curves corresponding to X will be symmetrical (with respect to X) to the point of $(\pi - \theta)$-evolutoid of the other. Analytically, it becomes clear if we replace in formula (3.2.6) R by $-R$, θ by $\pi - \theta$, and remove $\varepsilon(\gamma)$. Thus, in the case of a counter-clockwise γ, we choose the interior normals, and the exterior normals otherwise and apply the equations (2.4.5) or (2.4.3).

Since the the local properties of the evolutoidal transfomations, that is, the geometrical relationship between a point $X \in \gamma$ and its image $X_\theta \in \gamma_\theta$ do not depend on $\varepsilon(\gamma)$, we will restrict ourselves to the left-oriented case of γ, and use the equations (2.4.5) and (2.4.3) as a left-oriented particular case of a more general equation (3.2.6) whenever our concern is not about global properties of evolutoids.

3.3 Composition of two evolutoidal transformations

The problem of constructing successive evolutoids , that is, construction of evolutoids of evolutoids, evolutoids of evolutoids of evolutoids, and so on, was considered in 19th century. There are many interesting results on the topic in works of Réaumur, Aoust, Haton, Lancret, Habich, Chasles, Dewulf and others [8]. However, global properties of evolutoids were of major concern of these and many other mathematicians.

We will focus on the local properties of the evolutoidal transformation, and the rest of this work will be about the images of a single point on a curve, given by parametric equations, under two, three and more evolutoidal transformations.

Denote the curve, representing the result of $\psi-$evolutoidal transformation of γ_θ by $\gamma_{\theta\psi}$ and the image of $X(\varphi)$ by $X_{\theta\psi}(\varphi):\ \gamma \to \gamma_{\theta\psi},\ X \to X_{\theta\psi}$.

Theorem 3.3.1. (Commutation of a composition of evolutoidal transforms). *The result of two consecutive evolutoidal transformations applied to a curve does not depend on the order of application of the transforms:* $\gamma_{\theta\psi} = \gamma_{\psi\theta}$ *point-wise for any* $\theta, \psi \in [0, \pi]$.

Proof. Denote $a_\theta = \cos\theta\sin\theta,\ A_\theta = \cos^2\theta - \dot{R}\cos\theta\sin\theta,\ b_\theta = \sin^2\theta,\ B_\theta = \dot{R}\sin^2\theta - \cos\theta\sin\theta$, and the equation (2.4.5), we have:

$$\vec{X}_{\theta\psi} = \vec{X}_\theta + \frac{R_\theta}{\|\vec{v}_\theta\|}(-a_\psi\vec{v}_\theta + b_\psi\vec{n}_\theta) = \vec{X} + R(-a_\theta\vec{v} - a_\psi\vec{v}_\theta + b_\theta\vec{n} + b_\psi\vec{n}_\theta). \qquad (3.3.1)$$

and

$$\vec{X}_{\psi\theta} = \vec{X} + R(-a_\psi\vec{v} - a_\theta\vec{v}_\psi + b_\psi\vec{n} + b_\theta\vec{n}_\psi). \qquad (3.3.2)$$

Let us treat the equation above coordinate-wise:

$$\begin{aligned}
X_{\theta\psi} &= x + R(-a_\theta \dot{x} - b_\theta \dot{y} - b_\psi \dot{x} B_\theta - b_\psi \dot{y} A_\theta - a_\psi \dot{x} A_\theta + a_\psi \dot{y} B_\theta) = \\
&= x + R(\dot{x}(-a_\theta - b_\psi(\dot{R} b_\theta - a_\theta) - a_\psi(1 - a_\theta \dot{R} - b_\theta)) + \\
&+ \dot{y}(-b_\theta - b_\psi(1 - a_\theta \dot{R} - b_\theta) + a_\psi(\dot{R} b_\theta - a_\theta))) = \\
&= x + R(\dot{x}(-a_\psi - b_\theta(\dot{R} b_\psi - a_\psi) - a_\theta(1 - a_\psi \dot{R} - b_\psi)) + \\
&+ \dot{y}(-b_\psi - b_\theta(1 - a_\psi \dot{R} - b_\psi) + a_\theta(\dot{R} b_\psi - a_\psi))) = X_{\psi\theta}.
\end{aligned} \tag{3.3.3}$$

By the same technique of regrouping the like-terms, we get

$$Y_{\theta\psi} = Y_{\psi\theta}. \tag{3.3.4}$$

□

The fact that one can permute the angles taken for construction of successive evolutoids was proven by Haton de la Goupillière [18]. However he proved the commutativity in terms of the curvature function defining a curve up tp a parallel shift. Our proof is different. Let us give a geometrical interpretation of the Theorem 3.3.1 and its proof.

Denote $\overline{\theta} = \frac{\pi}{2} - \theta$, $\overline{\psi} = \frac{\pi}{2} - \psi$. Then by the construction, we have: $\widehat{XEX_\psi} = \psi$, $\widehat{XEX_\theta} = \theta$, $\widehat{EX_\psi X} = \widehat{EX_\theta X} = \frac{\pi}{2}$.

Denote by E_e the center of curvature of the evolute of γ at point $E = X_{\frac{\pi}{2}}$. (If the evolute has a cusp at E, then E_e coincides with E).

Lemma 3.3.2. *The foot of the perpendicular dropped from E_e to EX_θ is the center of curvature of γ_θ at X_θ.* (see Figure 3.1).

Proof. By the proposition 3.1.4, we have $|EE_e| = |R\dot{R}|$, and since XE is tangent to the evolute, $\widehat{E_eEX} = \frac{\pi}{2}$.

From $\triangle EE_\theta E_e :\ EE_\theta = EE_e \sin\theta = R\dot{R}\sin\theta$.

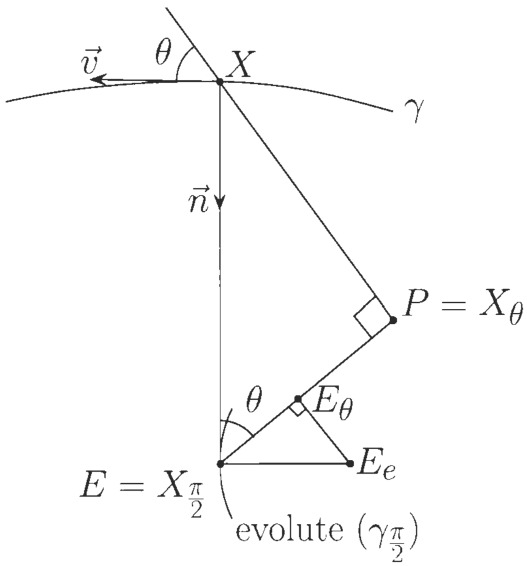

Figure 3.1: Center of curvature of an evolutoid.

From $\triangle EX_\theta X$: $EX_\theta = R\cos\theta$.

Hence, $|E_\theta X_\theta| = |R(\dot{R}\sin\theta - \cos\theta)|$. $\square$

Theorem 3.3.3. (Geometrical interpretation of the commutation of evolutoidal transformations) *Points $X_{\theta\psi}$ and $X_{\psi\theta}$ coincide and lie on the intersection of two perpendicular lines $E_\theta E_\psi$ and $X_\theta X_\psi$.*

Proof. Look at Figure 3.2. $\widehat{EX_\psi X_\theta} = \widehat{EXX_\theta} = \overline{\theta}$ - inscribed angles.

$\widehat{E_\theta EE_e} = \widehat{E_\theta E_\psi E_e} = \overline{\theta}$ - inscribed angles.

Therefore, $\widehat{E_\theta E_\psi X_\psi} = \frac{\pi}{2} - \overline{\theta} = \theta \Rightarrow E_\theta E_\psi \perp X_\theta X_\psi$.

Denote $X_\theta X_\psi \cap E_\theta E_\psi = P$.

Further,

$\widehat{XX_\theta X_\psi} = \widehat{XEX_\psi} = \psi$ - inscribed angles.

$\widehat{X_\theta E_\theta P} = \widehat{X_\psi X_\theta X} = \psi$ - the corresponding sides are perpendicular.

Thus, $P = X_{\theta\psi}$ by construction.

Finally, $\widehat{E_\theta X_\psi E_\psi} = \theta \;\Rightarrow\; P = X_{\psi\theta}$ by construction. $\square$

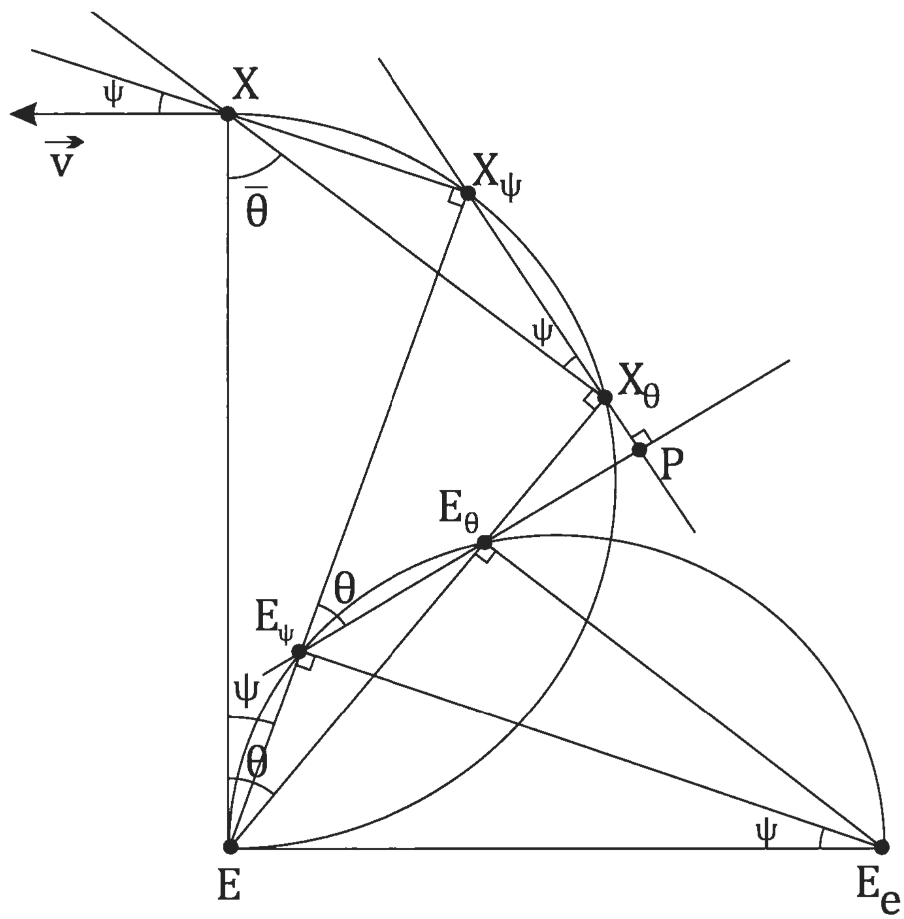

Figure 3.2: Geometrical interpretation of commutation of evolutoidal transformations

The geometrical interpretation and construction of $X_{\psi\theta} = X_{\theta\psi}$ presented in Theorem 3.3.3 are believed to be new. They open a broad way to use the variety of tools of Euclidean geometry to observe the local properties of multiple evolutoidal transfomations, i.e. to observe how a fixed point on a plane curve moves on the plane under compositions of different evolutoidal transformations apllied to the curve.

3.4 The range of $X_{\theta\psi}$. The Cardioid Theorem

Denote $X_{\theta\psi}$ by $P(\theta, \psi)$.

Definition 3.4.1. *The range of a point $X \in \gamma$ under two evolutoidal transformations is the locus of $\{P(\theta, \psi)\}_{\theta,\psi=0}^{\pi}$.*

Lemma 3.4.2. *Fix an $\alpha \in [0, \pi]$. Then $\{P(\theta, \psi)|_{(\theta+\psi) \bmod \pi = \alpha}\}_{\theta,\psi=0}^{\pi}$ is the segment between the points $P(\frac{\alpha}{2}, \frac{\alpha}{2})$ and $P(\frac{\alpha+\pi}{2}, \frac{\alpha+\pi}{2})$.*

Proof. Choose any fixed α and arbitrary θ and ψ such that $(\theta+\psi) \bmod \pi = \alpha$, $\alpha, \theta, \psi \in R \bmod \pi$. Without loss of generality we may assume that

$$\begin{cases} \theta = \frac{\alpha}{2} + t \\ \psi = \frac{\alpha}{2} - t. \end{cases} \tag{3.4.1}$$

Then the line $X_\theta X_\psi$ will be parallel to the tangent to the circle XEO at $X_{\frac{\alpha}{2}}$ (Figure

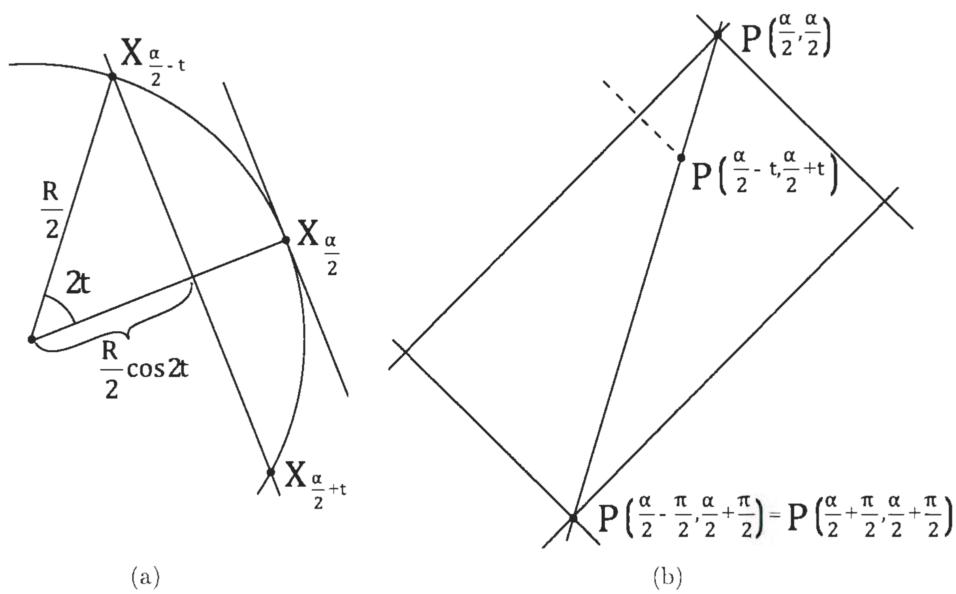

Figure 3.3: To Lemma 3.4.2.

3.3(a)).

By simple geometry, the distance between the two lines is $\frac{R}{2}(1 - \cos 2t)$. For the same reason, the line tangent to the circle EOE_e at $E_{\frac{\alpha}{2}}$ and the line $E_\theta E_\psi$ will be distance $\frac{\dot{R}R}{2}(1 - \cos 2t)$ apart.

By our construction, the two tangents are perpendicular and so are the lines $X_\theta X_\psi$ and $E_\theta E_\psi$.

Thus, the rectangle (Figure 3.3(b)) built on those two pairs of parallel lines has the same ratio between its sides, namely $\dot{R}$, regardless of the choice of α, θ, ψ.

Hence, the position of $P(\frac{\alpha}{2} + t, \frac{\alpha}{2} - t) = X_\theta X_\psi \cap E_\theta E_\psi,\ t \in [0, \frac{\pi}{2}]$ remains on the line segment connecting the point $P(\frac{\alpha}{2}, \frac{\alpha}{2})$ and $P(\frac{\alpha+\pi}{2}, \frac{\alpha+\pi}{2})$ corresponding to $t = 0$ and $t = \pi/2$ respectively. □

Corollary 3.4.3. *The segments $P(\frac{\alpha}{2}, \frac{\alpha}{2})P(\frac{\alpha+\pi}{2}, \frac{\alpha+\pi}{2})$ pass through O, the second intersection point of the circles XEO and EE_eO, for any $\alpha \in [0, \pi]$.*

Proof. Since the tangents to the two circles at E are perpendicular, so are the tangents at O.

Since $\widehat{EOE_e} = \widehat{EOX} = \frac{\pi}{2}$, we have: $O \in XE_e$.

From $\triangle XEE_e :\ \widehat{XEO} = \widehat{XE_eE} = \operatorname{arccot} \dot{R}$.

For a given α, choose $\theta = \operatorname{arccot} \dot{R}$ and $\psi = \alpha - \operatorname{arccot} \dot{R}$ and then $P(\theta, \psi) = O$.□

Lemma 3.4.2 and its corollary give us a nice way to construct locus of $\{P(\theta, \psi)\}_{\theta+\psi=\alpha}$, for a given constant α.

Draw the tangents to circles XEO and EE_eO at $X_{\frac{\alpha}{2}}$, $X_{\frac{\alpha+\pi}{2}}$ and $E_{\frac{\alpha}{2}}$, $E_{\frac{\alpha+\pi}{2}}$ respectively. Then the segment connecting the intersection points of the correspondent tangents will be the desired locus.

To describe the range of $\{P(\theta, \psi)\}_{\theta,\psi=0}^{\pi}$, we have to describe the locus spanned by segments $P(\theta, \theta)P(\theta + \frac{\pi}{2}, \theta + \frac{\pi}{2})$, letting θ run from 0 to $\frac{\pi}{2}$, or simply the locus traced by the endpoints of the segments.

Denote circles XOE and EE_eO by Ω_1 and Ω_2 and their centers by O_1 and O_2 respectively. Denote the circle built on $[O_1O_2]$ as its diameter by $\overline{\Omega}$ and $|O_1O_2| = 2r$. Denote the center of $\overline{\Omega}$ by C.

Lemma 3.4.4. *The locus of centres of the segments* $\{P(\theta, \psi)\}_{\theta+\psi=\text{const}}$ *is* $\overline{\Omega}$.

Proof. Choose any $\alpha \in [0, \frac{\pi}{2}]$. Construct the segment PQ, where $P = P(\alpha, \alpha)$ and $Q = P(\alpha + \frac{\pi}{2}, \alpha + \frac{\pi}{2})$ and denote by B the midpoint of PQ (Figure 3.4).
Note that $|PQ| = R\sqrt{1 + \dot{R}^2}$ as the length of the diagonal of a rectangle with sides R and $R\dot{R}$. Draw the lines l_1 and l_2 going through O_1 and O_2 parallel to the tangent

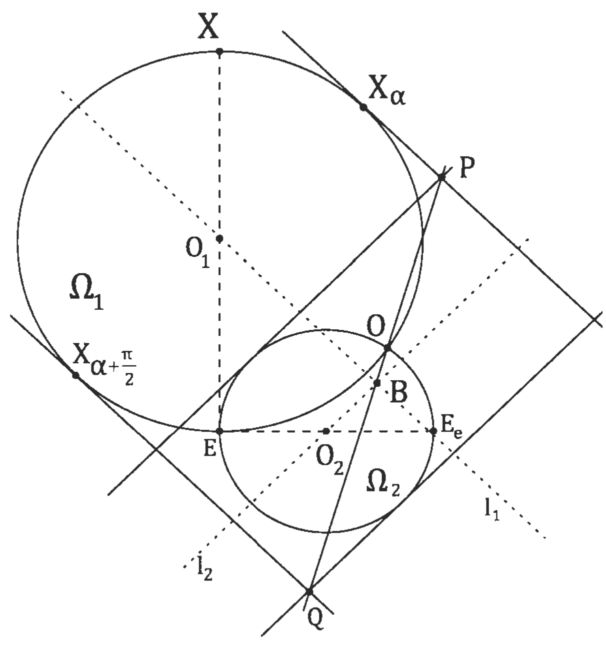

Figure 3.4: To Lemma 3.4.4.

to Ω_1 at X_α and to Ω_2 at E_α respectively. Obviously, l_1 and l_2 will pass through $B: \; B = l_1 \cap l_2$.
Since $l_1 \perp l_2$, B lies on the circle built on $[O_1O_2]$ as its diameter (on $\overline{\Omega}$).
On the other hand, each point on $\overline{\Omega}$ is the center of the segment $(P(\theta, \psi))_{\theta+\psi=2\alpha}$ for

some $\alpha \in R \bmod \frac{\pi}{2}$. It becomes clear if we reverse our chain of reasoning backward, constructing the corresponding $[PQ]$ for a given B. $\square$

Corollary 3.4.5. *Points E and O belong to $\overline{\Omega}$.*

Proof. The statement follows immediately from the fact that Ω_1 and Ω_2 intersect under the right angle. $\square$

Definition 3.4.6. *A cardioid is a curve, traced by a point on a circle, rolling upon a fixed circle of the same size.*

Theorem 3.4.7. (The Cardioid Theorem.) *The range of $X_{\theta\theta}$, $\theta \in [0, \pi]$, is a cardioid. The cardioid passes through X, E_e and O, O being its cusp, and is tangent to γ at X.*

Proof. Since $|O_1O_2|$ is a middle line of $\triangle XEE_e$, we have $|O_1O_2| = \frac{1}{2}|XE_e| = \frac{R\sqrt{1+\dot{R}^2}}{2}$. Consider $\overline{\Omega}$, defined above, and take any segment $[PQ]$, crossing $\overline{\Omega}$ at points O and B such that $|PB| = |BQ| = |O_1O_2| = 2r$.

Draw a segment $[AD]$ of the length $4r$ passing through the center of $\overline{\Omega}$ (Figure 3.5), denoted by C, parallel to PQ such that $|AC| = |CD|$. Then, $AQBC$ and $CBPD$ are equal parallelograms, since sides $[AC]$, $[QB]$, $[CD]$ and $[PB]$ are equal and parallel. Then, we have $|AQ| = |CB| = |DP| = r$.

Also, since $|AC| = |CD| = r$ and $|CF| = |CG| = r$, we have $|AF| = r$ and $|GD| = r$. From the trapezoids $OCDP$ and $OCAQ$, we get $\widehat{OCD} = \widehat{PDC}$ and $\widehat{QAC} = \widehat{ACO}$. Now, draw two circles of radii r centered at A and D (dotted circles on the picture). The arcs $\overset{\frown}{\mathrm{QF}} = \overset{\frown}{\mathrm{OF}}$ and $\overset{\frown}{\mathrm{OG}} = \overset{\frown}{\mathrm{PG}}$, because the corresponding central angles are equal.

Therefore, points Q and P take positions of a fixed point on a circle radius r, rolling upon $\overline{\Omega}$, and at the moments when the circles' common point is O the fixed point coincides with O.

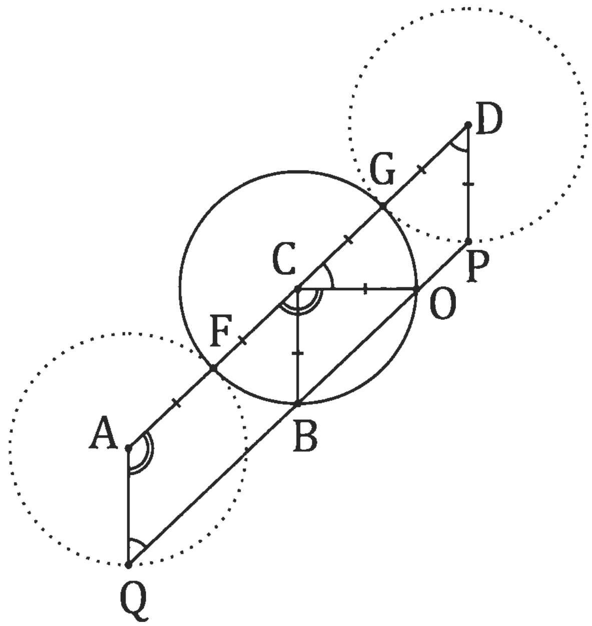

Figure 3.5: To The Cardioid Theorem.

By definition this point traces a cardioid with the cusp at O.

Replace P and Q by $P(\alpha, \alpha)$ and $P(\theta + \frac{\pi}{2}, \theta + \frac{\pi}{2})$ respectively, and the statement of the Theorem follows. $\square$

Thus, the whole image-set of $X_{\theta\psi}$, $\theta, \psi \in [0, \pi]$, is the closed region bounded by this cardioid, (see Figure 3.6)!

Definition 3.4.8. *For a plane curve γ and a given fixed point P, the pedal curve of γ is the locus of points X such that PX is perpendicular to a tangent to the curve passing through X. The point P is called the pedal point.*

The Cardioid Theorem has several nice generalizations and corollaries about properties of cardioids in particular and limaçons of Pascal in general which do not require lenthy proofs. One of them is the following Corollary.

Corollary 3.4.9. *A pedal curve of a circle with respect to one of its points is a*

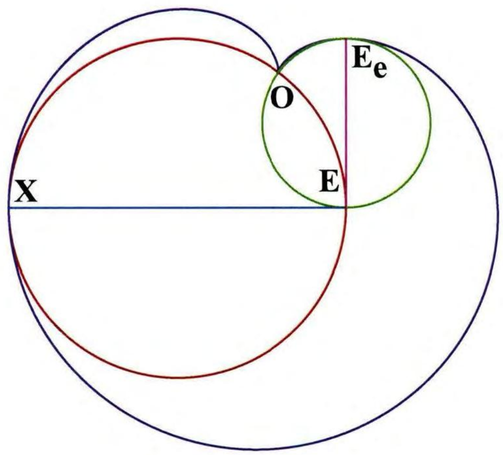

Figure 3.6: The locus $\{X_{\theta\theta}\}_{\theta=0}^{\pi}$ and two circles based on $[XE]$ and $[EE_e]$ as their diameters.

cardioid[5].

Proof. According to the definition 3.4.8, the statement of the corollary follows immediately from our construction of the set $\{X_{\theta\theta}\}_{\theta=0}^{\pi}$ if we take for X one of the vertices of γ, that is, one of the points on γ, where R attains its local maximum or minimum. Indeed, if X is a vertex, then $\dot{R} = 0$. Hence, E coincides with E_e and with O, so the locus of all possible $X_{\theta\theta}$ is the locus of points P such that PE is perpendicular to a tangent to the circle radius $\frac{R}{4}$ the center at $C \in XE: \ |CX| = 4|CE|$. By definition, this is the pedal curve to the circle with respect to E, and by the Cardioid Theorem, it is a cardioid. $\square$

Using the technique of the proof of the Cardioid Theorem, we may prove a nice statement generalizing the way of constructing a cardioid by means of finding the locus of points, which lie on intersection of perpendicular tangents to two perpendicular circles.

[5]This fact is known [14], but the approach of our proof is believed to be new. In Chapter7, we prove its generalization.

Theorem 3.4.10. *If two lines intersecting at a fixed angle are moved continuously tangent to two given circles, their intersection traces a limaçon of Pascal whose double point lies on the circle of similitude of the two given circles.*

This theorem was proved by J.H. Butchart in 1945, using a slightly different technique [3].

3.5 Analytic proof of the Cardioid Theorem

Since Lemma 3.4.2 implies that the image-set of the second iteration could be described by the locus of $\{X_{\theta\theta}\}_{\theta=0}^{\pi}$, let us obtain the equation of this locus analytically. By the vector form of the equation of θ-evolutoid of θ-evolutoid, we have

$$\vec{X}_{\theta\theta} = \vec{X} + R(-a_\theta(\vec{v} + \vec{v}_\theta) + b_\theta(\vec{n} + \vec{n}_\theta)), \tag{3.5.1}$$

or omitting subscripts θ and plugging in the expansions for $\vec{v}_\theta$ and $\vec{n}_\theta$, we get

$$\vec{X_{\theta\theta}} = \vec{X} + R(\vec{v}(-a - aA - bB) + \vec{n}(b - aB + bA)). \tag{3.5.2}$$

Using the notations c and s for $\cos\theta$ and $\sin\theta$ respectively and expanding the expressions for a, A, b, B in the latter equation, we finally obtain

$$\vec{X_{\theta\theta}} = \vec{X} + R(\vec{v}(-cs - (cs - \dot{R}s^2)(c^2 - s^2)) + \vec{n}(s^2 + 2cs(cs - \dot{R}s^2))). \tag{3.5.3}$$

For simplicity sake, let us denote cos and sin of multiple θ by c_n and s_n, where n is the multiplicity of θ, i.e. $\cos 4\theta$ is denoted by simply c_4.

To get rid of a constant vector $\vec{X}$ and to simplify the coefficients, we introduce a new vector of consideration, $\vec{F}$:

$$\vec{F} = \frac{4}{R}(\vec{X_{\theta\theta}} - \vec{X}) = (-\vec{F_v}, \vec{F_n}), \tag{3.5.4}$$

where

$$\begin{cases} F_v = 4(cs + (cs - \dot{R}s^2)c_2) \\ F_n = 4(s^2 + (cs - \dot{R}s^2)s_2). \end{cases}$$

Then

$$\begin{cases} F_v = 2s_2 + 2c_2(s_2 - \dot{R}(1-c_2)) = \dot{R}c_4 + s_4 + 2(s_2 - \dot{R}c_2) + \dot{R} \\ F_n = 2(1-c_2) + 2s_2(s_2 - \dot{R}(1-c_2)) = -c_4 + \dot{R}s_4 - 2(s_2\dot{R} + c_2) + 3. \end{cases}$$

Let

$$\tilde{F}_v = \frac{F_v - \dot{R}}{\dot{R}^2 + 1}, \quad \tilde{F}_n = \frac{F_n - 3}{\dot{R}^2 + 1}.$$

Denoting $\frac{\dot{R}}{\dot{R}^2+1}$ and $\frac{1}{\dot{R}^2+1}$ by $\cos\beta$ and $\sin\beta$ respectively (since $\cos^2\beta + \sin^2\beta = 1$), we can see

$$\begin{cases} \tilde{F}_v = \cos(4\theta - \beta) - 2\cos(2\theta + \beta) \\ \tilde{F}_n = \sin(4\theta - \beta) - 2\sin(2\theta + \beta). \end{cases}$$

Let us look for such μ and ν that

$$4\theta - \beta = 2\mu + \nu, \quad 2\theta + \beta = \mu + \nu.$$

We get

$$\mu = 2\theta - 2\beta, \quad \nu = 3\beta.$$

Now we apply linear change to the parameter $\mu = 2\theta - 2\,\mathrm{arccot}\,\dot{R}$ and obtain

$$\begin{cases} \tilde{F}_v = \cos(2\mu + 3\beta) - 2\cos(\mu + 3\beta) \\ \tilde{F}_n = \sin(2\mu + 3\beta) - 2\sin(\mu + 3\beta). \end{cases} \tag{3.5.5}$$

Vector $(\tilde{F}_v(\mu), \tilde{F}_n(\mu))$ is an equation of the trace of a fixed point on a unit circle rolling over a fixed unit circle centered in the origin, which is a cardioid. The cusp of this cardioid is located in the point $(\cos 3\beta, \sin 3\beta)$.

Chapter 4

Image-sets of higher order evolutoidal transformations

4.1 Gaussian map parameter

Consider the set of external (pointing away from the centers of curvature) normals $\vec{n}$ to an oval γ given by the C^3-map $s \to X(s)$, s being an arclength parameter. Fix a vector $\vec{w}$ in the plane and call its direction the *reference direction.* We will introduce a new parameter ψ by which γ may be defined via the curvature function $R(\psi)$ up to a parallel shift in the plane.

Definition 4.1.1. *The angle $\psi = \widehat{\vec{n}, \vec{w}}$ between the external normal $\vec{n}$ to the curve γ and the reference direction $\vec{w}$ is called the Gaussian parameter. The map $\psi \longmapsto R(\psi)$ is called a Gaussian parametrization.* (See Figure 4.1(b)).

Look at Figure 4.1(a). Here, as usual, E represents the center of curvature of γ at X, s is the arclength parameter of γ; $\vec{n}$ and $\vec{n} + d\vec{n}$ are the outer unit normals to γ at X and $X + dX$ respectively; $d\psi = \widehat{\vec{n}, \vec{n} + d\vec{n}}$; ds represents the arc of γ between X and $X + dX$. Since the unit vector tangent to γ at X is $\vec{v} = Rd\vec{n}/ds$, we have

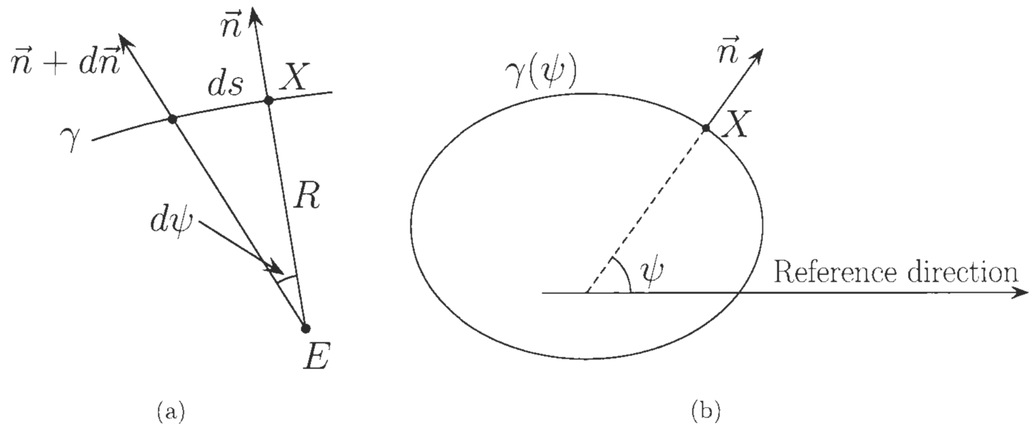

Figure 4.1: Gaussian parametrization

$ds = Rd\psi \;\Rightarrow\; R = ds/d\psi$. Hence

$$\frac{d\vec{n}}{d\psi} = \frac{d\vec{n}}{ds}\frac{ds}{d\psi} = \frac{\vec{v}}{R}R = \vec{v}, \tag{4.1.1}$$

and similarly

$$R\frac{d\vec{v}}{ds} = -\vec{n}. \tag{4.1.2}$$

Let us express the radius-vector $\vec{X}_\theta$ of the θ-evolutoid and its ψ-derivative $d\vec{X}_\theta/d\psi$ as functions of ψ. First of all,

$$\frac{d\vec{X}}{d\psi} = \frac{d\vec{X}}{ds}\frac{ds}{d\psi} = \vec{v}R. \tag{4.1.3}$$

Then, setting $a = \sin\theta\cos\theta,\ b = \sin^2\theta$, we get

$$\frac{d\vec{X}_\theta}{d\psi} = \frac{d\vec{X}}{d\psi}+\frac{dR}{d\psi}(-a\vec{v}-b\vec{n})+R(a\vec{n}-b\vec{v}) = \vec{v}(R-\frac{dR}{d\psi}a-Rb)+\vec{n}(-\frac{dR}{d\psi}b+aR). \tag{4.1.4}$$

Since $d\vec{X}_\theta/d\psi$ is the tangent vector to γ_θ at X_θ, let us denote this vector by $\vec{v}_\theta$. Note that if $\theta = \frac{\pi}{2}$, then $\vec{v}_\theta$ is parallel to the normal $\vec{n}$ to γ at $X(\psi)$. In general $\|\vec{v}_\theta\| \neq 1$, moreover, in some particular cases $\|\vec{v}_\theta\|$ can be zero.

By (3.2.7), $R_E = R\,dR/ds$. Then

$$R_E = R\frac{dR}{ds} = \frac{ds}{d\psi}\frac{dR}{ds} = \frac{dR}{d\psi}. \tag{4.1.5}$$

The simplicity of the expression for R_E via R, when R is a function of a Gaussian map parameter plays a significant role in further calculations. Also, using this type of parametrization, we can easily treat the case when $\|d\vec{X}/d\psi\| = 0$ (and hence $R = 0$), avoiding division by zero in the parametric equations of γ_θ (2.4.3).

4.2 Introduction to the general approach

The goal of this Section is to describe the shapes of image-sets of the n-th evolutoidal iteration ($n \geq 3$) of a curve at a given point[1], or simply the nth iteration.

For brevity, we will denote $X_{\underbrace{\theta_1\theta_1\ldots\theta_1}_{n_1}\ldots\underbrace{\theta_m\theta_m\ldots\theta_m}_{n_m}}$ by $X_{\theta_1^{n_1}\ldots\theta_m^{n_m}}$. The superscript for multiplicity one will be omitted. Analogously, we will denote by $\gamma_{\theta_1^{n_1}\ldots\theta_m^{n_m}}$, $R_{\theta_1^{n_1}\ldots\theta_m^{n_m}}$ and $E_{\theta_1^{n_1}\ldots\theta_m^{n_m}}$ the curve obtained by the same composition of evolutoidal transformations from the original curve, its radius of curvature at a point $X_{\theta_1^{n_1}\ldots\theta_m^{n_m}}$, and the point on the evolute of $\gamma_{\theta_1^{n_1}\ldots\theta_m^{n_m}}$ corresponding to $X_{\theta_1^{n_1}\ldots\theta_m^{n_m}}$.

Denote $\cos\theta_i$ and $\sin\theta_i$ by c_i and s_i respectively.

Lemma 4.2.1. (The radius of curvature of $\gamma_{\theta_1^{n_1}\ldots\theta_m^{n_m}}$) *The radius of curvature of $\gamma_{\theta_1^{n_1}\ldots\theta_m^{n_m}}$ at $X_{\theta_1^{n_1}\ldots\theta_m^{n_m}}$ can be calculated via the differential operator:*

$$R_{\theta_1^{n_1}\ldots\theta_m^{n_m}} = (c_1 - s_1\frac{d}{d\psi})^{n_1}\ldots(c_m - s_m\frac{d}{d\psi})^{n_m}R, \tag{4.2.1}$$

where ψ is the Gaussian map parameter of γ.

Proof. Let us convert formula (3.2.7) for a natural parametrization into the Gaussian map parameterization, using (4.1.5):

$$R_\theta = (\cos\theta - \sin\theta\frac{d}{d\psi})R. \tag{4.2.2}$$

Applying the differential operator n_i times with appropriate values of θ_i, ($i = 1, \ldots, m$) to $R(\psi)$ we will obtain the desired formula. $\square$

Remark. Thus, the radius of curvature of a curve resulting from n evolutoidal transformations depends only on the radii of curvature of the evolute, the evolute of

[1]We will always assume that a curve of consideration γ is continuously differentiable at a point of consideration X as many times as it is needed, so that $R, \frac{\partial R}{\partial\psi}, \frac{\partial^2 R}{\partial\psi^2}, \ldots, \frac{\partial^n R}{\partial\psi^n}$ are assumed to be continuous.

evolute and so on $(n-1)$ times, and on θ_i, $i = 1, ..., n$.

Denote by Γ_n the set $\{X_{\theta^n},\ \theta \in [0,\pi]\}$. It is clear that this is a curve, depending on parameter θ and the first $n+1$ derivatives of γ at X. Γ_1 is a circle. From the Cardioid Theorem 3.4.7, we know that Γ_2 of any curve γ is a cardioid, and the image-set of the second iteration is the region bounded by that cardioid. For further observation of image-sets of the nth iteration, we will focus our attention on the study of Γ_n, and we show later in Chapter 6 that the image-set of the nth iteration is a region bounded by arcs of Γ_n, in general. According to Remark to Lemma 4.2.1, the shape and the size of the image-set of the nth iteration of $X \in \gamma$ depend only on the set $\{R(\psi), R'(\psi), ..., R^{(n-1)}(\psi)\}$, or simpler $\{R, R', ..., R^{(n-1)}\}$. We will also use notation $\Gamma_n(R, R', R'', ..., R^{(n-1)})$ for Γ_n if we want to be specific about a particular image-set. Since the image-set of a point X on a curve does not depend on the curve's orientation and the way it is traced (by Theorem 3.2.14), we will consider only left-oriented curves traced counterclockwise at X. To further simplify the study of the shapes of Γ_n, let us apply an appropriate rotation and translation to the coordinate axes to move the point of consideration, $X \in \gamma$, to the origin, so that the center of curvature lies on the positive half of the x-axis, and the positive direction of the y-axis is opposite to that of the tangent to γ. Let us choose the negative direction of the x-axis for the reference direction of the Gaussian map parameter ψ, by which γ is parametrized.[2]

Let us fix $\theta \in [0,\pi]$ and construct the polygonal line with nodes at X, X_{θ^i}, $i = 1, ..., n$.

Lemma 4.2.2. *Vector* $\overrightarrow{X_{\theta^i}X_{\theta^{i+1}}} = R_{\theta^i}\sin\theta(\sin i\theta, \cos i\theta)$.

Proof. Look at Figure 4.2. By our construction of θ-evolutoid of γ_{θ^i}, we have

$$|X_{\theta^i}X_{\theta^{i+1}}| = |R_{\theta^i}\sin\theta|, \tag{4.2.3}$$

[2]The sign $R < 0$ is allowed, and the picture is symmetric to the case $R > 0$ with respect to the origin. In that case, the x-coordinate of the center of curvature will be negative, and the direction of the tangent to γ at X will coincide with that of the positive direction of the y-axis.

and line $X_{\theta^i}X_{\theta^{i+1}}$ will form angle θi with positive direction of y-axis. □

Note that some of the numbers R_{θ^i} could be zero. These are the roots of the trigono-

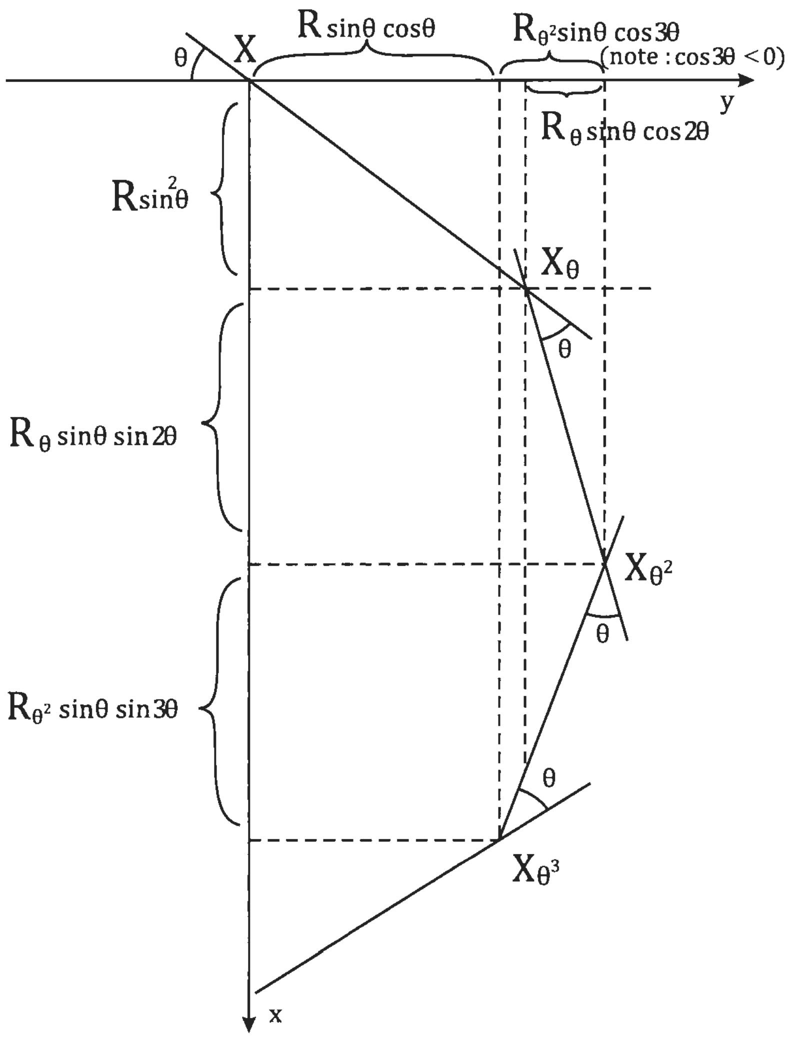

Figure 4.2: An illustration of the polygonal line construction of X_{θ^n} method for the first three iterations. Here $R, R_\theta, R_{\theta^2} > 0$.

metrical polynomial $P_i(\cos\theta, \sin\theta) = 0$, hence there are only finite number of $\theta \in [0, \pi]$ such that $R_{\theta^i} = 0$. If $R_{\theta^i} = 0$, then points X_{θ^i} and $X_{\theta^{i+1}}$ coincide.

An example of the development of Γ_n, $n = 2, 3, 4$, is shown in Figure 4.3(a). Lemma 4.2.2 gives clear tool to θ-parametrization of the equations of Γ_n.

Denote $\sin(\theta_1 + ... + \theta_k), \cos(\theta_1 + ... + \theta_k)$ by S_k, C_k respectively, $1 < k \leq n$.

Corollary 4.2.3. *The coordinates of the image of a point $X \in \gamma$ under the nth iteration with angles $\theta_1, ..., \theta_n$ are:*

$$\begin{cases} x = Rs_1^2 + R_{\theta_1}s_2S_2 + R_{\theta_1\theta_2}s_3S_3 + ... + R_{\theta_1...\theta^{n-1}}s_nS_n \\ y = Rs_1c_1 + R_{\theta_1}s_2C_2 + R_{\theta_1\theta_2}s_3C_3 + ... + R_{\theta_1...\theta^{n-1}}s_nC_n, \end{cases} \tag{4.2.4}$$

Proof. It follows from Lemmas 4.2.2 and 4.2.1, since the radius-vector of $X_{\theta_1...\theta_n}$ is a direct sum of $\overrightarrow{X_{\theta_1...\theta_i}X_{\theta_1...\theta_{i+1}}}$, $i = 0, ..., n-1$, if we set $X = X_{\theta_0}$. □

Corollary 4.2.4. *The parametric equations of Γ_n are*

$$\begin{cases} x = Rs^2 + R_\theta ss_2 + R_{\theta^2}ss_3 + ... + R_{\theta^{n-1}}ss_n \\ y = Rsc + R_\theta sc_2 + R_{\theta^2}sc_3 + ... + R_{\theta^{n-1}}sc_n, \end{cases} \tag{4.2.5}$$

where $s = \sin\theta$, $c = \cos\theta$, $s_k = \sin k\theta$, $c_k = \cos k\theta$, $k > 1$.

Proof. It follows immediately from Lemma 4.2.2. □

The following lemma will be also helpful in the future to prove Lemma 6.2.2.

Lemma 4.2.5. *For fixed $\theta, \alpha \in [0, \pi]$ the locus of points $\{X_{\theta^n(\alpha-t)(\alpha+t)}\}_{t=0}^{\frac{\pi}{2}}$ is the segment $[X_{\theta^n\alpha^2}X_{\theta^n(\alpha+\frac{\pi}{2})^2}]$.*

Proof. The statement follows from application of Lemma 3.4.2 to the curve γ_{θ^n} at point X_{θ^n}. □

Remark. Define a linear space L_n of n-tuples $(R, R', ..., R^{n-1})$, which determine the shape and size of Γ_n. Vectors $(0, 0, ..., 0, 1, 0, ..., 0)$ with $R^{(j)} = 0$, $j \neq i$ and $R^{(i)} = 1$ obviously form a basis in L_n. Since the parametric equations of Γ_n are linear with respect to $R^{(i)}$, $i = 0, ..., n$, the curves $\Gamma_n(R, ..., R^{(n-1)})$ and $\Gamma_n(\lambda R, ..., \lambda R^{(n-1)})$ are

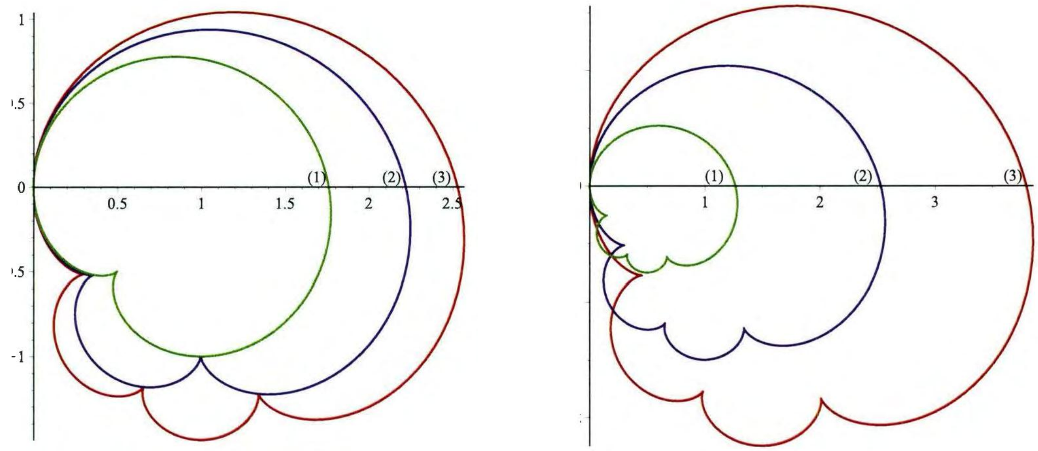

Figure 4.3: (a) An example of development of Γ_n, $n = 2, 3, 4$: the curves: (1) $\Gamma_2(1, -1)$; (2) $\Gamma_3(1, -1, 0)$; (3) $\Gamma_4(1, -1, 0, 0.5)$. (b) The homothetical curves (with respect to X): (1) $\Gamma_4(0.5. -0.5, 0, 0.25)$; (2) $\Gamma_4(1, -1, 0, 0.5)$; (3) $\Gamma_4(1.5, -1.5, 0, 0.75)$, the point of consideration, X, is in the origin in all three cases of (a) and (b).

homothetical (see Figure 4.3(b)) with respect to X, any line in L_n passing through the origin represents the shape of Γ_n. Note that different lines may represent the same shape of Γ_n, for instance, all curves Γ_2 are cardioids.

Thus, for further observation of shapes of Γ_n we may first try the basic cases and then consider their linear combinations, where the sum of two or more curves is understood as a coordinate-wise summation of their parametric equations (4.2.5). Also, we may realize a real projective space with homogeneous coordinates $(R : R' : \ldots : R^{(n-1)})$ as the set of lines in L_n passing through the origin, if the size of Γ_n is not of our concern.

Denote by $R_n = R_n(\theta)$ the radius of curvature of Γ_n. The following theorem establishes the relationship between $R_n(\theta)$ and $R_{\theta^{n-1}}$.

Theorem 4.2.6. (Radius of curvature of Γ_n.) *The raduis of curvature of the curve*

Γ_n *can be expressed via* $R_{\theta^{n-1}}$ *by the following equation*

$$R_n(\theta) = \left| \frac{n}{n+1} R_{\theta^{n-1}} \right|. \qquad (4.2.6)$$

Proof. Denote the coordinates of a point $X_{\theta^n} \in \Gamma_n$ by $(x_{\theta^n}, y_{\theta^n})$. First, let's prove by induction the two following equations

$$\begin{cases} \frac{\partial x_{\theta^n}}{\partial \theta} = n \sin_{n+1} R_{\theta^{n-1}} \\ \frac{\partial y_{\theta^n}}{\partial \theta} = n \cos_{n+1} R_{\theta^{n-1}} \ . \end{cases} \qquad (4.2.7)$$

$n = 1$. From (4.2.5), we get $\partial x_{\theta^n}/\partial \theta = Rs_2$, $\partial y_{\theta^n}/\partial \theta = Rc_2$. This matches (4.2.7). Suppose, the statement is true for all $k \leq n-1$, $n \geq 2$. By (4.2.5)

$$\begin{cases} x_{\theta^n} = x_{\theta^{n-1}} + ss_n R_{\theta^{n-1}} \\ y_{\theta^n} = y_{\theta^{n-1}} + sc_n R_{\theta^{n-1}}. \end{cases} \qquad (4.2.8)$$

Differentiating formula (4.2.1) for $\theta_1 = ... = \theta_{n-1}$ with respect to θ

$$\frac{\partial R_{\theta^{n-1}}}{\partial \theta} = -(n-1)(sR_{\theta^{n-2}} + cR'_{\theta^{n-2}}), \qquad (4.2.9)$$

where $R'_{\theta^{n-2}} = \partial R_{\theta^{n-1}}/\partial \psi$.

Now, differenting x_{θ^n} in (4.2.8) with respect to θ, we have

$$\frac{\partial x_{\theta^n}}{\partial \theta} = (n-1)s_n R_{\theta^{n-2}} + R_{\theta^{n-1}}(cs_n + nsc_n) - (n-1)ss_n(sR_{\theta^{n-2}} + cR'_{\theta^{n-2}}).$$

Combining the like-terms and using formula (4.2.9), we obtain the $\partial x_{\theta^n}/\partial \theta = ns_{n+1}R_{\theta^{n-1}}$. Analogously, we obtain $\partial y_{\theta^n}/\partial \theta = nc_{n+1}R_{\theta^{n-1}}$.

Let us calculate $\partial x^2_{\theta^n}/\partial^2\theta$ and $\partial y^2_{\theta^n}/\partial^2\theta$.

$$\begin{cases} \frac{\partial x^2_{\theta^n}}{\partial^2\theta} = n((n+1)c_{n+1}R_{\theta^{n-1}} + s_{n+1}R'_{\theta^{n-1}}) \\ \frac{\partial y^2_{\theta^n}}{\partial^2\theta} = n(-(n+1)s_{n+1}R_{\theta^{n-1}} + c_{n+1}R'_{\theta^{n-1}}). \end{cases} \tag{4.2.10}$$

Plugging formulas (4.2.8) and (4.2.10) in formula (2.4.4), we get
$R_n(\theta) = \left|\frac{n^3R^3_{\theta^{n-1}}}{(n+1)n^2R^2_{\theta^{n-1}}}\right| = \left|\frac{n}{n+1}R_{\theta^{n-1}}\right|.$ □

Corollary 4.2.7. *The curve Γ_n is singular at a point X_{θ_n} if and only if $\gamma_{\theta^{n-1}}$ is singular at the point $X_{\theta^{n-1}}$.*

Corollary 4.2.7 allows us to veiw $\Gamma_n(\theta)$ as a smooth curve wherever $R_{\theta^{n-1}} \neq 0$.

Lemma 4.2.8. *Let $\gamma_{\theta^{k-1}}$ be regular at $X_{\theta^{k-1}}$, and let γ_{θ^k} be regular at X_{θ_k}. Then the tangent to Γ_k and the θ-secant to γ_{θ^k} at X_{θ^k} coincide.*

Proof. We will prove it by induction.
$n = 1$. In this case Γ_1 is the circle based on $[XE]$, so the basis of the induction follows from the construction of the image-set of the second iteration (see Theorem 3.3.3).
Suppose, the statement is true for all $k \leq n$. Then consider two close points, $X_{\theta^n} \in \gamma_{\theta^n}$ and $X_{(\theta+d\theta)^n} \in \gamma_{(\theta+d\theta)^n}$ ($d\theta \ll \theta$), on Γ_n, see Figure 4.4. To avoid bulky notations in the Lemma, we denote X_{θ^n}, $X_{(\theta+d\theta)^n}$, E_{θ^n}, $E_{(\theta+d\theta)^n}$, γ_{θ^n}, $\gamma_{(\theta+d\theta)^n}$ by X_n, X'_n, E_n, E'_n, γ_n, γ'_n, $n > 0$, and use similar notations with subscript $n+1$ for $X_{\theta^{n+1}}$, etc . Denote also by M the point of intersection of the tangents to γ_n at X_n and to γ'_n at X'_n. The arc $X_nX'_n \in \Gamma_n$ can be considered as a line segment, and, by the induction step, is $(\theta + d\theta)$-secant to γ'_n at X'_n, i.e. $\widehat{X_nX'_nM} = \theta + d\theta$.
It is clear that $\widehat{X_nMX'_n} = nd\theta$. That implies that the angle adjacent to $\widehat{MX_nX'_n}$ is equal to $\theta + (n+1)d\theta$.
Denote the circles based on $[X_nE_n]$ and $[X'_nE'_n]$ as their diameters by Ω_n and Ω'_n

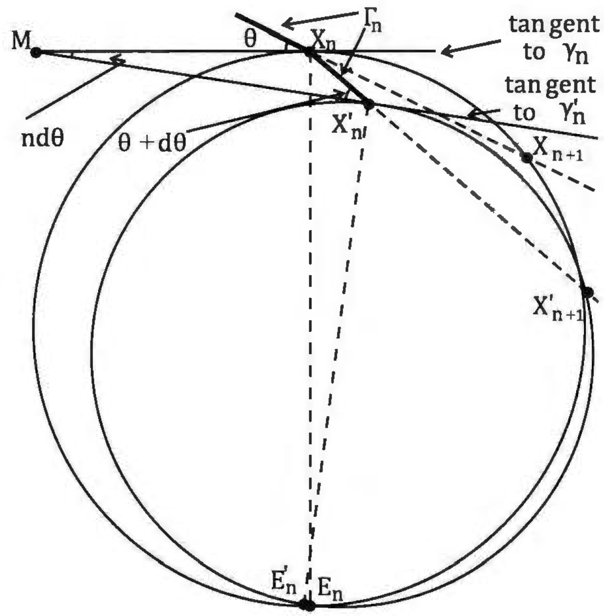

Figure 4.4: To Lemma 4.2.8.

respectively.

Construct X_{n+1} and X'_{n+1} by the routine procedure of continuation of θ-secant to γ_n at X_n and $(\theta + d\theta)$-secant to γ'_n at X'_n down to their intersections with the circles Ω_n and Ω'_n respectively. Note that $\widehat{X'_{n+1}X_nX_{n+1}} = (n+1)d\theta$.

Getting $d\theta \to 0$, we make $\Omega'_n \to \Omega_n$, $X'_n \to X_n$ and $X'_{n+1}X_{n+1}$ tangent to Γ_{n+1} and θ-secant to γ_{n+1} at X_{n+1}. □

Consider the image-sets of the n-th iteration of $X \in \gamma$ and $E = X_{\frac{\pi}{2}} \in \gamma_{\frac{\pi}{2}}$. Their shapes and sizes will depend on $R, R', ...R^{(n-1)}$ and $R', R'', ...R^{(n)}$ respectively. Denote the former by $\Gamma_n(X)$ and the latter by $\Gamma_n(E)$.

Proposition 4.2.9. *Lines, tangent to $\Gamma_n(X)$ and $\Gamma_n(E)$ at points corresponding to the same values of θ, are perpendicular and intersect at points $X_{\theta^{n+1}}$, $\theta \in [0, \pi]$.*

Proof. Points on $\Gamma_n(E)$ are $X_{\frac{\pi}{2}\theta^n} = X_{\theta^n\frac{\pi}{2}}$, since the order of application of evolutoidal transformations does not matter (see Figure 4.5). In other words, they are centers

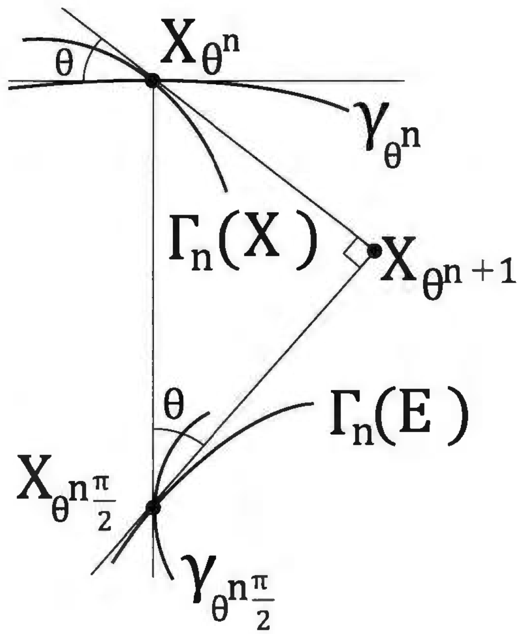

Figure 4.5: Tangential construction of Γ_{n+1}.

of curvature of γ_{θ^n}, $\theta \in [0, \pi]$. By Lemma (4.2.8), tangents to $\Gamma_n(X)$ at X_{θ^n} and to $\Gamma_n(E)$ at $X_{\theta^n \frac{\pi}{2}}$ are θ-isoclines to curves γ_{θ^n} and $\gamma_{\theta^n \frac{\pi}{2}}$ respectively. Then the statement follows from Definition 2.4.1. $\square$

Theorem 4.2.10. *The curve Γ_{n+1} is enveloped by the circles based on $[X_{\theta_n} E_{\theta_n}]$ as their diameters, $\theta \in [0, \pi]$.*

Proof. From Lemma (4.2.8), it follows that circles based on $[X_{\theta^n} E_{\theta^n}]$ are tangent to Γ_{n+1} at $X_{\theta^{n+1}}$ for any $\theta \in [0, \pi]$. Hence, Γ_{n+1} is enveloped by the circles. $\square$

Before continuing development of the topic on image-sets of the n-th iteration for general n, let us take a close look on the 3rd iteration and study $\Gamma_3(R, R', R'')$ for variety of $(R, R', R'') \in L_3$.

Chapter 5

The 3rd iteration: Construction

In this Chapter, we provide the necessary background for construction of an image of a point $X \in \gamma$ under three successive evolutoidal transformation.

5.1 Similar-perspective triangles

Let us consider two coplanar intersecting circles Ω_1 and Ω_2, and R_1, R_2 be their corresponding radii. Denote by A and B the points of intersection of the circles: $\Omega_1 \cap \Omega_2 = \{A, B\}$. We do not allow the points A and B coincide unless $R_2 = 0$. Let α be adjacent to the outer angle between the tangents to the circles at A (or at B). In the degenerate case $R_2 = 0$, α can be assigned any value we wish.

Define *rotational homothety with respect to* A as a transformation $T = T_A[\alpha, R]$, $R = \frac{R_2}{R_1}$ equal to the composition of two affine maps of the plane onto itself:

(a) the rotation of the plane around A by angle α so that the tangent to Ω_1 at A is mapped onto the tangent to Ω_2 at A;

(b) the homothety centered at A with ratio R.

If a plane Π is mapped onto itself by $T = T_A[\alpha, R]$, $A \in \Pi$, we will denote the image of any planar set of points $G \in \Pi$ under T by $T_A[\alpha, R](G)$ or simpler by $T(G)$.

Note that indeed, as the notation suggests, $T_A[\alpha, R]$ depends only on the ratio $R = R_1/R_2$ but not on R_1 and R_2 themselves. In other words, replacing the circles Ω_1 and Ω_2 in the construction by their images under the same homothety with center A has no effect on T. In other words, replacing the circles Ω_1 and Ω_2 in the above construction by their images under a homothety with center A has no effect on T. Obviously, $T(\Omega_1) = \Omega_2$.

Remark. We will count $\alpha > 0$ if the rotational part of T is counter-clockwise and $\alpha < 0$ otherwise.

To distinguish the line passing through two points, X and Y, on the plane and the segment between the points, let us denote the line by XY and the segment by $[XY]$. We will count the angle between two not parallel coplanar lines a_1 and a_2 as the angle α and denote it by $\widehat{a_1, a_2} = \alpha$, $\alpha > 0$ if the rotation around the point of their intersection by $(\alpha \bmod \pi)$ maps a_1 onto a_2. Clearly, $\widehat{a_1, a_2} = -\widehat{a_2, a_1}$ or $\widehat{a_1, a_2} = \pi - \widehat{a_2, a_1}$.

Lemma 5.1.1. *Let points $P \in \Omega_1$ and $P' = T(P) \in \Omega_2$. Then $B \in [PP']$.*

Proof. We will prove the statement if we show that $\widehat{PBA} + \widehat{ABP'} = \pi$.

Draw the chord in Ω_1 tangent to Ω_2 at B and denote the second endpoint of the chord by C (see Figure 5.1). The angle $\widehat{T(C)AC} = \alpha$, and $T(C) \in \Omega_2$.

Let $B' \in \Omega_2$ and BB' be tangent to Ω_1. Since the inscribed in Ω_1 angle $\widehat{CAB}$ subtends $[CB]$, and $[BB']$ is tangent to Ω_1 from the side of A, it is equal to the adjacent to $\widehat{B'BC} = \pi - \alpha$. So $\widehat{CAB} = \alpha$. Therefore, $B = T(C)$.

Further, $T(\triangle CPA) = \triangle BP'A \Rightarrow \widehat{ACP} = \widehat{ABP'}$, (because T is conformal). Also $\widehat{ACP} = \pi - \widehat{PBA}$, since $\widehat{ACP}$ and $\widehat{PBA}$ are inscribed in Ω_1 angles subtending the same arc from different sides. Hence, $\widehat{PBA} + \widehat{ABP'} = \pi$. $\square$

In this Section, we consider special relation between similar triangles called homology. We will call the sides of similar triangles opposing the same angles *corresponding or proportional sides.*

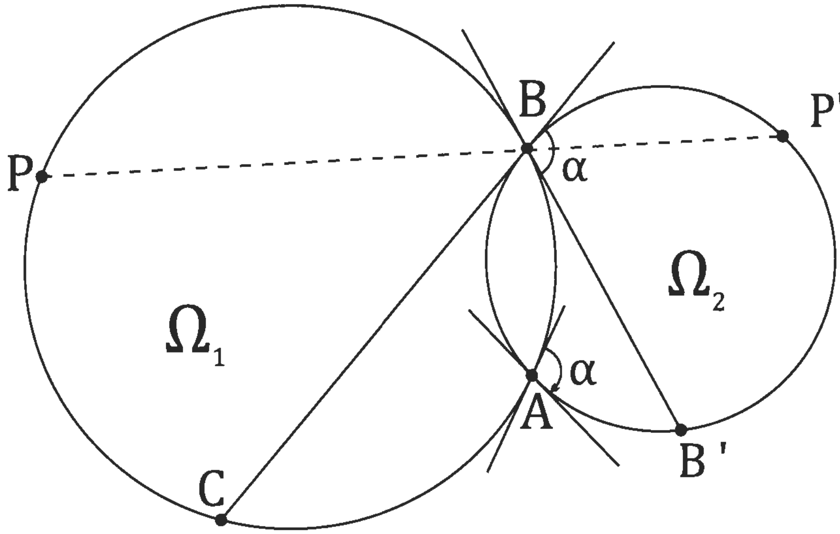

Figure 5.1: To Lemma 5.1.1.

Definition 5.1.2. *We will call two similar triangles homological if the lines joining vertices with same angles are concurrent. The concurrency point is called the center of homology.*

Definition 5.1.3. *Two homological similar triangles are called perspective if the corresponding sides are not parallel.*

Theorem 5.1.4. (Desargues Theorem) *Let $\triangle ABC$ and $\triangle abc$ be two distinct triangles. Then the lines Aa, Bb and Cc are concurrent if and only if the points $AB \cap ab$, $AC \cap ac$ and $BC \cap bc$ are collinear.*

The Desargues Theorem gives rise to an equivalent definition for similar perspective triangles.

Definition 5.1.5. *Two similar triangles with sides $\{A_i\}_{i=1}^3$ and $\{a_i\}_{i=1}^3$ respectively are called perspective if there are permutations $\{i_1, i_2, i_3\}$ and $\{j_1, j_2, j_3\}$ such that $\frac{|A_{i_k}|}{|a_{j_k}|} = const$ and the points $\tilde{A}_{i_k} \cap \tilde{a}_{j_k}$ are collinear, $k = 1, 2, 3$, where $\tilde{A}_{i_k}$ and $\tilde{a}_{j_k}$*

are lines containing the corresponding sides. The line, passing through the points $\tilde{A}_{i_k} \cap \tilde{a}_{j_k}$, $k = 1, 2, 3$, is called the axis of homology of the two triangles.

Lemma 5.1.6. *Let triangle $\triangle P$ be inscribed in Ω_1. Then $T(\triangle P)$ and $\triangle P$ are similar perspective, and $T(\triangle P)$ is inscribed in Ω_2.*

Proof. $\triangle P$ and $T(\triangle P)$ are homological and B is the center of homology by Lemma 5.1.1, and the vertices of $T(\triangle P)$ lie on Ω_2.

Further, since T is conformal, $\triangle P$ and $T(\triangle P)$ are similar. Finally, since $A \neq B$, we have: $\alpha \in (0, \pi)$, and hence the corresponding sides of the triangles are not parallel.□

Lemma 5.1.7. *Let a triangle $\triangle P$ be inscribed in Ω_1. Let $A, A^* \in \Omega_1$. Consider two maps T=$T_A[\alpha, R]$ and $T^* = T_{A^*}[\alpha, R]$, $R \geq 0$. Then $T(\triangle P)$ and $T^*(\triangle P)$ are congruent, and their corresponding sides are parallel.*

Proof. Congruence of the images of the triangle and parity of their corresponding sides follow from the equality of the rotations and ratios of homothety of T and T^*.□

Theorem 5.1.8. (Generalization of Simson's Theorem[1]) *Let $\triangle P$ be a triangle inscribed in a circle Ω_1 and let $\triangle P^* = L_\alpha(\triangle P)$, where $L_\alpha, |\alpha| \leq \pi$ is a rotation around the center of Ω_1. If we draw lines passing through A and parallel to the sides of $\triangle P^*$, then the points of intersection of those lines with the sides of $\triangle P$ are collinear.*

Proof. Let $T = T_A[\alpha, R]$, $R = \frac{R_2}{R_1} \neq 0$ be a rotational homothety with respect to A. By Lemma 5.1.6, $T(\triangle P)$ and $\triangle P$ are similar perspective.

Fixing α and approaching $R_2 \to 0$, we merge the center of the rotational homothety and the center of homology, simultaneously shrinking $T(\triangle P)$ into a point. □

Remark. Thus, Theorem 5.1.8 is the limiting case of Lemma 5.1.6 when $R_2 \to 0$.

[1]The Simson's Theorem states: Let points N, K, L be the feet of perpendiculars dropped from a point on a circle to sides of a triangle, inscribed into the circle. Then N, K, L are collinear. The line passing through them is called *Wallace-Simson line* (in some sources just *Simson line*) [20].

Definition 5.1.9. *A line passing through the intersection points described in* 5.1.8 *we will call Generalized Simson's Line and denote by* $GSL(A, \alpha, \triangle P)$, *where* $A \in \Omega_1$ *is the concurrency point,* $\triangle P$ *is the triangle of consideration and* α *is the angle of rotation of* $\triangle P$.

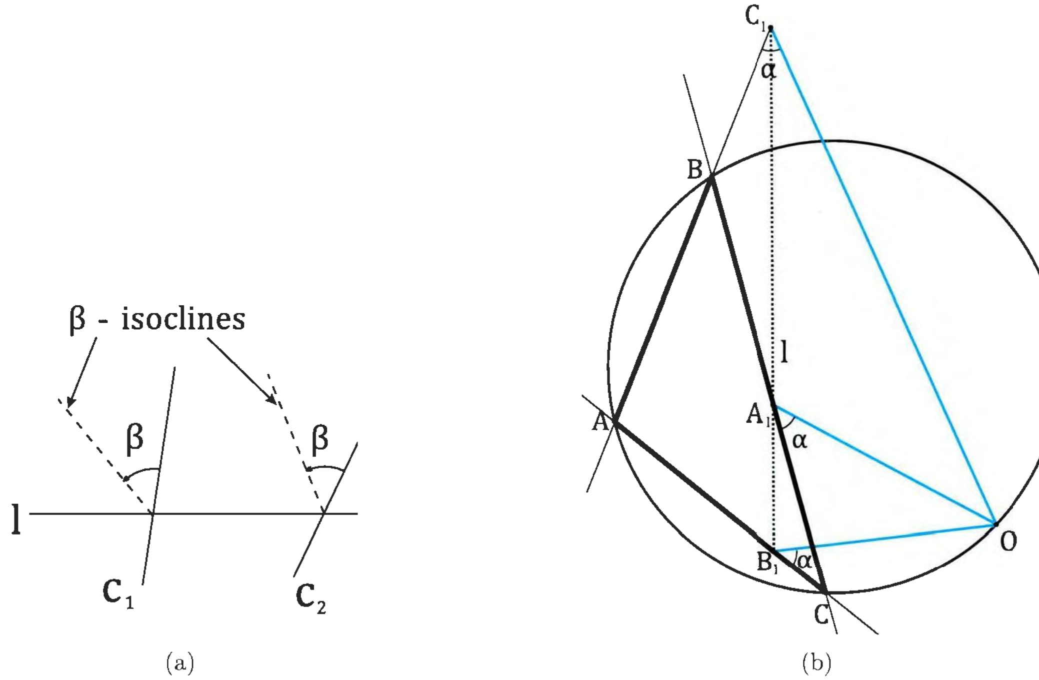

Figure 5.2: (a) β-isoclines to lines c_1 and c_2 along a line l; (b) construction of $l = GSL(O, \alpha, \triangle ABC)$.

Definition 5.1.10. *Let* Π *be plane,* $a_i \in \Pi$ *be a set of lines,* $i = 1, 2, \ldots$ *Lines* $b_{i_n} \in \Pi$ *are called* α*-isoclines to* a_i *if* $\widehat{a_i, b_{i_n}} = \alpha$, $n, i \in \mathbb{N}$. *The points* $a_i \cap b_{i_n}$ *are called vertices of* α*-isoclines.*

An example of β-isoclines to two lines c_1 and c_2 with vertices along line l is show in Figure 5.2(a).

Let Ω be a circle circumscribed around a triangle $\triangle ABC$ and a point $O \in \Omega$. Let

$l^* = GSL(O, \alpha, \triangle ABC)$ and let $l \not\parallel AB, l \not\parallel BC,\ l \not\parallel AC$. Finally, introduce the family of lines parallel to l: $L' = \{l' |\ l' \parallel l,\ l' \neq l\}$.

Lemma 5.1.11. *Let α-isoclines to the sides of $\triangle ABC$ at the points of their intersections with a line $l' \in L'$ intersect pairwise in points A'', B'', C''. Triangles $\triangle ABC$ and $\triangle A''B''C''$ are similar perspective. The center of homology is O.*

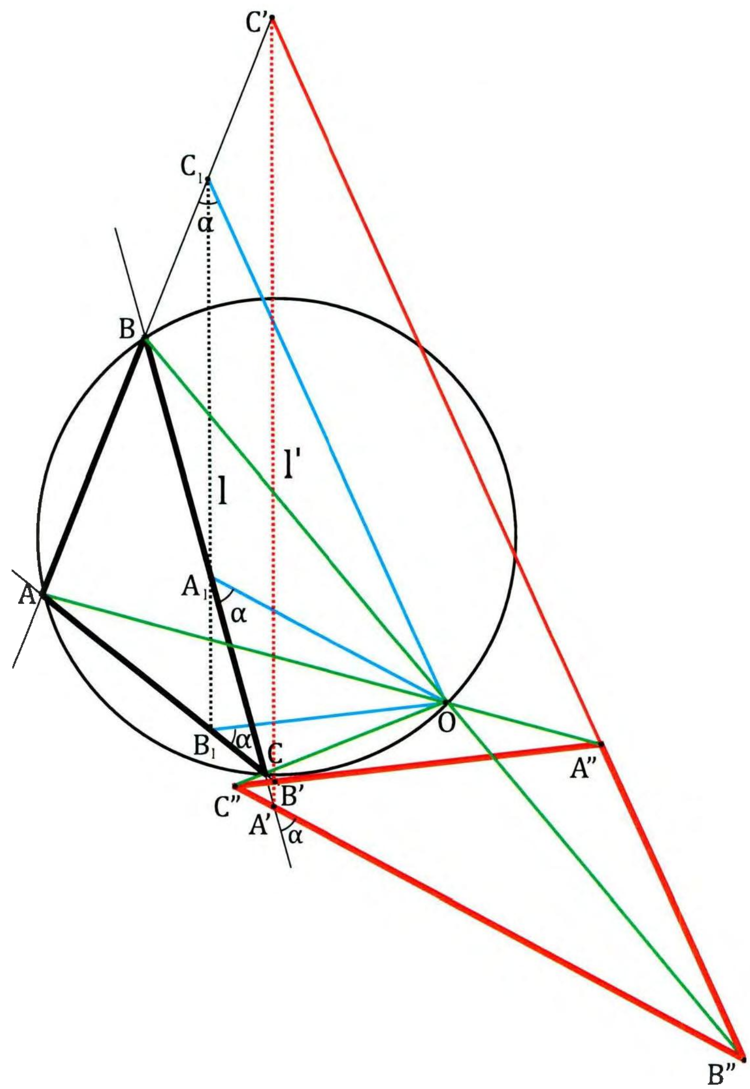

Figure 5.3: To Lemma 5.1.11.

Proof. Denote the points $l \cap AB = C_l$, $l \cap BC = A_l$, $l \cap AC = B_l$. We have OA_l, OB_l, OC_l are α-isoclines to BC, AC and AB respectively as it is in Figure 5.2(b). Choose a point $A' \in BC$ such that $A' \neq A_l$ and draw the line passing through A' and parallel to OA_l. Denote by B'' the point of intersection of this line and OB. Draw the line parallel to OC_l and passing through B'', denoting the intersection point of these lines by C'. Draw also the line $l' \in L'$, passing through A', as it is shown in Figure 5.3. Now, we have:

$\triangle BC_lO \sim \triangle BC'B''$, since all sides are parallel.

$\triangle BA_lO \sim \triangle BA'B''$ for the same reason.

Therefore, $\frac{|BO|}{|BB''|} = \frac{|BA_l|}{|BA'|} = \frac{|BC_l|}{|BC'|}$. The latter equality implies that $A'C' = l'$.

Since $\widehat{BA'B''} = \widehat{BC'B''} = \pi - \alpha$, B'' is the intersection point of corresponding isoclines to AB and BC at points of their intersections with l'. By construction $B'' \in OB$.

Set $l' \cap AC = B'$. Repeating the same chains of reasoning and construction routines with α-isocline to AC at B', that is, the line parallel to OB_l and passing through B', we will get that it intersects $C'B''$ and $A'B''$ at some points lying on OA and OC. Denote the points by A'' and C'' respectively. Hence, by construction, the triangles $\triangle ABC$ and $\triangle A''B''C''$ are homological, center of homology being at O.

Finally, $\triangle ABC \sim \triangle A''B''C''$, since we can make their corresponding sides parallel by rotation $\triangle A''B''C''$ by α around, for example, any of its vertices. □

Corollary 5.1.12. *Any two triangles, similar perspective to a given one, and constructed as in Lemma* 5.1.11 *with respect to two lines $l', l'' \in L'$, are homothetic with respect to O.*

Proof. By Lemma 5.1.11, the lines, passing through corresponding vertices of the two triangles are concurrent, the point of concurrency being O. The parity of the corresponding sides follows from the construction. □

Proposition 5.1.13. *Given a circle Ω, let $K, K' \in \Omega$, $\widehat{KK'} = \alpha$. Let a triangle $\triangle ABC$ be inscribed into Ω. Then for any $\beta \in \mathbb{R} \bmod \pi$, one of the angles between the lines $GSL(K, \beta, \triangle ABC)$ and $GSL(K', \beta, \triangle ABC)$ is $\frac{\alpha}{2}$.*

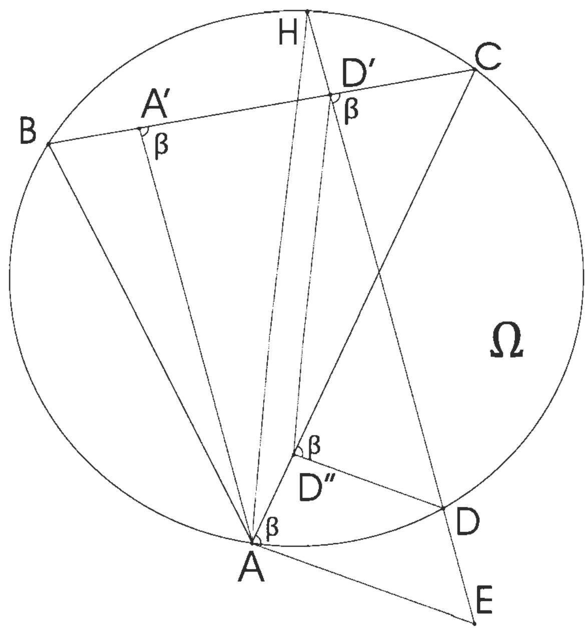

Figure 5.4: To Proposition 5.1.13.

Proof. Choose a point $D \in \Omega$ such that $D \notin \{A, B, C\}$ and choose $\beta \in R \bmod \pi$. Let points $D' \in BC$ and $A' \in BC$ be such that the angles $\widehat{AA'C} = \widehat{DD'C} = \beta$.

Denote the point $DD' \cap \Omega$ by H and find the points $E \in DD'$ and $D'' \in AC$ such that $\widehat{DD''C} = \widehat{CAE} = \beta$, see Figure 5.4.

Let us show that $D'D'' \| AH$.

Indeed, since $\widehat{DD''C} = \widehat{DD'C} = \beta$, we may circumscribe a circle around quadrangle $D''D'CD$. Therefore, $\widehat{D''CD} = \widehat{D''D'D}$ (inscribed angles subtending the same chord $(D'D'')$ from the same side). But $\widehat{AHD} = \widehat{D''CD}$, since they both are inscribed in Ω and subtend the same arc $\widehat{AC}$. Hence $\widehat{AHD} = \widehat{D''D'D}$.

On the other hand, $D'D'' = GSL(D, \beta, \triangle ABC)$ and $AA' = GSL(A, \beta, \triangle ABC)$. The angle between these two lines is equal to $\widehat{AHD}$, which is one half of the angular measure of $\widehat{AD}$.

The cases $D = A$ is trivial, and we may treat the cases when D coincides with either B or C as limiting cases for D approaching one of the two vertices, getting the same result.

Let us generalize the above mentioned. Consider two arbitrary taken points $K, K' \in \Omega$, and set $\widehat{AK} = \alpha$ and $\widehat{AK'} = \delta$. Obviously, $\widehat{K'K} = |\alpha - \delta|$.

Denote $l = GSL(K, \beta, \triangle ABC)$ and $l' = GSL(K', \beta, \triangle ABC)$. Then $\widehat{l, l'} = \widehat{l, AA'} - \widehat{l', AA'} = |\frac{\alpha}{2} - \frac{\delta}{2}| = \frac{1}{2}\widehat{KK'}$. $\square$

Let a triangle $\triangle ABC$ be inscribed in a circle Ω and $\alpha \in R \bmod \pi$. Let also L' be a family of parallel lines.

Lemma 5.1.14. *There exists a unique line $l^* \in L'$ such that α-isoclines to the lines AB, BC and AC at the points of their intersection with l^* are concurrent. The concurrency point lies on Ω.*

Proof. Consider first the case when L' is such that a line $l \in L'$ (generator of L') intersects each of the sides of $\triangle ABC$.

Given an α, take a point $D' \in \Omega$ and construct $GSL(D', \alpha, \triangle ABC)$. It will intersect a generator of L' under angles β and $\pi - \beta$. Let $D \in \Omega$ be such that $\widehat{DD'} = 2\beta$. By proposition 5.1.13, the angle between $GSL(D', \alpha, \triangle ABC)$ and $GSL(D, \alpha, \triangle ABC)$ will be β.

Hence, $GSL(D, \alpha, \triangle ABC)$ will either belong to L' or form angle 2β with its generator, depending on the direction of β-rotation of Ω mapping D' onto D. We will choose the first option, that is, D is such that $GSL(D, \alpha, \triangle ABC) \in L'$. Denote $GSL(D, \alpha, \triangle ABC)$ by l^*. Take a line $l \in L'$, $l \neq l^*$. But by Lemma 5.1.11, α-isoclines to the lines AB, BC and AC at the points of their intersection with l will not be concurrent. Thus l^* is the desired line by construction.

In case, when a generator of L' is parallel to one of the sides of $\triangle ABC$, the line l^* obviously coincides with that side since it is the only member of L', for which α-isoclines defined in this Lemma make sense. $\square$

Theorem 5.1.15. (Conditions of perspectivity for similar triangles). *Two similar triangles are perspective if and only if:*

(a) Their circumscribing circles intersect at two distinct points (A and B).

(b) A rotational homothety, centered at either A or B and mapping one of the circles onto another, maps also one of the triangles onto another.

If the center of homology is B then the center of rotational homothety is A and visa versa.

Proof. 1. The direct statement follows from Lemma 5.1.6.

2. To prove the converse, let us consider two similar perspective triangles $\triangle P_1$ and $\triangle P_2$ and let l be their axis of homology. Define the family of parallel lines L, generated by l.

Applying Lemma 5.1.14 to each of this triangles and L, we find that the triangles' homology center is one of the two points of intersection of the circles Ω_1 radius R_1 and Ω_2 radius R_2 circumscribed around $\triangle P_1$ and $\triangle P_2$ respectively. Denote this point by B, and another point of intersection of the circles by A. Thus, lines passing through corresponding vertices of $\triangle P_1$ and $\triangle P_2$ are concurrent at $B \in \Omega_1 \cap \Omega_2$.

By Lemma 5.1.1, $T_1 = T[A, \alpha, \frac{R_2}{R_1}]$ and $T_2 = T[A, -\alpha, \frac{R_1}{R_2}]$ are such that $T_1(\triangle P_1) = \triangle P_2$ and $T_2(\triangle P_2) = \triangle P_1$, where α is the properly signed outer angle of intersection of Ω_1 and Ω_2. $\square$

One may ask, 'What is the relationship between the topic of the thesis and the similar triangle questions?' The answer surprisingly comes from observation of the behaviour of the third iteration of an evolutoidal transform of the same smooth curve γ at the same point $X(\varphi)$, namely, the problem of finding the position of a point $X_{\theta_1\theta_2\theta_3}$ on

θ_3-evolutoid of θ_2-evolutoid of θ_1-evolutoid of γ, that is, on $\gamma_{\theta_1\theta_2\theta_3}$.

Since we have discovered before, that evolutoidal transformations commute, the order of application of the transforms is not important - the result will be the same. In other words, $X_{\theta_1\theta_2\theta_3} = X_{\theta_2\theta_1\theta_3} = X_{\theta_2\theta_3\theta_1} = ... = X_{\theta_3\theta_2\theta_1}$.

Following the construction described in Theorem 3.3.3, we get the Lemma.

Lemma 5.1.16. *The tangent line to $\gamma_{\theta_1\theta_2\theta_3}$ at $X_{\theta_1\theta_2\theta_3}$ is the axis of homology of two similar perspective triangles $\triangle X_{\theta_1}X_{\theta_2}X_{\theta_3}$ and $\triangle E_{\theta_1}E_{\theta_2}E_{\theta_3}$.*

Proof. Let us show, that the points $X_{\theta_1\theta_2} = X_{\theta_2\theta_1}$, $X_{\theta_1\theta_3} = X_{\theta_3\theta_1}$ and $X_{\theta_3\theta_2} = X_{\theta_2\theta_3}$ are collinear, and $X_{\theta_1\theta_2\theta_3}$ lies on the line passing through these points.

Consider any of the three points, say, $X_{\theta_1\theta_2}$, and the point $X_{\theta_1\theta_2\theta_3}$ on the curve $\gamma_{\theta_1\theta_2\theta_3}$. According to our construction, the line $X_{\theta_1\theta_2}X_{\theta_1\theta_2\theta_3}$ is tangent to $\gamma_{\theta_1\theta_2\theta_3}$ at $X_{\theta_1\theta_2\theta_3}$. By the same reason, $X_{\theta_1\theta_3}, X_{\theta_2\theta_3} \in X_{\theta_1\theta_2}X_{\theta_1\theta_2\theta_3}$.

By construction, the two triangles $\triangle X_{\theta_1}X_{\theta_2}X_{\theta_3}$ and $\triangle E_{\theta_1}E_{\theta_2}E_{\theta_3}$ are similar perspective with the center of homology at E, and the line passing through $X_{\theta_1\theta_2}, X_{\theta_2\theta_3}$ and $X_{\theta_1\theta_3}$ is their axes of homology. $\square$

Note that the positions of tangents to $\gamma_{\theta_1\theta_2\theta_3}$ depend only on radii of curvature of γ and its evolute.

Finally, we broadly used the notion of Simson's line, and the envelope of Simson's lines of a triangle is a deltoid. This amazing (though long known) property of Simson's lines will give us a good insight concerning deltoid's projections in Chapter 6.

Among the publications of many mathematicians, who studied similar perspective triangles by the early 20th century, the paper by Frank Wood [23] looks most resembling (but not identical) to our results in this Section (except Lemma 5.1.16), although the context and proofs are different. His attention was focused on special points of triangles (Miguel points) and the Desargues configuration arising from similar perspective triangles, while our focus is on Generalized Simson Lines.

5.2 The Homology Axis Theorem

In Chapter 3 we gave a synthetic construction of the second iteration of the evolutoidal transformation. In this Section we will describe a more involved construction of the third iteration based on the key Proposition 5.1.13 and Lemma 5.1.16.

Let the radius of curvature and its first two derivatives of a curve γ at a point X be R, R' and R''.

Consider the polygonal line with nodes at $X_{(\frac{\pi}{2})^i}$, $i = 0, ..., 3$, where $X_{(\frac{\pi}{2})^0} = X$. The first segment goes downward from $X_{(\frac{\pi}{2})^0}$ to $X_{(\frac{\pi}{2})^1}$. Draw the circles Ω_i, $i = 1, 2, 3$ based on the segments $[X_{(\frac{\pi}{2})^{i-1}}, X_{(\frac{\pi}{2})^i}]$ as their diameters. It is clear that $|X_{(\frac{\pi}{2})^{i-1}}, X_{(\frac{\pi}{2})^i}| = |R^{(i-1)}|$.

Different scenarios of the development of this polygonal line: cup-shaped, ladder-shaped (or degenerated versions of them) depend on the signs of R, R' and R'' (or they may be equal to zero). But we will often have to consider only one scenario, namely, $R, R'' > 0$, $R' < 0$, since the generalization on the case of arbitrary taken R, R', R'' comes naturally. Sometimes, we will use the old notations of centers of curvature, remembering $X_{(\frac{\pi}{2})^i} = E_{e^{i-1}}$, $i = 1, 2, ...$

Definition 5.2.1. *Given a chain of intersecting circles, Ω_1, $\Omega_2, ...,$ the iterational transformation $P_{i,i+1}$ of Ω_i onto Ω_{i+1} is a point-wise one-to-one mapping such that $\forall N \in \Omega_i$ the point $E_{e^{i-1}}$ lies on line passing through N and $P_{i,i+1}(N)$. Naturally, we will denote the result of k consecutive iterational transformations of the same point $M \in \Omega_i$ by $P_{i,i+k}(M)$.*

Remark. To avoid bulky notations, we will denote $P_{12}(X_{\theta_i})$ and $P_{13}(X_{\theta_j})$ by X'_{θ_i} and X''_{θ_j}. Clearly, $X'_\theta = X_{\theta\frac{\pi}{2}}$ and $X''_\theta = X_{\theta(\frac{\pi}{2})^2}$.

Lemma 5.2.2. *The center of curvature of curve $\gamma_{\theta_1\theta_2}$ at $X_{\theta_1\theta_2}$ lies on the intersection of lines $X'_{\theta_1}X'_{\theta_2}$ and $X''_{\theta_1}X''_{\theta_2}$.*

Proof. Take any $\theta_1, \theta_2 \in [0, \pi]$. Assume $\theta_1 \leq \theta_2$. Construct the circles Ω_1, Ω_2 and Ω_3, as they were described above in the beginning of this Section (see Figure 5.5), and the pairs of points $X_{\theta_1}, X_{\theta_2} \in \Omega_1$, $X'_{\theta_1}, X'_{\theta_2} \in \Omega_2$ and $X''_{\theta_1}, X''_{\theta_2} \in \Omega_3$.

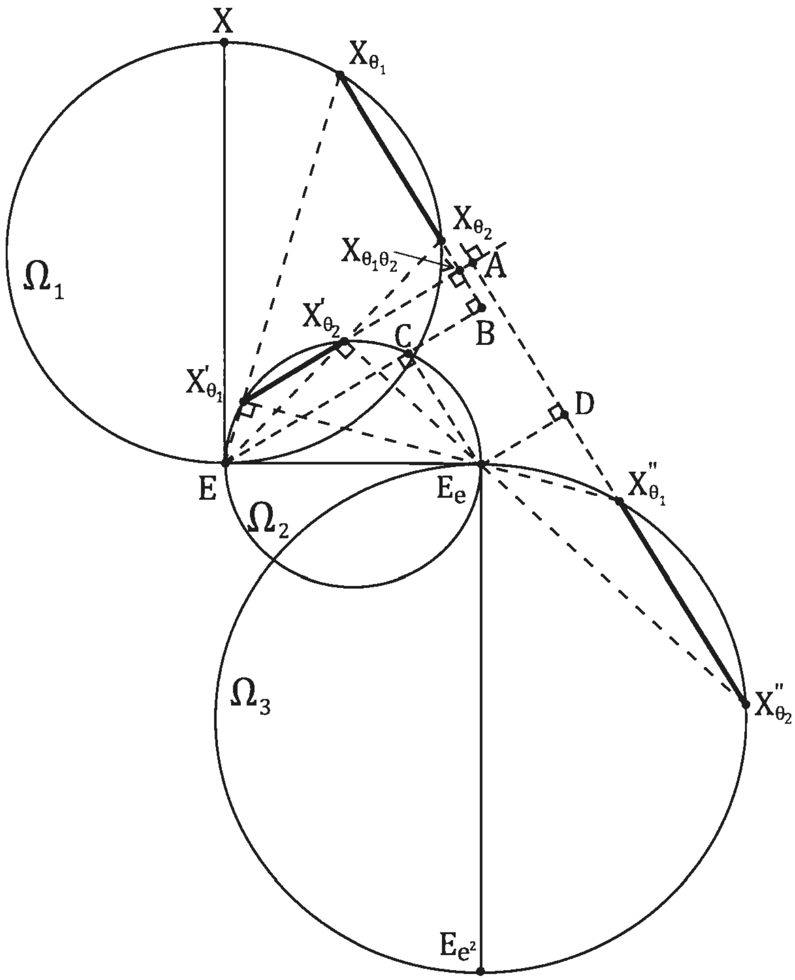

Figure 5.5: To Lemma 5.2.2

As it was proved in Theorem 3.3.3, the point $X_{\theta_1\theta_2} = X_{\theta_1}X_{\theta_2} \cap X'_{\theta_1}X'_{\theta_2}$. It is clear that $\gamma_{\theta_1\theta_2}$ is tangent to line $X_{\theta_1}X_{\theta_2}$ at $X_{\theta_1\theta_2}$, so the center of curvature of $\gamma_{\theta_1\theta_2}$ at $X_{\theta_1\theta_2}$, that is $E_{\theta_1\theta_2}$, lies on $X'_{\theta_1}X'_{\theta_2}$.

Continue line $X''_{\theta_1}X''_{\theta_2}$ up to the intersection with $X'_{\theta_1}X'_{\theta_2}$, denoting the intersection point by A, and drop perpendiculars from E to line $X_{\theta_1}X_{\theta_2}$, denoting the foot of the perpendiculars by B, and from E_e to lines EB and $X''_{\theta_1}X''_{\theta_2}$, denoting the feet of the perpendiculars by C and D respectively.

From $\triangle X_{\theta_1}EB$, we have $|EB| = Rc_{\theta_1}c_{\theta_2}$.

From $\triangle ECE_e$, we have $\widehat{CE_eE} = \theta_1 + \theta_2$, hence $|EC| = R'\sin(\theta_1 + \theta_2)$.

Finally, from $\triangle P_{13}(X_{\theta_2})DE_e$, we obtain $|E_eD| = R''s_{\theta_1}s_{\theta_2}$.

Clearly, $|X_{\theta_1\theta_2}A| = ||BC| - |E_eD||$, which brings us to the desired result after expanding the absolute value signs. □

Corollary 5.2.3. *Let $\alpha \in [0, \pi]$ be a fixed constant. Then the locus of the centers of curvature of the curves $\{\gamma_{\theta(\theta+\alpha)}\}_{\theta=0}^{\pi}$ at points $\{X_{\theta(\theta+\alpha)}\}_{\theta=0}^{\pi}$ respectively, is a limaçon of Pascal. In particular, when $\alpha = 0$ the locus is a cardioid.*

Proof. The lines $X'_\theta X'_{\theta+\alpha}$ and $X''_\theta X''_{\theta+\alpha}$ are perpendicular to each other and tangent to the circles C_2 and C_3 concentric to Ω_2 and Ω_3 respectively. The radii of the circles C_2 and C_3 depend on α. The sought locus and the locus $\{X'_\theta X'_{\theta+\alpha} \cap X''_\theta X''_{\theta+\alpha}\}_{\theta=0}^{\pi}$ coincide by Lemma 5.2.2. If $\alpha = 0$, the sought locus is the locus of intersections of corresponding tangents to Ω_2 and Ω_3 at points X'_θ and X''_θ respectively. Then the statement follows from Theorems 3.4.7 and 3.4.10. □

The results obtained in Section 5.1 suggest an interesting construction of the third iteration.

Theorem 5.2.4. (Homology Axis theorem). *Consider $\theta_1, \theta_2, \theta_3 \in [0, \pi]$ and two pairs of similar perspective triangles (degenerated cases when $\theta_i = \theta_j$ for some $i \neq j$ should be treated as limiting):*

1. $\triangle X_{\theta_1}X_{\theta_2}X_{\theta_3}$ and $\triangle X'_{\theta_1}X'_{\theta_2}X'_{\theta_3}$ with the axis of homology l_1,

2. $\triangle X''_{\theta_1}X''_{\theta_2}X''_{\theta_3}$ and $\triangle X'_{\theta_1}X'_{\theta_2}X'_{\theta_3}$ with the axis of homology l_2.

The point $X_{\theta_1\theta_2\theta_3} \in \gamma_{\theta_1\theta_2\theta_3}$ is the intersection point of l_1 and l_2.

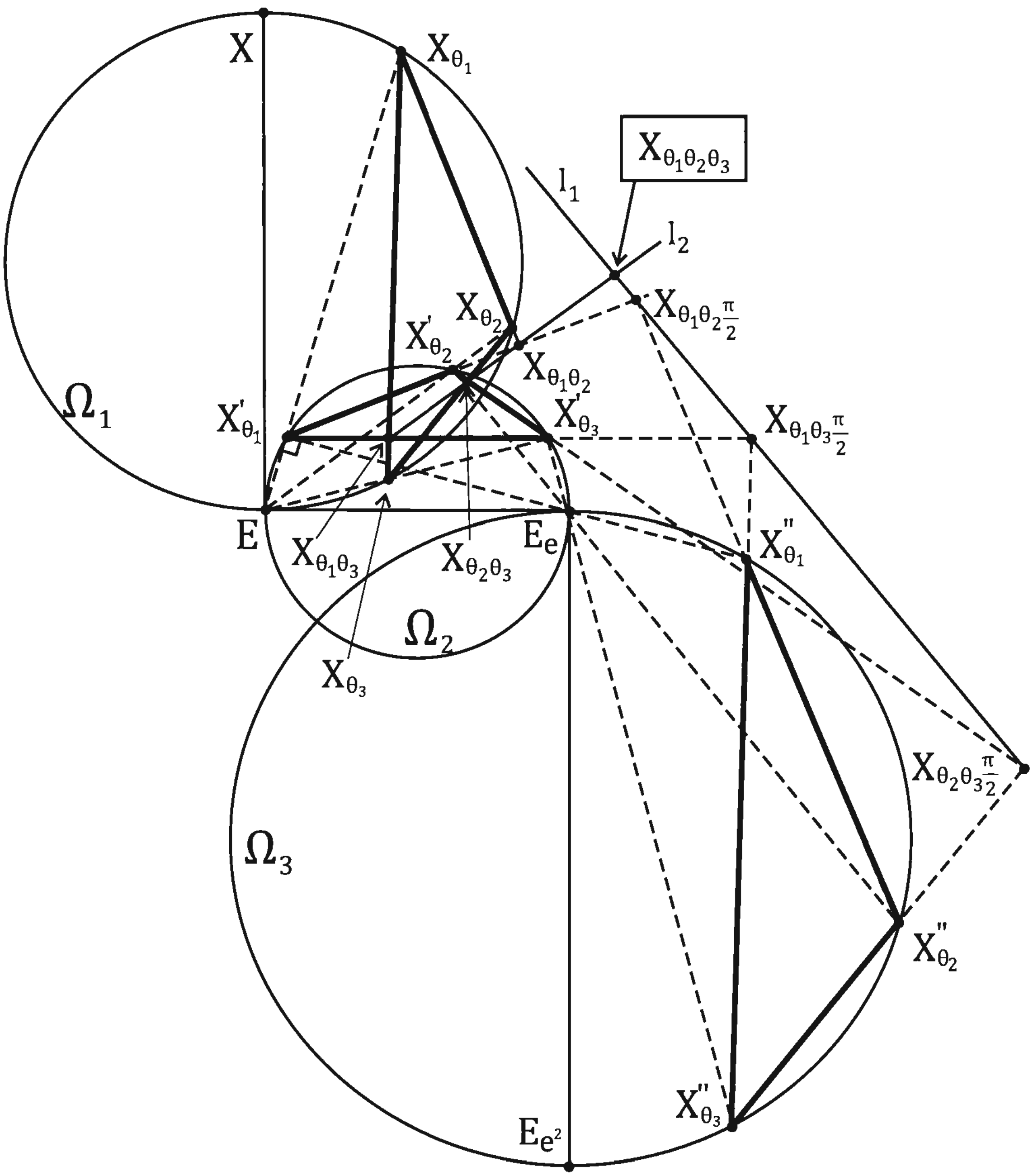

Figure 5.6: To Theorem 5.2.4

Proof. Denote $\triangle X_{\theta_1}X_{\theta_2}X_{\theta_3}$, $\triangle X'_{\theta_1}X'_{\theta_2}X'_{\theta_3}$, $\triangle X''_{\theta_1}X''_{\theta_2}X''_{\theta_3}$ by $\triangle_1$, $\triangle_2$, $\triangle_3$ respectively (Figure 5.6). Let their circumcircles be Ω_i of radii R_i respectively.

If we apply homothety H_E centered at E with ratio $\frac{R_3}{R_1}$ to Ω_1, then the homology axis of $H_E(\triangle_1)$ and $\triangle_2$ will be parallel to l_1 by Lemma 5.1.12 and perpendicular to l_2 by Lemma 5.1.13, since $\widehat{EE_e} = \pi$. Therefore, $l_2 \perp l_1$.

Since l_1 is tangent to $\gamma_{\theta_1\theta_2\theta_3}$ at $X_{\theta_1\theta_2\theta_3}$ by Lemma 5.1.16, then by the construction of θ_3-evolutoid of $\gamma_{\theta_1\theta_2}$, the point $X_{\theta_1\theta_2\theta_3}$ is the foot of the perpendicular dropped from the center of curvature of $\gamma_{\theta_1\theta_2}$, that is $E_{\theta_1\theta_2}$, to l_1. But by Lemma 5.2.2, $E_{\theta_1\theta_2} \in l_2$. Hence, $X_{\theta_1\theta_2\theta_3} = l_2 \cap l_1$. $\square$

Thus, the axis of homology of $\triangle_2$ and $\triangle_3$ is normal, whereas that of $\triangle_2$ and $\triangle_1$ is tangent to $\gamma_{\theta_1\theta_2\theta_3}$ at $X_{\theta_1\theta_2\theta_3}$.

Chapter 6

The 3rd iteration: Image-sets

In the previous chapter we were concerned with the construction of individual positions of points under the third iteration, and in this chapter we study their collective properties as the parameters $\theta_{1,2,3}$ vary.

6.1 The Cayley Sextic Normal Front Theorem

Let us consider a few simple triples of (R, R', R'') and find the shapes of Γ_3 determined by the triples, denoting such Γ_3 by $\Gamma_3(R, R', R'')$. If we are only concerned about the shape of $\Gamma_3(R, R', R'')$, we use the homogeneous coordinate notation $\Gamma_3(R : R' : R'')$. Many of the shapes can be described as or related to sinusoidal spirals, hence we begin with a definition of these curves.

We will use the notations $\sin\theta = s,\ cos\theta = c,\ \sin k\theta = s_k,\ \cos k\theta = c_k$ in this Section.

Definition 6.1.1. *The sinusoidal spirals are a family of curves defined by the equation in polar coordinates*

$$r^n = a^n \cos(n\theta), \tag{6.1.1}$$

where a is a non-zero constant and n is a rational number other than 0. We will call *n the order of the spiral.*

Note, that according to the definition, a circle and a cardioid are sinusoidal spirals of orders 1 and $\frac{1}{2}$ respectively.

Definition 6.1.2. *A Cayley sextic is a sinusoidal spiral of the order* $\frac{1}{3}$. (Figure 6.1(a))

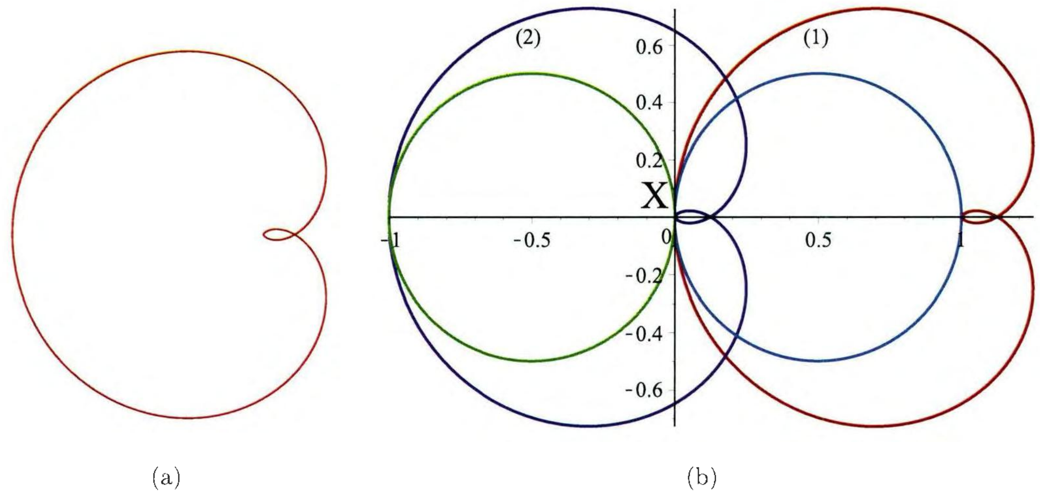

Figure 6.1: (a) a Cayley sextic; (b) to Lemma 6.1.3: Cayley sextics and the circles whose second pedals with respect to the origin they are (1) The curve $\Gamma_3(1,0,0)$, (2) The curve $\Gamma_3(0,0,1)$.

Then it is straightforward to establish the following results.

Lemma 6.1.3. *The curves $\Gamma_3(0,0,1)$ and $\Gamma_3(1,0,0)$ are congruent Cayley sextics, each symmetric with respect to line XE, point X and E being their poles respectively.*

Proof. Let us calculate R_θ and R_{θ^2} for (R, R', R'')=(0,0,1) and then plug them in equations (4.2.5).

We have: $R_{\theta^0} = R = 0$, $R_\theta = Rc - R's = 0$, $R_{\theta^2} = Rc^2 - 2scR' + R''s^2 = s^2$. Then

$$\begin{cases} x = R''s^3 s_3 \\ y = R''s^3 c_3. \end{cases} \tag{6.1.2}$$

On the other hand, the parametric equations of Cayley sextic are:

$$\begin{cases} x = \cos t \cos^3 \frac{t}{3} \\ y = \sin t \cos^3 \frac{t}{3} \ . \end{cases}$$

Substituting $\theta = \frac{t}{3} + \frac{\pi}{2}$, we get the desired result.

Let us take a different look at the construction of $\Gamma_3(0,0,1)$. It is clear, $\Gamma_2(0,0)$ is point X. Then by Lemma 4.2.9 $\Gamma_3(0,0,1)$ is the pedal curve of the cardioid representing the image-set of the second iteration of $E \in \gamma_{\frac{\pi}{2}}$ with respect to its cusp, which was just proven to be Cayley sextic with the same pole and axes of symmetry. By the same reason, $\Gamma_3(1,0,0)$ is the pedal curve of the cardioid $\Gamma_2(1,0)$ with respect to its cusp, point E. The congruence of $\Gamma_3(0,0,1)$ and $\Gamma_3(1,0,0)$ is obvious, since they both are double pedal for the same size circles (Figure 6.1(b)). ☐

Thus, by the way, we have proven a well-known relationship between Cardioids and Cayley sextic: *the pedal curve of a cardioid with respect to its cusp is Cayley sextic.*

Lemma 6.1.4. *The curve $\Gamma_3(1,0,1)$ is a circle (double circle) of radius $\frac{3}{4}$ centered at $(\frac{3}{4},0)$.*

Proof. We have $R_{\theta^0} = R = 1$, $R_\theta = Rc - R's = c$, $R_{\theta^2} = Rc^2 - 2scR' + R''s^2 = 1$. Then

$x = s(s+cs_2+s_3) = s(s+2(1-s^2)s+(1-2s^2)s+2(1-s^2)s) = 6s(s-s^3) = 6s^2c^2 = \frac{3}{2}s_2^2$,

and

$y = s(c+cc_2+c_3) = s(c+c(2c^2-1)+c(2c^2-1)+2c(1-c^2)) = sc(6c^2-3) = \frac{3}{2}s_2c_2$.

Clearly, the set of points with coordinates $(\frac{3}{2}s_2^2, \frac{3}{2}s_2c_2)$ is the desired circle (Figure 6.2(a)) passed twice as θ runs from 0 to π. ☐

Note that coordinates of points of $\Gamma_3(1,0,1)$ are sums of coordinates of points of

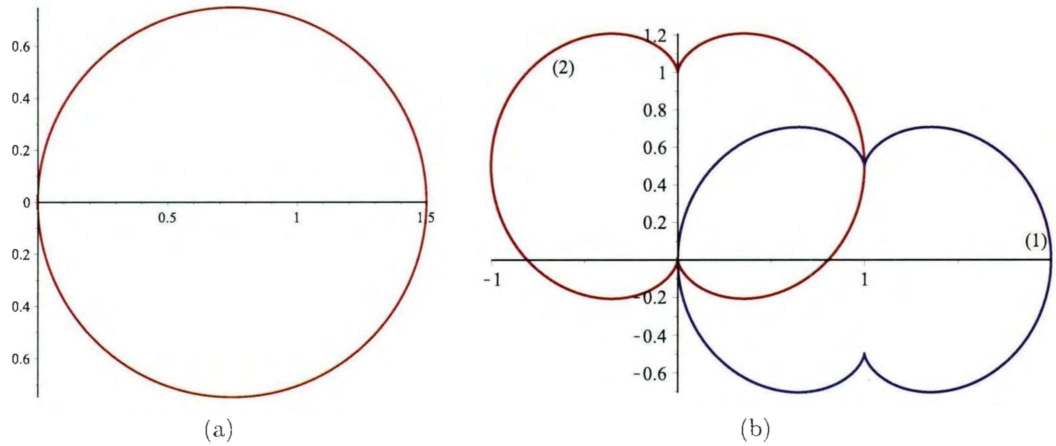

Figure 6.2: (a) To Lemma 6.1.4: the double circle curve $\Gamma_3(1,0,1)$; (b) to Lemma 6.1.6. Two congruent nephroids: (1) The curve $\Gamma_3(1,0,-1)$, (2) The curve $\Gamma_3(0,1,0)$.

$\Gamma_3(1,0,0)$ and $\Gamma_3(0,0,1)$ corresponding the same values of θ. So, we may formally write $\Gamma_3(1,0,1) = \Gamma_3(1,0,0) + \Gamma_3(0,0,1)$.

Definition 6.1.5. *The trajectory traced by a fixed point on a circle of radius R, which rolls with no friction over a fixed circle of radius $2R$, is a nephroid.* [14] *Parametric equations for the nephroid, with cusps on the x-axis, are given by*

$$x = R(3\cos t - \cos 3t), \quad y = R(3\sin t - \sin 3t). \tag{6.1.3}$$

When the cusps lie on the y-axis, parametric equations are given by

$$x = R(3\cos t + \cos 3t), \quad y = R(3\sin t + \sin 3t). \tag{6.1.4}$$

The moving circle is called a generating circle.

Lemma 6.1.6. *Curves $\Gamma_3(1,0,-1)$ and $\Gamma_3(0,1,0)$ are two congruent nephroids.*

Proof. Consider first $\Gamma_3(0,1,0)$. We have $R_{\theta^0} = R = 0$, $R_\theta = Rc - R's = -s$, $R_{\theta^2} = Rc^2 - 2scR' + R''s^2 = -2sc$. Then:

$$\begin{cases} x = -s^2 s_2 - 2s^2 c s_3 = -s^2(s_2 + 2cs_3) \\ y = -s^2 c_2 - 2s^2 c c_3 = -s^2(c_2 + 2cc_3). \end{cases}$$

Applying rotation of axes by $\frac{\pi}{2}$ and their reflection with respect to y-axis, we get

$x' = s^2 c_2 + 2s^2 cc_3 = \frac{1}{2}(1 - c_2)c_2 + (1 - c_2)cc_3 = \frac{c_2}{2} - \frac{c_2^2}{2} + cc_3 - cc_2c_3 = \frac{c_2}{2} - \frac{1}{4} - \frac{c_4}{4} + \frac{c_2}{2} + \frac{c_4}{2} - \frac{c_2^2}{2} - \frac{c_2c_4}{2} = -\frac{1}{4} + c_2 + \frac{c_4}{4} - \frac{1}{4} - \frac{c_4}{4} - \frac{c_2}{4} - \frac{c_6}{4} = -\frac{1}{2} + \frac{3}{4}c_2 - \frac{1}{4}c_6.$

An analogous routine leads to

$y' = \frac{3}{4}s_2 - \frac{1}{4}s_6.$

Now, the curve $\Gamma_3(1, 0, -1)$ is treated by the same means. We have $R_{\theta^0} = 1$, $R_\theta = c$, $R_{\theta^2} = c_2$. Then, applying reflection with respect to y-axis:

$x' = -s^2 - css_2 - c_2ss_3 = -\frac{1}{2} + \frac{c_2}{2} - \frac{s_2^2}{2} - \frac{c_2^2}{2} + \frac{c_2c_4}{2} = -1 + \frac{3}{4}c_2 + \frac{1}{4}c_6.$

By the same means

$y' = cs + csc_2 + c_2sc_3 = \frac{3}{4}s_2 + \frac{1}{4}s_6.$

Thus both curves are nephroids (Figure 6.2(b)) with generating circles of radius $\frac{1}{4}$.□

Definition 6.1.7. *A parallel of a curve (or a parallel curve) is the envelope of a family of congruent circles centered on the curve. It can also be defined as a curve whose points are at a fixed normal distance from a given curve (a normal front of a curve).* [14]

Clearly, parallel curves have the same evolute, which is the envelope of their normals. The alternative definition of evolute of a curve Γ is the following: *The locus of cusps of curves parallel to Γ is its evolute.* So when a parallel curve touches the evolute, it has a singularity (generically, it forms a cusp). An example of a family of parallel curves is shown in Figure 6.3.

Lemma 6.1.8. *A curve $\Gamma_3(r_1, 0, r_2)$, $r_1, r_2 \in \mathbb{R}$ has a shape of a normal front of a Cayley sextic.*

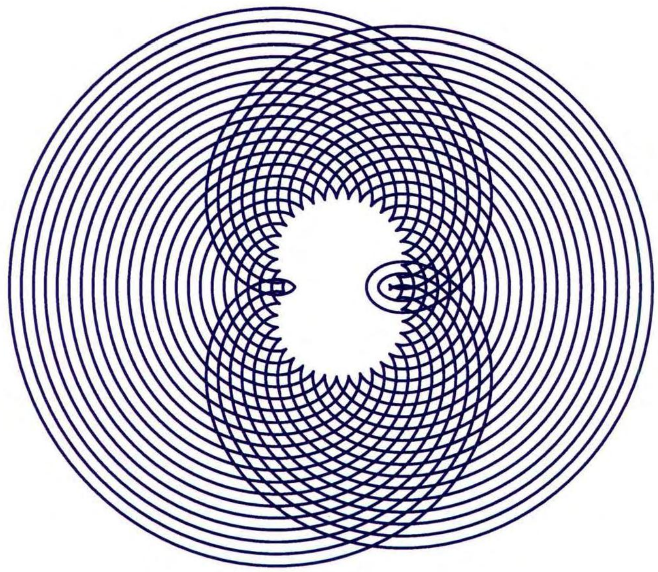

Figure 6.3: A family of curves parallel to a Cayley sextic. The Cayley sextic is the rightmost curve (bold). Note that the cusps of these curves lie on the evolute of the Cayley sextic (a nephroid) in the middle.

Proof. Routinely, we get $R_{\theta^0} = r_1$, $R_\theta = r_1 c$, $R_{\theta^2} = c^2 r_1 + s^2 r_2 = r_1 + s^2(r_2 - r_1)$, and then calculate the coordinates of X_{θ^3} using the results obtained in Lemmas 6.1.4 and 6.1.3:

$$\begin{cases} x = r_1 s^2 + r_1 c s s_2 + r_1 s s_3 + (r_2 - r_1)s^3 s_3 = \frac{3}{2} r_1 s_2^2 + (r_2 - r_1)s^3 s_3 \\ y = r_1 + r_1 c s c_2 + r_1 s c_3 + (r_2 - r_1)s^3 c_3 = \frac{3}{2} r_1 s_2 c_2 + (r_2 - r_1)s^3 c_3. \end{cases} \tag{6.1.5}$$

Thus, $\vec{X}_{\theta^3} = \frac{3}{2} r_1 (s_2^2, s_2 c_2) + (r_1 - r_2)(s^3 s_3, s^3 c_3)$ in our coordinate system. The second term represents a radius-vector of $\Gamma_3(0, 0, r_1 - r_2)$, which is a Cayley sextic. Let us modify the first term:

$\frac{3}{2} r_1 (s_2^2, s_2 c_2) = \frac{3}{4} r_1 (1 - c_4, s_4) = \frac{3}{4} r_1 (1, 0) - \frac{3}{4} r_1 (c_4, -s_4)$.

By Lemma 4.2.2, the tangent vector to $\Gamma_3(0, 0, r_1 - r_2)$ at X_{θ^3} is (s_4, c_4), and then the vector $\frac{3}{4} r_1 (c_4, -s_4)$ is normal to $\Gamma_3(0, 0, r_1 - r_2)$ at X_{θ^3}. Besides, it has constant length.

Thus, to obtain $\Gamma_3(r_1, 0, r_2)$, we have to first translate by constant vector $(\frac{3}{4}r_1, 0)$ each point of Cayley sextic, representing $\Gamma_3(0, 0, r_2 - r_1)$, and then translate it by $\frac{3}{4}r_1$ toward the corresponding center of curvature by $\frac{3}{4}r_1$. $\square$

Lemma 6.1.9. *A curve* $\Gamma_3(r_1, r_2, -r_1)$, $r_1, r_2 \in \mathbb{R}$ *is a nephroid.*

Proof. Consider $\Gamma_3(r_1, r_2, -r_1)$, $r_1, r_2 \in \mathbb{R}$. Without loss of generality, we may assume $r_2, r_1 \neq 0$ (the case $r_1 = 0$ or $r_2 = 0$ were considered in Lemma 6.1.6). We have:

$$\Gamma_3(r_1, r_2, -r_1) = \Gamma_3(0, r_2, 0) + \Gamma_3(r_1, 0, -r_1), \tag{6.1.6}$$

By the same Lemma, $\Gamma_3(0, r_2, 0)$ has equations:

$$\begin{cases} x = r_2(1 - \frac{3}{4}c_2 - \frac{1}{4}c_6) \\ y = r_2(\frac{3}{4}s_2 + \frac{1}{4}s_6). \end{cases}$$

and $\Gamma_3(r_1, 0, -r_1)$ has equations:

$$\begin{cases} x = r_1(-\frac{3}{4}s_2 + \frac{1}{4}s_6) \\ y = r_1(\frac{1}{2} - \frac{3}{4}c_2 + \frac{1}{4}c_6). \end{cases}$$

Therefore, the equations of $\Gamma_3(r_1, r_2, -r_1)$ are:

$$\begin{cases} x = \frac{1}{4}(4r_2 - 3(r_2c_2 + r_1s_2) - (r_2c_6 - r_1s_6)) \\ y = \frac{1}{4}(2r_1 + 3(r_2s_2 - r_1c_2) + (r_2s_6 + r_1c_6)). \end{cases} \tag{6.1.7}$$

Denote $\arcsin \frac{r_2}{\sqrt{r_1^2+r_2^2}} = \beta$ and $\frac{1}{4}\sqrt{r_1^2+r_2^2} = C$. Then rewrite equations (6.1.7):

$$\begin{cases} x = C(4r_2 - 3\sin(2\theta + \beta) + \sin(6\theta - \beta)) \\ y = C(2r_1 - 3\cos(2\theta + \beta) + \cos(6\theta - \beta)). \end{cases} \tag{6.1.8}$$

Now, setting $\theta = \theta' + \frac{\beta}{2}$, we obtain:

$$\begin{cases} x = C(4r_2 - 3\sin(2\theta' + 2\beta) + \sin(6\theta' + 2\beta)) \\ y = C(2r_1 - 3\cos(2\theta' + 2\beta) + \cos(6\theta' + 2\beta)). \end{cases} \tag{6.1.9}$$

Therefore, the curve $\Gamma_3(r_1, r_2, -r_1)$ is a nephroid with the segment, connecting the cusps, rotated by 2β clockwise. $\square$

Theorem 6.1.10. *A curve Γ_3 has a shape of a curve parallel to a Cayley sextic.*

Proof. Consider the parallels to the Cayley sextic representing $\Gamma_3(0, 0, 2)$ translated by $\frac{3}{4}r_1$ along x-axis. One of its normal fronts is the nephroid $\Gamma_3(1, 0, -1)$ by Lemma 6.1.8. Let us take any $\theta \in [0, \pi]$ and consider a pair of points X_{θ^3} and $X_{(\theta+\frac{\pi}{2})^3}$ of the nephroid. The two points have been displaced from their counterparts on the Cayley sextic along parallel lines in the same direction, since $(\cos 4\theta, -\sin 4\theta) = (\cos 4(\theta + \frac{\pi}{2}), -\sin 4(\theta + \frac{\pi}{2}))$. The vector of further development of the front for one of the points is directed inside the nephroid, for the other - outside. Hence, we can *define*[1] *a normal front of Cayley sextic as the normal fronts of two opposite arcs of a nephroid, with endpoints in its cusps*[2]*, the points of one of the arcs being displaced toward, and the points of the other - away from, corresponding centres of curvature by the same distance. The cusps' displacement direction is treated as limiting.*

[1]What we are defining is actually a description of an involute of a nephroid. [5, Ch.9̃]
[2]We will call these arcs main arcs of a nephroid.

Now, consider $\Gamma_3(R, R', R'')$. Denote $(R, R', R'') = (r_1, r_2, r_3)$. We have:

$$\Gamma_3(r_1, r_2, r_3) = \Gamma_3(\frac{1}{2}r_1 - \frac{1}{2}r_3, r_2, \frac{1}{2}r_3 - \frac{1}{2}r_1) + \Gamma_3(\frac{1}{2}r_1 + \frac{1}{2}r_3, 0, \frac{1}{2}r_3 + \frac{1}{2}r_1). \quad (6.1.10)$$

Obviously, the first curve on the RHS of (6.1.10) is a nephroid whose normal vectors at points corresponding to θ are $(c_4, -s_4)$ and the second curve is a double circle whose points have coordinates $\frac{3}{4}(\frac{1}{2}r_3 + \frac{1}{2}r_1)(1 - c_4, s_4)$. In other words, the expression on the RHS may interpreted as the sum of three radius-vectors: a constant vector $\frac{3}{4}(\frac{1}{2}r_3 + \frac{1}{2}r_1)(1, 0)$, a radius vector of a point X_{θ^3} on the nephroid $\Gamma_3(\frac{1}{2}r_1 - \frac{1}{2}r_3, r_2, \frac{1}{2}r_3 - \frac{1}{2}r_1)$, and finally, a constant length vector $\frac{3}{4}(\frac{1}{2}r_3 + \frac{1}{2}r_1)(-c_4, s_4)$, which is normal to the nephroid and is directed inside one of its main arc and outside another.

Hence, $\Gamma_3(r_1, r_2, r_3)$ is a parallel of the Cayley sextic. $\square$

Clearly, a parallel to a Cayley sextic is a connected curve. It follows from Lemma 6.1.8, since $\Gamma_3(r_1, 0, r_2)$ must be a continuous and closed curve.

Definition 6.1.11. *Given a Cayley sextic, Γ, we will call the family of its parallels $P(\Gamma)$, and Γ itself will be referred to as a generator of the family. For two curves $C_1, C_2, \in P(\Gamma)$, the difference between their normal displacements from Γ is called normal distance between C_1 and C_2. To avoid ambiguity, when the normal displacement from Γ to a parallel curve $C \in P(\Gamma)$ is directed away from the evolute, the distance will be negative, and positive otherwise.*

A brief and routine examination of the equations (6.1.2) shows that the curve has two vertices (local extrema of radius of curvature). One of the vertices is at the pole, where the curve is singular (the radius of curvature is zero); the singularity is not a cusp.

Lemma 6.1.12. *Let Γ be a Cayley sextic and the distance between its vertices be R. Then $P(\Gamma)$ has two generators, the normal distance between the generators being R,* *and one nephroid distance $\frac{R}{2}$ away from the generators.*

Proof. Consider the curve $\Gamma_3(0,0,1)$ and let $C \in P(\Gamma_3(0,0,1))$ be normal distance k away from the generator of the family. It follows from Theorem 6.1.10, that the equation of $C \in P(\Gamma_3(0,0,1))$ is

$$\begin{cases} x = -s^3 s_3 - kc_4 = -s^3 s_3 + k(1-c_4) - k \\ y = -s^3 c_3 + ks_4 \ . \end{cases} \tag{6.1.11}$$

That implies that the curve $\Gamma_3(-1,0,0)$ translated $-\frac{3}{4}$ units along x-axis is a member of $P(\Gamma_3(0,0,1))$. Denote that curve by Γ'. Clearly, Γ' is a Cayley sextic, too, and hence each of members of $P(\Gamma_3(0,0,1))$ is also a member of $P(\Gamma')$.

On the other hand, since the pole is the only point when the Cayley sextic touches the evolute, any its parallel C distance $k \neq R$ away from the generator is not a Cayley sextic. Indeed, for $k \in (-\infty, 0) \cup (R, \infty)$, C is a smooth curve, and for $k \in (0, R)$, C has two cusps.

By the symmetry reason and from Lemma 6.1.6, the parallel of nephroidal shape in the family $P(\Gamma)$ is unique and equally distant from the generators. □

Theorem 6.1.13. (The Cayley Sextic Normal Front Theorem) *The curve $\Gamma_3(r_1, r_2, r_3)$ is a Cayley sextic if and only if $r_2^2 = r_1 r_3$. If and only if $r_1 = -r_3$, $\Gamma_3(r_1, r_2, r_3)$ is a nephroid. Otherwise, it is an unnamed normal front of a Cayley sextic.*

Proof. We can represent $\Gamma_3(r_1, r_2, r_3)$ as a linear combination of two curves:

$$\Gamma_3(r_1, r_2, r_3) = \Gamma_3(\frac{r_1 - r_3}{2}, r_2, \frac{r_3 - r_1}{2}) + \Gamma_3(\frac{r_1 + r_3}{2}, 0, \frac{r_3 + r_1}{2}). \tag{6.1.12}$$

The first curve on the RHS of (6.1.12) is a nephroid (by Lemma 6.1.9), the second is a double circle (by Lemma 6.1.4). From the equations (6.1.8) of the nephroid we conclude that the nephroid is $C = \sqrt{\frac{(r_1-r_3)^2}{4} + r_2^2}$ times bigger than the nephroid $\Gamma_3(1, 0, -1)$. Hence its normal distance from the generators of the family of parallels it belongs to is $\frac{3}{4}\sqrt{\frac{(r_1-r_3)^2}{4} + r_2^2}$ (see Lemma 6.1.8).

Looking at the double circle equations

$$\begin{cases} x = \frac{3}{4}\frac{(r_1+r_3)}{2} - \frac{3}{4}\frac{(r_1+r_3)}{2}c_4 \\ y = \frac{3}{4}\frac{(r_1+r_3)}{2}s_4, \end{cases} \tag{6.1.13}$$

we conclude that if $\Gamma_3(r_1, r_2, r_3)$ is a Cayley sextic, then

$$\frac{3}{4}\sqrt{\frac{(r_1-r_3)^2}{4} + r_2^2} = \frac{3}{4}\frac{(r_1+r_3)}{2}. \tag{6.1.14}$$

The condition $r_2^2 = r_1 r_3$, making $\Gamma_3(r_1, r_2, r_3)$ a Cayley sextic, follows immediately. The condition $r_1 + r_3 = 0$, making $\Gamma_3(r_1, r_2, r_3)$ a nephroid, follows from Lemma 6.1.12.

The reverse chain of reasoning proves the converse statement. $\square$

Lemma 6.1.14. *If $RR'' - R'^2 > 0$, $\Gamma_3(R, R', R'')$ is smooth, if $RR'' - R'^2 = 0$ it has one singular point (the curve is a Cayley sextic), if $RR'' - R'^2 < 0$ it has two singular points.*

Proof. By Theorem 4.2.6 and Corollary 4.2.7, the solutions of

$$R_{\theta^2} = 0 \tag{6.1.15}$$

gives the us the answer on singularity of Γ_3 question. We have:

$R_{\theta^2} = Rc^2 - 2R'sc + R''s^2 = 0 \;\Rightarrow\; R - R's_2 + \frac{1}{2}(R'' - R)(1 - c_2) = 0.$

Thus, we obtain:

$$\frac{R+R''}{2} = \sqrt{\frac{(R''-R)^2}{4} + R'^2}\ \sin\left(2\theta + \arccos\frac{R'}{\sqrt{\frac{(R''-R)^2}{4} + R'^2}}\right). \tag{6.1.16}$$

This equation has no solution if $RR'' - R'^2 > 0$, since absolute value of sine can not exceed 1. It has one solution on $[0, \pi]$ if $RR'' - R'^2 = 0$:

$$\theta = \frac{\pi}{4} - \frac{1}{2}\arccos\frac{2R'}{R+R''}. \tag{6.1.17}$$

Finally, the equation (6.1.15) has two roots on $[0, \pi]$, if $RR'' - R'^2 < 0$. $\square$

Since the number $RR'' - R'^2$ plays important role in determination whether Γ_3 is smooth or not, we will call it *the discriminant of the 3rd iteration*.

6.2 The Deltoid Theorem

Next we consider the 3rd iteration $X_{\theta_1\theta_2\theta_3}$ where $\theta_1 + \theta_2 + \theta_3 = k \bmod \pi$, for some constant k. It will help us to understand the distribution of $X_{\theta_1\theta_2\theta_3}$ inside the *image-set of the 3rd iteration.*

Definition 6.2.1. *We will call the image-set of $X_{\theta_1\theta_2\theta_3}$ when $\theta_1 + \theta_2 + \theta_3 = k \bmod \pi$, where k is some constant, a constant sum image-set in general and k-image-set in particular.*

As it follows from Lemma 4.2.2, tangents to $\gamma_{\theta_1\theta_2\theta_3}$ and $\gamma_{\theta_1'\theta_2'\theta_3'}$ are parallel if

$$(\theta_1 + \theta_2 + \theta_3) \bmod \pi = (\theta_1' + \theta_2' + \theta_3') \bmod \pi = k, \ \ k \in [0, \pi). \tag{6.2.1}$$

Thus, we may call constant sum image-sets by *parallel tangent image-set.*

Given a curve γ let a point $X \in \gamma$ and a constant $k \in [0, \pi)$. Then the locus of points $\{X_{\theta^2(k-2\theta)}\}_{\theta=0}^{\pi}$ will be denoted by $\tilde{\Gamma}_3^k$. Clearly, it is a curve parametrized by θ.

Lemma 6.2.2. *The locus of points $X_{\theta_1\theta_2\theta_3}$, $\theta_1 + \theta_2 + \theta_3 = k \bmod \pi$, is bounded by $\tilde{\Gamma}_3^k$.*

Proof. Since $X_{\theta_1\theta_2\theta_3} \in [X_{\theta_1\alpha^2} X_{\theta_1(\alpha+\frac{\pi}{2})^2}]$, where $\alpha = \frac{\theta_2+\theta_3}{2}$, the statement follows immediately from Lemma 4.2.5. □

Definition 6.2.3. *We will call the curve $\tilde{\Gamma}_3^k$ the boundary of constant sum image-sets, or for brevity sake, the constant sum boundary. If we would like to be specific about k, we will refer to $\tilde{\Gamma}_3^k$ as k-sum boundary.*

Definition 6.2.4. *Deltoid* (Figure 6.4(a)) *is the roulette created by a point on the circumference of a circle as it rolls without slipping along the inside of a circle with three times its radius. It can also be defined as a similar roulette where the radius of* *the outer circle is $\frac{3}{2}$ times that of the rolling circle. A deltoid can be represented (up to rotation and translation) by the following parametric equations*

$$\begin{cases} x = 2R\cos(t) + R\cos(2t) \\ y = 2R\sin(t) - R\sin(2t), \end{cases} \tag{6.2.2}$$

where R is the radius of the rolling circle. [14]

Proposition 6.2.5. *If $R = R'' = 1$ and $R' = 0$, the k-sum boundaries are deltoids, inscribed in the double circle $\Gamma_3(1,0,1)$. The cusps of the deltoids lie in $X_{(\frac{k}{3}+m\frac{\pi}{3})^3}$, $m = 0, 1, 2$.*

Proof. Let $k \in [0, \pi]$ be a fixed number and consider the the equations of the curve $\tilde{\Gamma}_3^k(1,0,1)$:

$$\begin{cases} x = s^2 + css_2 + \sin(k - 2\theta)\sin k \\ y = sc + scc_2 + \sin(k - 2\theta)\cos k. \end{cases} \tag{6.2.3}$$

Simple manipulations with formulas (6.2.3) yield:

$$\begin{cases} x = \dfrac{1}{2} - \dfrac{c_2}{2} + \dfrac{1}{4} - \dfrac{c_4}{4} + \dfrac{c_2}{2} - \dfrac{\cos(2k-2\theta)}{2} = \dfrac{3}{4} - \dfrac{\cos(2\theta - 2k)}{2} - \dfrac{c_4}{4} \\ y = \dfrac{s_2}{2} + \dfrac{s_4}{4} + \dfrac{\sin(2k-2\theta)}{2} - \dfrac{s_2}{2} = -\dfrac{\sin(2\theta-2k)}{2} + \dfrac{s_4}{4}. \end{cases}$$

Substituting $\theta = \frac{\theta'}{2} - k$, we get:

$$\begin{cases} x = \dfrac{3}{4} - \dfrac{\cos(\theta' - 4k)}{2} - \dfrac{\cos(2\theta' - 4k)}{4} \\ y = -\dfrac{\sin(\theta' - 4k)}{2} + \dfrac{\sin(2\theta' - 4k)}{4}. \end{cases} \tag{6.2.4}$$

Finally, reflecting the curve (6.2.4) with respect to the x- and y-axes, we obtain the equations (6.2.2).

The positions of the cusps are obvious. □

Thus, we obtain an interesting construction of a deltoid. Take a unit circle Ω_1 and

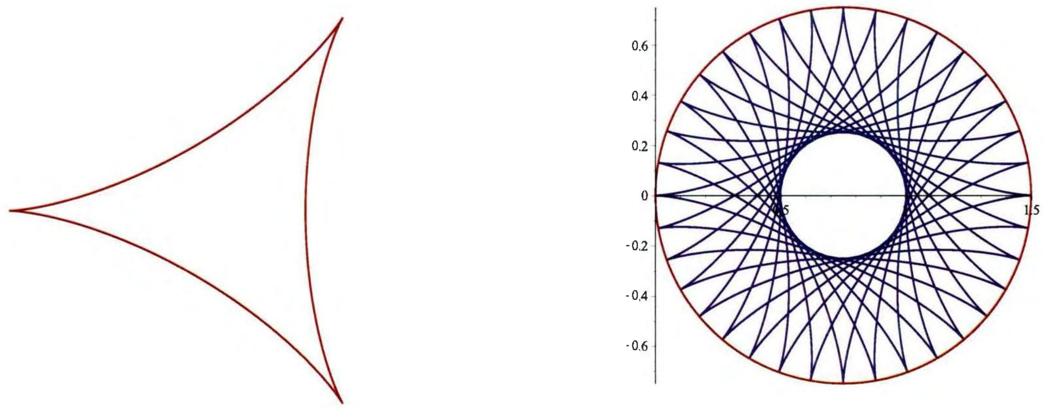

(a) (b)

Figure 6.4: (a) A deltoid; (b) to Lemma 6.2.5: The double circle $\Gamma_3(1, 0, 1)$ and a few constant sum image-sets' boundaries.

let points O and X be its center and a fixed point on the circumference respectively. Let point $E \in \Omega_1$ be opposite to X.

Let $\widehat{XOA}$ be counted clockwise and $A_X = (\frac{1}{2}\widehat{XOA}) \operatorname{mod} \pi$ be the coordinate of a point A on the circumference. Pick any number $k \in [0, \pi)$ and let $A, B, C \in \Omega_1$ be such that $(A_X + B_X + C_X) \operatorname{mod} \pi = k$. Let $\triangle A'B'C'$ be symmetrical to $\triangle ABC$ with respect to O. Denote by $\overline{ABC}$ the point of intersection of Simson lines of the two triangles with respect to E. Let Ω_2 be a circle such that its radius is $\frac{3}{2}$ and Ω_1 is its incircle at X.

Theorem 6.2.6. *The locus of $\{\overline{ABC}\}_{(A_X+B_X+C_X) \operatorname{mod} \pi = k}$ is a closed region bounded by a deltoid inscribed in the circle Ω_2. The bounding deltoid is attained by considering only triangles $\triangle ABC$ with at least two vertices coinciding.*

Proof. The statement follows from Theorem 5.2.4 and Proposition 6.2.5. $\square$

Lemma 6.2.7. *If Γ_3 has a singularity at $X_{\theta_0^3}$, then $\tilde{\Gamma}_3^k$ passes through that point for any $k \in [0, \pi]$.*

Proof. Suppose Γ_3 has a singularity at $X_{\theta_0^3}$. That implies that $R_{\theta_0^2} = 0$, and then $X_{\theta_0^3} = X_{\theta_0^2 \alpha}$ for any $\alpha \in [0, \pi]$. Then the statement of Lemma follows immediately. □

Lemma 6.2.8. (Lemma about three congruent deltoids) *Given any $k \in \mathbb{R} \bmod \pi$, the curves $\tilde{\Gamma}_3^k(0,1,0)$ and $\tilde{\Gamma}_3^k(1,0,-1)$ are deltoids congruent to $\tilde{\Gamma}_3^k(1,0,1)$.*

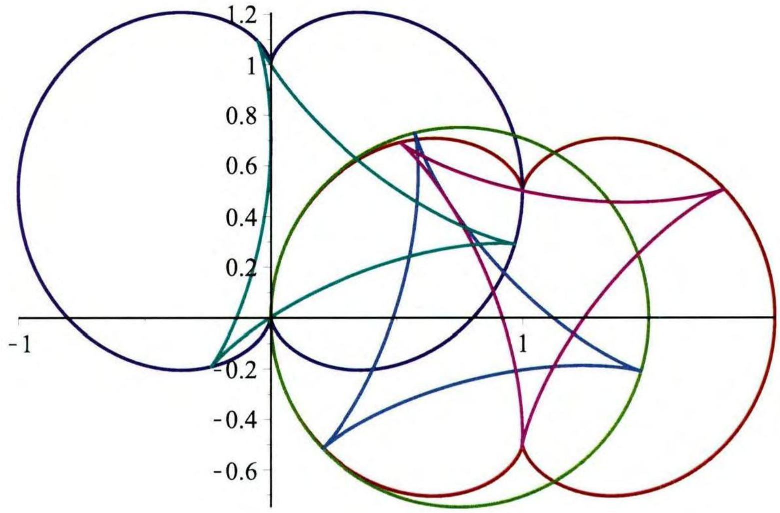

Figure 6.5: To Lemma 6.2.8. The upper nephroid, $\Gamma_3(0,1,0)$, with $\tilde{\Gamma}_3^k(0,1,0)$, the lower nephroid, $\Gamma_3(1,0,-1)$, with $\tilde{\Gamma}_3^k(1,0,-1)$ and the double circle, $\Gamma_3(1,0,1)$, with $\tilde{\Gamma}_3^k(1,0,1)$, where $k = 1$ in all three cases.

Proof. Consider first $\tilde{\Gamma}_3^k(0,1,0)$.

$$\begin{cases} x = -s^2 s_2 - s_2 s_{k-2\theta} s_k \\ y = -s^2 c_2 - s - 2 s_{k-2\theta} c_k. \end{cases}$$

Working out the coordinate expressions, we get:

$$\begin{cases} x = -\frac{1}{2}(1 - c_2) s_2 - \frac{1}{2} s_2 (c_2 - c_{2k-2\theta}) = \frac{1}{4} s_{2k} - \frac{1}{2} s_2 + s_{4\theta-2k} \\ y = -\frac{1}{2}(1 - c_2) c_2 - \frac{1}{2}(s_{2k-2\theta} - s_2) s_2 = \frac{1}{2} + \frac{1}{4} c_{2k} - \frac{1}{2} c_2 - \frac{1}{4} c_{4\theta-2k} \ . \end{cases} \tag{6.2.5}$$

Substituting $\theta = \frac{1}{2}\theta' + k$ and reflecting the curve with respect to the x- and y-axes, we finally obtain a model equation of a deltoid:

$$\begin{cases} x = -\frac{1}{4}\sin 2k + \frac{1}{2}\sin(\theta' + 2k) - \frac{1}{4}\sin(2\theta' + 2k) \\ y = -\frac{1}{2} - \frac{1}{4}\cos 2k + \frac{1}{2}\cos(\theta' + 2k) + \frac{1}{4}\cos(2\theta' + 2k). \end{cases} \tag{6.2.6}$$

Now, consider the equations of $\tilde{\Gamma}_3^k(1, 0, -1)$.

$$\begin{cases} x = s^2 + css_2 + c_2 s_{k-2\theta} s_k \\ y = cs + csc_2 + c_2 s_{k-2\theta} c_k. \end{cases}$$

Performing the same routine:

$$\begin{cases} x = \frac{1}{2} - \frac{1}{2}c_2 + \frac{1}{4} - \frac{1}{4}c_4 + \frac{1}{2}c_2^2 - \frac{1}{2}c_2 c_{2\theta-2k} = 1 - \frac{1}{4}c_{2k} - \frac{1}{2}c_2 - \frac{1}{4}c_{4\theta-2k} \\ y = \frac{1}{2}s_2 + \frac{1}{4}s_4 - \frac{1}{2}c_2 s_{2\theta-2k} - \frac{1}{2}c_2 s_2 = \frac{1}{4}s_{2k} + \frac{1}{2}s_2 - \frac{1}{4}s_{4\theta-2k}. \end{cases} \tag{6.2.7}$$

Substituting $\theta = \frac{1}{2}\theta' + k$ and reflecting the curve with respect to the x- and y-axes, we obtain again a model equation of a deltoid:

$$\begin{cases} x = -1 + \frac{1}{4}c_{2k} + \frac{1}{2}\cos(\theta' + 2k) + \frac{1}{4}\cos(2\theta' + 2k) \\ y = -\frac{1}{4}s_{2k} - \frac{1}{2}\sin(\theta' + 2k) + \frac{1}{4}\sin(2\theta' + 2k). \end{cases} \tag{6.2.8}$$

The sizes of the deltoids (6.2.6), (6.2.8) and (6.2.4) are the same. $\square$

Definition 6.2.9. *Since $\Gamma_3(R, R', R'')$ is a Cayley sextic if $RR'' - R'^2 = 0$, we will call the cone $RR'' - R'^2 = 0$ in L_3 the Cayley sextic cone.*

Definition 6.2.10. *Since $\Gamma_3(R, R', R'')$ is a nephroid if $R + R'' = 0$, we will call the plane $R + R'' = 0$ in L_3 the nephroidal plane.*

Lemma 6.2.11. (Nephroidal plane deltoids) *The curves* $\tilde{\Gamma}_3^k(r_1, r_2, -r_1)$ *are deltoids inscribed in the nephroid* $\Gamma_3(r_1, r_2, -r_1)$ *and passing through the nephriod's cusps.*

Proof. Let us represent $\tilde{\Gamma}_3^k(r_1, r_2, -r_1)$ as the sum:

$$\tilde{\Gamma}_3^k(r_1, r_2, -r_1) = \tilde{\Gamma}_3^k(0, r_2, 0) + \tilde{\Gamma}_3^k(r_1, 0, -r_1), \tag{6.2.9}$$

and work on the coordinate sum of the corresponding parametric equations (6.2.6) and (6.2.8) ignoring for a while the constant terms and the argument shift $2k$ for simplicity sake. We have:

$$\begin{cases} x = \frac{r_1}{2}c_{\theta'} + \frac{r_1}{4}c_{2\theta'} + \frac{r_2}{2}s_{\theta'} - \frac{r_2}{4}s_{2\theta'} = \frac{1}{2}(r_1 c_{\theta'} + r_2 s_{\theta'}) + \frac{1}{4}(r_1 c_{2\theta'} - r_2 s_{2\theta'}) \\ y = -\frac{r_1}{2}s_{\theta'} + \frac{r_1}{4}s_{2\theta'} + \frac{r_2}{2}c_{\theta'} + \frac{r_2}{4}c_{2\theta'} = \frac{1}{2}(-r_1 s_{\theta'} + r_2 c_{\theta'}) + \frac{1}{4}(r_1 s_{2\theta'} + r_2 c_{2\theta'}). \end{cases} \tag{6.2.10}$$

Denote $\rho = \sqrt{r_1^2 + r_2^2}$, and $\frac{r_1}{\rho} = \cos\alpha$, $\frac{r_2}{\rho} = \sin\alpha$. Then:

$$\begin{cases} x = \frac{\rho}{2}\cos(\theta' - \alpha) + \frac{\rho}{4}\cos(2\theta' + \alpha) \\ y = -\frac{\rho}{2}\sin(\theta' - \alpha) + \frac{\rho}{4}\sin(2\theta' + \alpha). \end{cases} \tag{6.2.11}$$

Remembering the ignored constant shift of the argument by $+2k$ and constant terms in the equations for the x- and y-coordinates, we get:

$$\begin{cases} x = -r_1 + \frac{r_1}{4}\cos 2k - \frac{r_2}{4}\sin 2k + \frac{\rho}{2}\cos(\theta' - \alpha + 2k) + \frac{\rho}{4}\cos(2\theta' + \alpha + 2k) \\ y = -\frac{r_1}{4}\sin 2k - \frac{r_2}{2} - \frac{r_2}{4}\cos 2k - \frac{\rho}{2}\sin(\theta' - \alpha + 2k) + \frac{\rho}{4}\sin(2\theta' + \alpha + 2k). \end{cases} \tag{6.2.12}$$

By a routine change of variables $\theta' = \theta'' - 2\alpha$, we get the model equation of a deltoid.

$$\begin{cases} x = -r_1 + \frac{r_1}{4}c_{2k} - \frac{r_2}{4}\sin 2k + \frac{\rho}{2}\cos(\theta'' - 3\alpha + 2k) + \frac{\rho}{4}\cos(2\theta'' - 3\alpha + 2k) \\ y = -\frac{r_1}{4}\sin 2k - \frac{r_2}{2} - \frac{r_2}{4}\cos 2k - \frac{\rho}{2}\sin(\theta'' - 3\alpha + 2k) + \frac{\rho}{4}\sin(2\theta'' - 3\alpha + 2k). \end{cases} \tag{6.2.13}$$

The deltoids (6.2.13) pass through the nephroid's cusps by Lemma 6.2.7 and their cusps lie on the nephroid, since $X_{(\frac{k}{3}+\frac{m\pi}{3})^3}$, $m = 0, 1, 2$, belong to both $\Gamma_3(r_1, r_2, -r_1)$ and $\tilde{\Gamma}_3^k(r_1, r_2, -r_1)$. ☐

Lemma 6.2.12. *Fix a $k \in \mathbb{R} \bmod \pi$. The chords $[X_{\theta^2(k-2\theta)} X_{(\theta+\frac{\pi}{2})^2(k-2\theta)}]$ of a deltoid representing $\tilde{\Gamma}_3^k(r_1, r_2, -r_1)$ are tangent to it.*

Proof. For $\tilde{\Gamma}_3^k(r_1, r_2, -r_1)$, we have: $R = r_1$, $R_\theta = r_1 c - r_2 s$, $R_{\theta^2} = r_1 c_2 - r_2 s_2$. Calculate the coordinates of $X_{\theta^2(k-2\theta)} = (x_1, y_1)$ and $X_{(\theta+\frac{\pi}{2})^2(k-2\theta)} = (x_2, y_2)$:

$$\begin{cases} x_1 = r_1 s^2 + (r_1 c - r_2 s) s s_2 + (r_1 c_2 - r_2 s_2) s_{k-2\theta} s_k \\ y_1 = r_1 s c + (r_1 c - r_2 s) s c_2 + (r_1 c_2 - r_2 s_2) s_{k-2\theta} c_k. \end{cases} \tag{6.2.14}$$

$$\begin{cases} x_2 = r_1 c^2 + (-r_1 s - r_2 c) c(-s_2) + (-r_1 c_2 + r_2 s_2)(-s_{k-2\theta}) s_k \\ y_2 = -r_1 s c + (-r_1 s - r_2 c) c(-c_2) + (-r_1 c_2 + r_2 s_2)(-s_{k-2\theta}) c_k. \end{cases} \tag{6.2.15}$$

Clearly, $x_2 - x_1 = r_1 c_2 + r_2 s_2$ and $y_2 - y_1 = -r_1 s_2 + r_2 c_2$, so

$$|X_{\theta^2(k-2\theta)} X_{(\theta+\frac{\pi}{2})^2(k-2\theta)}| = \sqrt{(x_2 - x_1)^2 + (y_2 - y_1)^2} = \sqrt{r_1^2 + r_2^2}. \tag{6.2.16}$$

From the geometry of deltoid, we know that the tangents to a deltoid with generating circle of radius a, measured between two points, where they cut the curve again, are of constant length $4a$.[13] By Lemma 6.2.11 we know that the radius of a circle generating the deltoid $\tilde{\Gamma}_3^k(r_1, r_2, -r_1)$ is $\frac{\sqrt{r_1^2+r_2^2}}{4}$, which is 4 times smaller than the chord $[X_{\theta^2(k-2\theta)}X_{(\theta+\frac{\pi}{2})^2(k-2\theta)}]$. $\square$

Lemma 6.2.13. (Lemma of three concurrent circles) *If point $(R, R', R'') \in L_3$ lies on the Cayley sextic cone, the three circles based on the segments*[3] $[X_{(\frac{\pi}{2})^{(i-1)}}X_{(\frac{\pi}{2})^i}]$, *i=1,2,3, as their diameters, are concurrent. The concurrency point is the pole of the Cayley sextic $\Gamma_3(R, R', R'')$.*

Proof. Let us use the old notation for the circles: Ω_1, Ω_2, Ω_3 whose diameters are the corresponding segments $[X_{(\frac{\pi}{2})^{(i-1)}}X_{(\frac{\pi}{2})^i}]$, i=1,2,3, see Figure 6.6.

By definition 6.2.9, $RR'' = R'^2$.

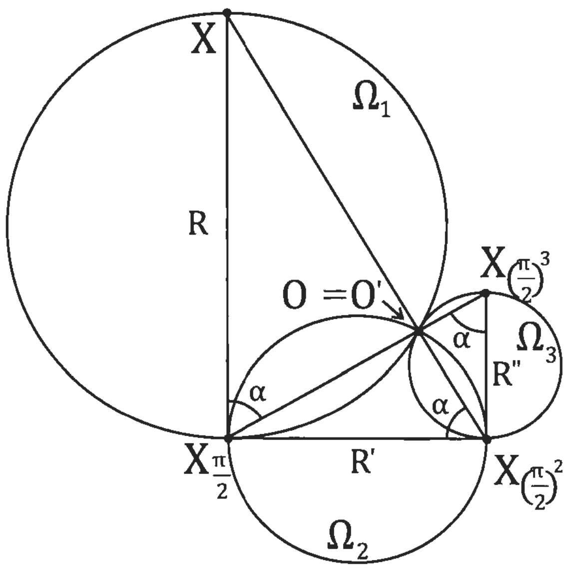

Figure 6.6: To Lemma 6.2.13.

If $R' = 0$, then either $R = 0$ or $R'' = 0$, so two of the three circles are degenerated into points, and the statement is obvious.

If $R' \neq 0$, then neither $R = 0$ nor $R'' = 0$. Denote by O and O' the feet of the perpendiculars dropped from $X_{\frac{\pi}{2}}$ and $X_{(\frac{\pi}{2})^2}$ to $[XX_{(\frac{\pi}{2})^2}]$ and $[X_{\frac{\pi}{2}}X_{(\frac{\pi}{2})^3}]$ respectively.

[3]We will count $X_{(\frac{\pi}{2})^0} = X$.

Obviously point O is one of the points of intersection of Ω_1 and Ω_2, whereas point O' is that of Ω_2 and Ω_3.

Since $\frac{R}{R'} = \frac{R'}{R''}$, the angles $\widehat{XX_{\frac{\pi}{2}}X}_{(\frac{\pi}{2})^2} = X_{\frac{\pi}{2}}\widehat{X_{(\frac{\pi}{2})^3}}X_{(\frac{\pi}{2})^2} = \arctan\frac{R}{R'}$, hence $X_{\frac{\pi}{2}}X_{(\frac{\pi}{2})^3} \perp XX_{(\frac{\pi}{2})^2}$. Therefore O and O' coincide.

Further, let us denote $\arctan\frac{R}{R'}$ by α and calculate R_{α^2}:

$R_{\alpha^2} = R\cos^2\alpha - R'\sin 2\alpha + R''\sin^2\alpha = \frac{1}{\cos^2\alpha}(R - 2R + R) = 0.$

Therefore, γ_{α^2} is singular at X_{α^2}, and so is Γ_3 at X_{α^3} by Cor 4.2.7. Since Γ_3 is a Cayley sextic, its only singularity is in the pole, so X_{α^3} is the pole. Clearly, X_{α^3} coincides with X_{α^2}, which is the point O. $\square$

Lemma 6.2.14. *If $(R, R', R'') \in L_3$ belongs to the Cayley sextic cone, then curves $\tilde{\Gamma}_3^k(R, R', R'')$ are chords of the Cayley sextic $\Gamma_3(R, R', R'')$ spanned twice (double segments), passing through the pole.*

Proof. Consider a curve γ_α and construct the image-set of the second iteration of $X_\alpha \in \gamma_\alpha$. Suppose $RR'' = R'^2$. Let $R' \neq 0$ (see Figure 6.7). Take any $k, \alpha \in [0, \pi)$

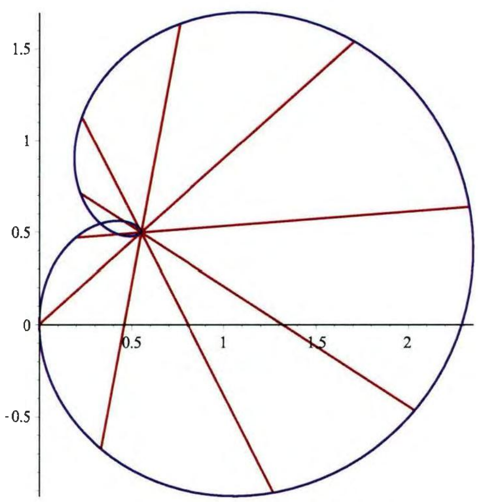

Figure 6.7: To Lemma 6.2.14. The curve $\Gamma_3(1, 0.9, 0.81)$ with a few chords, passing through the pole.

and fix k. Then a segment $[X_{\alpha(\frac{k-\alpha}{2})^2}X_{\alpha(\frac{k-\alpha+\pi}{2})^2}]$ will be a chord of $\tilde{\Gamma}_3^k(R, R', R'')$, which is the collection of endpoints of all such segments as α runs from 0 to π.

By the routine construction, the center of curvature of γ_α at X_α is $X_{\alpha\frac{\pi}{2}} = [X_\alpha X_{\frac{\pi}{2}}] \cap \Omega_1$. The center of curvature of the evolute of γ_α, $\gamma_{\alpha\frac{\pi}{2}}$, at $X_{\alpha\frac{\pi}{2}}$ is $X_{\alpha(\frac{\pi}{2})^2} = [X_{\alpha\frac{\pi}{2}} X_{(\frac{\pi}{2})^2}] \cap \Omega_3$, since $X_{\alpha(\frac{\pi}{2})^2} = X_{(\frac{\pi}{2})^2\alpha}$, so the line $X_{\alpha\frac{\pi}{2}} X_{(\frac{\pi}{2})^2}$ meets line $X_{\alpha\frac{\pi}{2}} X_\alpha$ at a right angle.

Then the image-set of the second iteration of $X_\alpha \in \gamma_\alpha$ will be a cardioid with the cusp at O. By Lemma 3.4.2, the segment $[X_{\alpha(\frac{k-\alpha}{2})^2} X_{\alpha(\frac{k-\alpha+\pi}{2})^2}]$ passes through O. It will form angle $2(\frac{k-\alpha}{2}) = \operatorname{arccot} \frac{R'}{R}$ with γ_α (see Lemma 3.4.4) or angle $k + \operatorname{arccot} \frac{R'}{R}$ with γ, i.e. the angle does not depend on α. Thus, all segments $[X_{\alpha(\frac{k-\alpha}{2})^2} X_{\alpha(\frac{k-\alpha+\pi}{2})^2}]$ constituting k-image-set, are collinear, and therefore $\tilde{\Gamma}_3^k(R, R', R'')$ is a line segment passing through the pole.

Note, that the image-sets of the second iteration of points $X_{\operatorname{arccot} \frac{R'}{R} - \alpha} \in \gamma_{\operatorname{arccot} \frac{R'}{R} - \alpha}$ and $X_{\operatorname{arccot} \frac{R'}{R} + \alpha} \in \gamma_{\operatorname{arccot} \frac{R'}{R} + \alpha}$, $\alpha \in [0, \frac{\pi}{2}]$ are the same, so the corresponding constant sum segments will totally overlap, therefore $\tilde{\Gamma}_3^k(R, R', R'')$ is spanned twice as α runs from 0 to π.

If $R' = R = 0$ and $R'' \neq 0$, then the argument is not valid but we can easily prove the statement in this case by examining the parametric equations of $\tilde{\Gamma}_3^k(R, R', R'')$. We have $R_{\theta^2} = s^2$, $R = R_\theta = 0$ and then:

$$\begin{cases} x = \sin^2\theta \sin(k - 2\theta) \sin k \\ y = sin^2\theta \sin(k - 2\theta) \cos k. \end{cases} \tag{6.2.17}$$

Clearly, the equations (6.2.17) for a fixed k are parametric equations of a segment, and since the function $\sin^2\theta \sin(k - 2\theta)$ is $\frac{\pi}{2}$-periodic, the segment is spanned twice as θ runs from 0 to π. $\square$

Lemma 6.2.15. *Let a point (r_1, r_2, r_3) belong to the Cayley sextic cone. Then for any $r^* \in \mathbb{R}$ and $k \in \mathbb{R} \bmod \pi$, the segment $\tilde{\Gamma}_3^k(r_1, r_2, r_3)$ is tangent to a curve $\tilde{\Gamma}_3^k(r_1, r_2, r^*)$*

at $X_k \in \gamma_k$. (Figure 6.8(a)).

If $r_1 = 0$, *i.e.* $(r_1, r_2, r_3) = (0, 0, r_3)$, *the segment* $\tilde{\Gamma}_3^k(0,0,r_3)$ *is tangent to a curve* $\tilde{\Gamma}_3^k(0, r_*, r^*)$ *at the origin for any* $r_*, r^* \in \mathbb{R}$. (Figure 6.8(b)).

Proof. Obviously, the segment $\tilde{\Gamma}_3^k(r_1, r_2, r_3)$ and the curve $\tilde{\Gamma}_3^k(r_1, r_2, r^*)$ have a common point, corresponding to $\theta = 0$, namely $X_k \in \gamma_k$, since $X_k = X_{k0^2}$. It is also clear that $X_{k0^2} \in [X_{0(\frac{k}{2})^2} X_{0(\frac{k}{2}+\frac{\pi}{2})^2}]$, because it is equivalent to the statement $X_{k0} \in [X_{(\frac{k}{2})^2} X_{(\frac{k}{2}+\frac{\pi}{2})^2}]$, which follows from Lemma 3.4.2.

Consider the equations of $\tilde{\Gamma}_3^k(r_1, r_2, r_3)$:

$$\begin{cases} x = r_1 s^2 + (r_1 c - r_2 s) s s_2 + (r_1 c^2 - r_2 s_2) s_k s_{k-2\theta} + r_3 s^2 s_k s_{k-2\theta} \\ y = r_1 s c + (r_1 c - r_2 s) s c_2 + (r_1 c^2 - r_2 s_2) c_k s_{k-2\theta} + r_3 s^2 c_k s_{k-2\theta}, \end{cases} \tag{6.2.18}$$

and those of $\tilde{\Gamma}_3^k(r_1, r_2, r^*)$

$$\begin{cases} x = r_1 s^2 + (r_1 c - r_2 s) s s_2 + (r_1 c^2 - r_2 s_2) s_k s_{k-2\theta} + r^* s^2 s_k s_{k-2\theta} \\ y = r_1 s c + (r_1 c - r_2 s) s c_2 + (r_1 c^2 - r_2 s_2) c_k s_{k-2\theta} + r^* s^2 c_k s_{k-2\theta}. \end{cases} \tag{6.2.19}$$

Differentiating these equations with respect to θ at $\theta = 0$, we notice that the corresponding equations differ only by the last term and derivatives of the last term in each equation vanish. Hence the segment $\tilde{\Gamma}_3^k(r_1, r_2, r_3)$ is tangent to $\tilde{\Gamma}_3^k(r_1, r_2, r^*)$.

Further, consider the equations curve $\tilde{\Gamma}_3^k(0, r_*, r^*)$

$$\begin{cases} x = -r_* c s s_2 - r_* s_2 s_k s_{k-2\theta} + r^* s^2 s_k s_{k-2\theta} \\ y = -r_* s^2 c_2 - r_* s_2 c_k s_{k-2\theta} + r^* s^2 c_k s_{k-2\theta}. \end{cases} \tag{6.2.20}$$

Clearly, both curves, $\tilde{\Gamma}_3^k(0, r_*, r^*)$ and $\tilde{\Gamma}_3^k(0, 0, r_3)$, pass through the origin when the parameter is equal to zero. Then differentiating these equations with respect to θ at

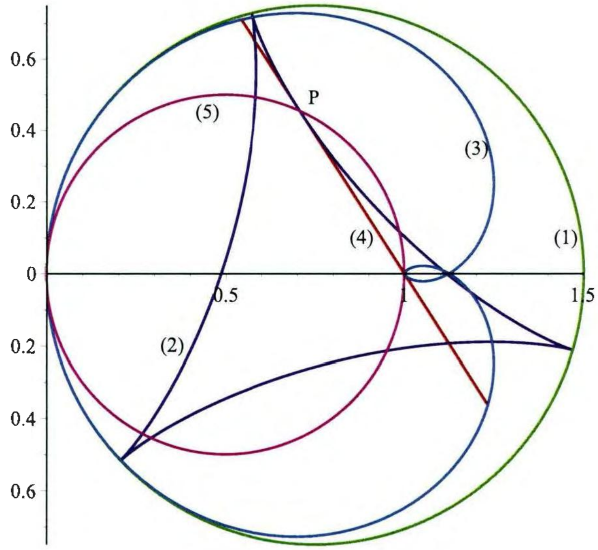

(a)

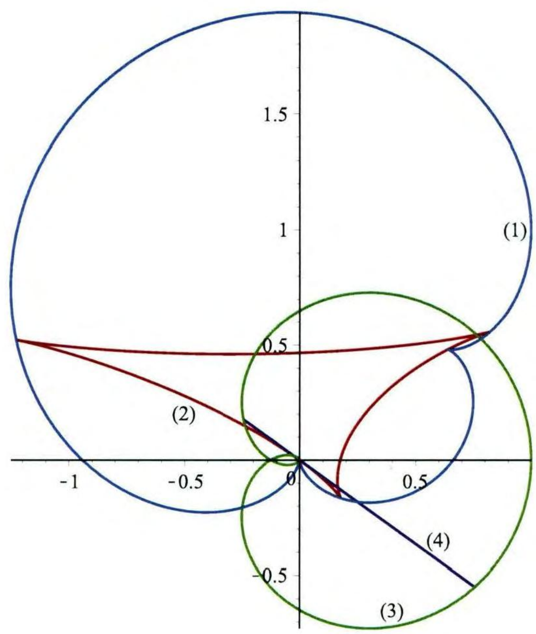

(b)

Figure 6.8: To Lemma 6.2.15. In both Figures, segment (4) is tangent to curve (2). (a) Curves: (1) $\Gamma_3(1,0,1)$, (2) $\tilde{\Gamma}_3^1(1,0,1)$, (3) $\Gamma_3(1,0,0)$, (4) $\tilde{\Gamma}_3^1(1,0,0)$, (5) $\Gamma_1(1)$, point $P = X_1 \in \gamma_1$. Note, curves (5),(4),(2) pass through P; (b) Curves: (1) $\Gamma_3(0,1,-1)$, (2) $\tilde{\Gamma}_3^{2.2}(0,1,-1)$, (3) $\Gamma_3(0,0,-1)$, (4) $\tilde{\Gamma}_3^{2.2}(0,0,-1)$. Note, curves (2),(4) pass through the origin.

$\theta = 0$, yields

$$\begin{cases} x = -2r_* s_k^2 \\ y = -2r_* s_k c_k. \end{cases} \tag{6.2.21}$$

Thus, the tangent vector to $\tilde{\Gamma}_3^k(0, r_*, r^*)$ at the origin is proportional to the vector (s_k, c_k), and as it follows from the equation (6.2.17), the segment $\tilde{\Gamma}_3^k(0, 0, r_3)$ lies along this vector. $\square$

To economize on notations, we will call anything pertaining to the image-set of the nth iteration of a point on a curve, whose value and the first $n-1$ derivatives at this point are $R, R', ..., R^{(n-1)}$ by *that of* $(R, R', ..., R^{(n-1)}) \in L_n$. We will also denote by $X_{\theta_1 \ldots \theta_n}(R, R', ..., R^{(n-1)})$ a point $X_{\theta_1 \ldots \theta_n} \in \gamma_{\theta_1 \ldots \theta_n}$ of $(R, R', ..., R^{(n-1)}) \in L_n$.

Lemma 6.2.16. *Let $\alpha_1, \alpha_2, k \in \mathbb{R} \bmod \pi$, $\alpha_1 \neq \alpha_2$ and k is fixed. Suppose a line passing through $X_{(\alpha_1)^2(k-2\alpha_1)}$ and $X_{(\alpha_2)^2(k-2\alpha_2)}$ on $\tilde{\Gamma}_3^k(0, r_*, 0)$ is parallel to $\tilde{\Gamma}_3^k(0, 0, r^*)$, $r_*, r^* \in \mathbb{R}$. Then the corresponding points on $\tilde{\Gamma}_3^k(0, 0, r^*)$ coincide.*

Proof. The radius-vectors of points $X_{(\alpha_1)^2(k-2\alpha_1)}(0, r_*, 0)$ and $X_{(\alpha_2)^2(k-2\alpha_2)}(0, r_*, 0)$ are

$$\vec{X}_{(\alpha_1)^2(k-2\alpha_1)} = r_*(-s_{\alpha_1}^2 s_{2\alpha_1} - s_{2\alpha_1} s_{k-2\alpha_1} s_k, -s_{\alpha_1}^2 c_{2\alpha_1} - s_{2\alpha_1} s_{k-2\alpha_1} c_k), \tag{6.2.22}$$

$$\vec{X}_{(\alpha_2)^2(k-2\alpha_2)} = r_*(-s_{\alpha_2}^2 s_{2\alpha_2} - s_{2\alpha_2} s_{k-2\alpha_2} s_k, -s_{\alpha_2}^2 c_{2\alpha_2} - s_{2\alpha_2} s_{k-2\alpha_2} c_k) \tag{6.2.23}$$

respectively. Since these two points lie on the line parallel to $\tilde{\Gamma}_3^k(0, 0, r^*)$, we have $\vec{X}_{(\alpha_1)^2(k-2\alpha_1)} - \vec{X}_{(\alpha_2)^2(k-2\alpha_2)} = \beta(s_k, c_k)$, for some $\beta \in \mathbb{R}$, and then we conclude that

$$s_{\alpha_1}^2 s_{2\alpha_1} = s_{\alpha_2}^2 s_{2\alpha_2}, \tag{6.2.24}$$

$$s_{\alpha_1}^2 c_{2\alpha_1} = s_{\alpha_2}^2 c_{2\alpha_2}. \tag{6.2.25}$$

On the other hand, the radius-vectors of the corresponding points on $\tilde{\Gamma}_3^k(0,0,r^*)$ are

$$\vec{X}_{(\alpha_1)^2(k-2\alpha_1)} = r^*(s^2_{\alpha_1}s_{k-2\alpha_1}s_k, s^2_{\alpha_1}s_{k-2\alpha_1}c_k), \tag{6.2.26}$$

$$\vec{X}_{(\alpha_2)^2(k-2\alpha_2)} = r^*(s^2_{\alpha_2}s_{k-2\alpha_2}s_k, s^2_{\alpha_2}s_{k-2\alpha_2}c_k). \tag{6.2.27}$$

Then we have: $s^2_{\alpha_2}s_{k-2\alpha_2} = s^2_{\alpha_2}(s_k c_{2\alpha_2} - c_k s_{2\alpha_2}) = s^2_{\alpha_1}s_{k-2\alpha_1}$, which implies that $X_{(\alpha_1)^2(k-2\alpha_1)} = X_{(\alpha_2)^2(k-2\alpha_2)}$ on $\tilde{\Gamma}_3^k(0,0,r^*)$. □

Corollary 6.2.17. *The distance* $|X_{(\alpha_1)^2(k-2\alpha_1)}(0,r_*,r^*)X_{(\alpha_2)^2(k-2\alpha_2)}(0,r_*,r^*)|$ *does not depend on* r^*, *if the line passing through them is parallel to* $\tilde{\Gamma}_3^k(0,0,r^*)$ (Figure 6.9).

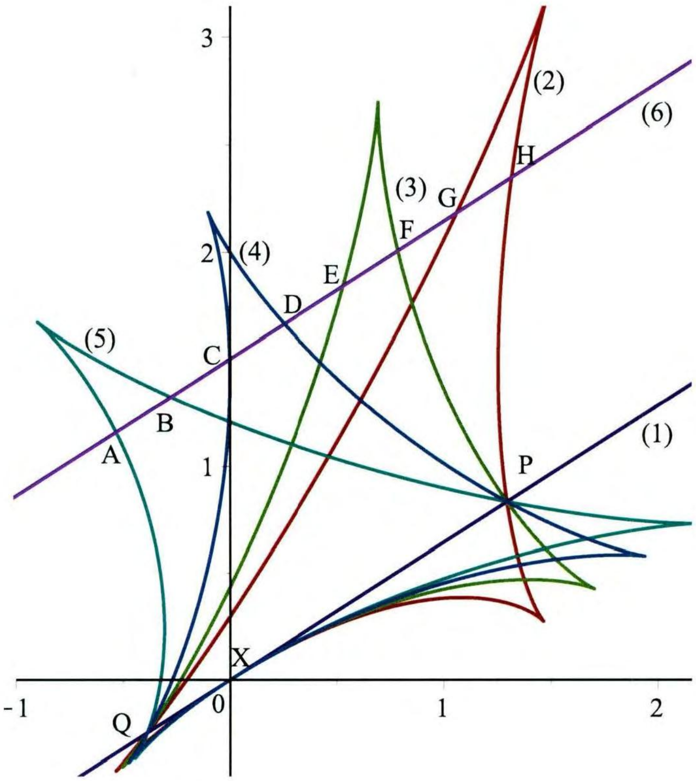

Figure 6.9: Curves (1)-(5), passing through points P, X, Q, are: line $y = x\cot 1$, $\tilde{\Gamma}_3^1(0,2,-2)$, $\tilde{\Gamma}_3^1(0,2,-1)$, deltoid $\tilde{\Gamma}_3^1(0,2,0)$, $\tilde{\Gamma}_3^1(0,2,1)$. Line (6) is $y = x\cot 1 + 1.5$. Note, $|AB| = |CD| = |EF| = |GH|$ as lines (1) and (6) are parallel.

Proof. Since $\tilde{\Gamma}_3^k(0, r_*, r^*) = \tilde{\Gamma}_3^k(0, 0, r^*) + \tilde{\Gamma}_3^k(0, r_*, 0)$, we have
$|\vec{X}_{(\alpha_1)^2(k-2\alpha_1)}(0, r_*, r^*) - \vec{X}_{(\alpha_2)^2(k-2\alpha_2)}(0, r_*, r^*)| = |(\vec{X}_{(\alpha_1)^2(k-2\alpha_1)}(0, r_*, 0)$
$- \vec{X}_{(\alpha_2)^2(k-2\alpha_2)}(0, r_*, 0)) + (\vec{X}_{(\alpha_1)^2(k-2\alpha_1)}(0, 0, r^*) - \vec{X}_{(\alpha_2)^2(k-2\alpha_2)}(0, 0, r^*))|$.
By the Lemma above $|\vec{X}_{(\alpha_1)^2(k-2\alpha_1)}(0, 0, r^*) - \vec{X}_{(\alpha_2)^2(k-2\alpha_2)}(0, 0, r^*))| = 0$, so distance between such points is constant for a fixed r_* and any $r^* \in \mathbb{R}$. $\square$

Corollary 6.2.18. *The distance from a point $X_{(\alpha)^2(k-2\alpha)}(0, r_*, 0)$ to the line $x \cos k = y \sin k$ is equal to the distance between the origin and the corresponding point on $\tilde{\Gamma}_3^k(0, 0, r_*)$, that is $X_{(\alpha)^2(k-2\alpha)}(0, 0, r_*)$.*

Proof. Considering equation (6.2.22), we notice that the distances from the points $X_{(\alpha)^2(k-2\alpha)}(0, r_*, 0)$ and $(-r_* s_\alpha^2 s_{2\alpha}, -r_* s_\alpha^2 c_{2\alpha})$ to the line $x \cos k = y \sin k$ are the same. The latter can be calculated by simple geometry, as vector with the same coordinates $(-r_* s_\alpha^2 s_{2\alpha}, -r_* s_\alpha^2 c_{2\alpha})$ forms angle $k-2\alpha$ with vector (s_k, c_k) and $\|r_*(-s_\alpha^2 s_{2\alpha}, -s_\alpha^2 c_{2\alpha})\| = |r_* s_\alpha^2|$. Then to find the distance between that point and the line, we have to multiply $|r_* s_\alpha^2|$ by $|s_{k-2\alpha}|$, which, by equation (6.2.26), is the distance between $X_{(\alpha)^2(k-2\alpha)}(0, 0, r_*)$ and the origin. $\square$

For the future, we will count the distance from a point on $\tilde{\Gamma}_3^k(0, 0, r^*), r^* \in \mathbb{R}$, to the origin negative if the number $r^* s_\alpha^2 s_{k-2\alpha}$ is negative.

Lemma 6.2.19. *Given a fixed $r_* \in \mathbb{R}$, the area covered by a k-image-set of $(0, r_*, r^*)$ is equal to the area of the deltoid $\tilde{\Gamma}_3^k(0, r_*, 0)$ for any $k \in [0, \pi]$ and any $r^* \in \mathbb{R}$.*

Proof. Denote by C the region, bounded by $\tilde{\Gamma}_3^k(0, r_*, r^*)$. By Corollary 6.2.17, if we cut C by slices along the lines parallel to $\tilde{\Gamma}_3^k(0, 0, 1)$ and take the limit of the sum of the areas of those slices getting their width approach 0, we will obtain the same result as that of following the same procedure with the deltoid $\tilde{\Gamma}_3^k(0, r_*, 0)$, since the lengths of corresponding slices of the figure and the deltoid are the same (Figure 6.9). $\square$

Lemma 6.2.20. *Let a point A be the foot of perpendicular dropped from the point $X_{(\alpha)^2(k-2\alpha)}(0, r_*, 0)$ to the line $x \cos k = y \sin k$. Denote by B and C the points $X_{(\alpha)^2(k-2\alpha)}(0, r_*, 0)$ and $X_{(\alpha)^2(k-2\alpha)}(0, r_*, r^*)$ respectively. Then angle $\widehat{BAC} = \arctan \frac{r^*}{r_*}$.*

Proof. By Corollary 6.2.18, $\frac{|BC|}{|AB|} = \frac{r^*}{r_*}$. From the right triangle $\triangle ABC$, we have $\tan \widehat{BAC} = \frac{|BC|}{|AB|} = \frac{r^*}{r_*}$. □

Denote the homothety with the pole at point A and ratio δ by $H(A, \delta)$. If a point P is mapped to a point P' by this homothety, we will write $P' = H(A, \delta)[P]$.

For brevity sake denote $\tilde{\Gamma}_3^k(r_1, r_2, r_3)$ by $C(r_1, r_2, r_3)$, for curves denoted like that, k is the same unless otherwise specified.

Lemma 6.2.21. *Suppose $(r_1, r_2, r_3) \in L_3$ belongs to the Cayley sextic cone. Let $r^* \neq r_3$ and consider three curves $C_1 = C(r_1, r_2, r_3)$, $C_2 = C(r_1, r_2, -r_1)$, $C_3 = C(r_1, r_2, r^*)$ with points, corresponding to the same parameter θ, denoted by $F_{i\theta}$ respectively, $i = 1, 2, 3$. Then for all $\theta \in [0, \pi]$, the points $F_{1\theta}, F_{2\theta}, F_{3\theta}$ are lying along a line parallel to $C(0, 0, 1)$ and $F_{3\theta} = H(F_{1\theta}, \frac{r_3 - r^*}{r_3 + r_1})[F_{2\theta}]$.* (Figure 6.10).

Proof. Consider the linear combinations $C_2 - C_1$ and $C_3 - C_1$:

$$C_1 - C_2 = (r_3 + r_1)C(0, 0, 1), \tag{6.2.28}$$

$$C_1 - C_3 = (r_3 - r^*)C(0, 0, 1). \tag{6.2.29}$$

From the equations (6.2.28), (6.2.29), we conclude that points $F_{2\theta}$ and $F_{3\theta}$ lie the proportional distances away from $F_{1\theta}$ along a line parallel to $C(0, 0, 1)$.

Therefore $F_{3\theta} = H(F_{1\theta}, \frac{r_3 + r_1}{r_3 - r^*})[F_{2\theta}]$ for all $\theta \in [0, \pi]$. □

Corollary 6.2.22. *Let $C_1 = C(r_1, r_2, r_3) \in L_3$ be a Cayley sextic. If the line passing through two points on $C(r_1, r_2, r^*)$, $r^* \in \mathbb{R}$, is parallel to C_1 then the distance between the two points does not depend on r_*.* □

Thus, we see that curves $\tilde{\Gamma}_3^k(R, R', R'')$ have the relationship with deltoids similar to that between rectangles and parallelograms having equal bases and heights (Cavalieri's principle).

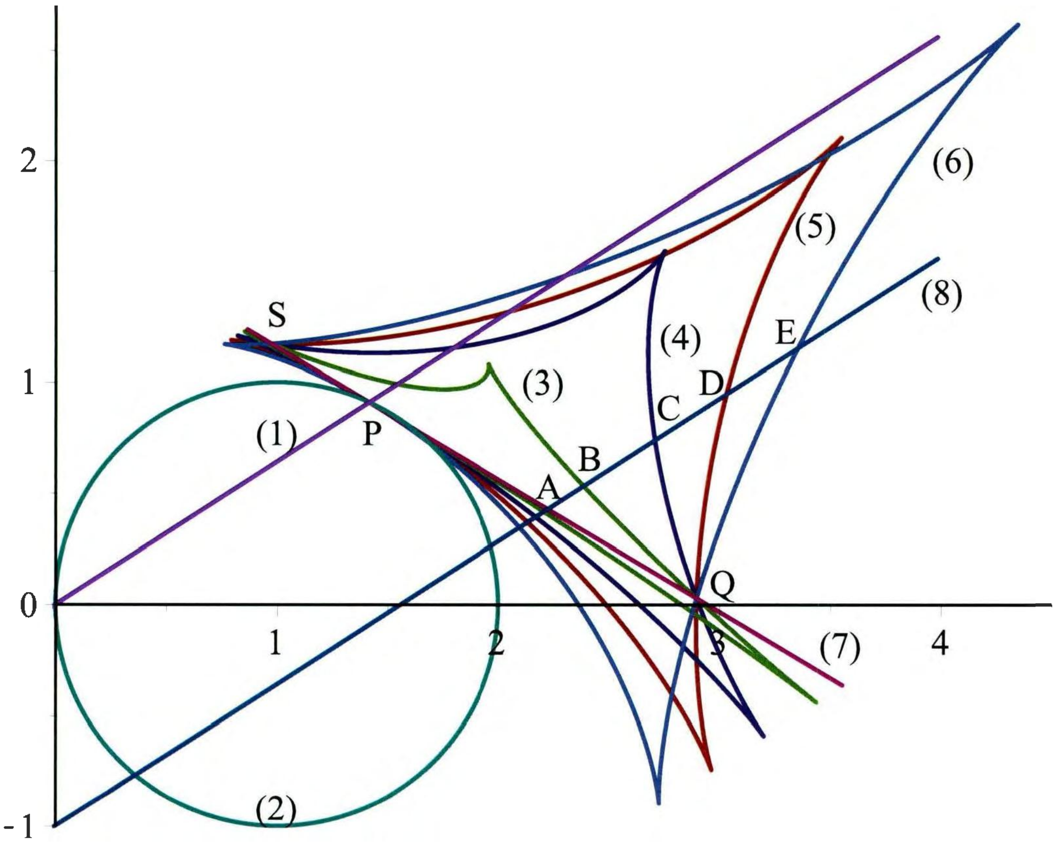

Figure 6.10: To Lemmas 6.2.21 and 6.2.23. Curves (1)-(8) are: line $y = x \cot 1$, circle $\Gamma_1(2)$, $\tilde{\Gamma}_3^1(2, 1, 0)$, $\tilde{\Gamma}_3^1(2, 1, -1)$, deltoid $\tilde{\Gamma}_3^1(2, 1, -2)$, $\tilde{\Gamma}_3^1(2, 1, -3)$, segment $\tilde{\Gamma}_3^1(2, 1, 0.5)$, line $y = x \cot 1 - 1$. Point P is passed through by curves (1)-(7), points S and Q belong to curves (3)-(7). Note, $|AD| = 5|AB| = \frac{5}{3}|AC| = \frac{5}{7}|AE|$ as lines (1) and (8) are parallel.

Lemma 6.2.23. *Given* $(r_1, r_2, r^*) \in L_3$, $r_1 \neq 0$, *the area covered by a k-image-set of* (r_1, r_2, r_3) *is equal to the area of the deltoid* $\tilde{\Gamma}_3^k(r_1, r_2, -r_1)$ *times* $|\frac{r_3 - r^*}{r_3 + r_1}|$ *for any* $k \in \mathbb{R} \bmod \pi$ *and any* $r^* \in \mathbb{R}$.

Proof. The proof is similar to that of Lemma 6.2.19, but now, the length of the slices of k-image-set of (r_1, r_2, r^*) cut along the line $x \cos k = y \sin k$ will be $|\frac{r_3 - r^*}{r_3 + r_1}|$ times that of the deltoid $\tilde{\Gamma}_3^k(r_1, r_2, -r_1)$ by Lemma 6.2.21. $\square$

Theorem 6.2.24. (The Deltoid Theorem) *Let perpendicular planes Π^*, $\Pi^{**} \in \mathbb{R}^3$ intersect along a line l^* tangent to a deltoid $D \subset \Pi^*$, and a line l_* be such that $l_* \nparallel \Pi^{**}$. Then a family of lines parallel to l_* passing through D will cut on Π^{**} a curve which is of shape of $\tilde{\Gamma}_3^k(R, R', R'')$ for some $(R, R', R'') \in L_3$ and some $k \in [0, \pi]$. The converse statement is true as well: given two perpendicular planes Π^*, $\Pi^{**} \in \mathbb{R}^3$ and a deltoid $D \in \Pi^*$, for any $(R, R', R'') \in L_3$ and any $k \in [0, \pi)$ there is a line $l_* \nparallel \Pi^{**}$ such that a curve similar to $\tilde{\Gamma}_3^k(R, R', R'')$ is cut on Π^{**} by lines parallel to l_* passing through D.*

Proof. Let Π_1 be a plane with Cartesian coordinate system xOy. Suppose, we are to find the shape of $\tilde{\Gamma}_3^k(r_1, r_2, r^*) \in \Pi_1$.

Draw the deltoid, $D = \tilde{\Gamma}_3^k(r_1, r_2, -r_1)$ and a line $l_1 \in \Pi_1$ containing

a) the segment $\tilde{\Gamma}_3^k(r_1, r_2, r_3)$, $r_3 = \frac{r_2^2}{r_1}$ if $r_1 \neq 0$, or

b) the segment $\tilde{\Gamma}_3^k(0, 0, r_2)$ if $r_1 = 0$.

Denote the segment we chose out of a) or b) by C^*.

It follows from Lemma 6.2.15 that l_1 is tangent to D at some point.

Let a plane $\Pi_2 \perp \Pi_1$ be such that $\Pi_1 \cap \Pi_2 = l_1$ and a deltoid D' be the result of rotation of D by 90 degrees around l_1.

Construct $\tilde{\Gamma}_3^k(r_1, r_2, r^*) \in \Pi_1$ and connect its points with the corresponding points of D'. As it follows from Lemmas 6.2.20 and 6.2.21, the triangles with vertices in corresponding points of D, D' and the segment C^* are similar, hence the lines are parallel. Denote the family of these lines by $\mathcal{L}$.

If we move Π_1 along the line perpendicular to Π_2, the figure on Π_1, cut by the lines from $\mathcal{L}$ passing though D', will change neither the size nor the shape.

By Lemma 6.2.14, we know that $\tilde{\Gamma}_3^k(r_1, r_2, r_3)$, $r_1 \neq 0$ passes through the pole of the corresponding Cayley sextic and through $X_k \in \gamma_k$. Since the latter depends only on r_1, the former may take any position in semi-plane $x \leq r_1$, should we vary r_2 (and consequently, r_3). Hence $\tilde{\Gamma}_3^k(r_1, r_2, r_3)$ may form any angle with $\tilde{\Gamma}_3^k(0, 0, r_3)$. That implies that any family of parallel lines, such that they are neither parallel to Π_2 nor perpendicular to Π_1, passing through D' will cut on Π_1 a curve similar to some $\tilde{\Gamma}_3^k(R, R', R'')$, $(R, R', R'') \in L_3$.

On the other hand, there is nothing special about the tangency point of D and C^* (and therefore the orientation of D with respect to C^*), it varies for different k with fixed $(r_1, r_2, -r_1) \in L_3$, taking all possible positions from a cusp to a cusp of the deltoid. It follows from the fact that the deltoid makes a $\frac{\pi}{3}$-rotation when k run from 0 to π (see Lemma 6.2.11). Indeed, the cusps of the deltoids envelope the nephroid, and no k-image-set coincide ($X_{(\frac{k_1}{3})^3} \neq X_{(\frac{k_2}{3})^3}$, $k_1 \neq k_2$). Meanwhile, C^* makes a π-rotation as k runs from 0 to π.

That implies that the orientation of D' with respect to C^* could be any, which completes the proof of the converse statement. □

Remark. In the Deltoid Theorem, we actually deal with the projections (shadows) of a deltoid. The projection directions are not orthogonal to the projection plane in general. We will look at envelopes of those projections closely in Section 6.4.

6.3 The Triple Envelope Theorem

Before resuming work on the 3rd iteration, we will prove an important statement over a general n iteration image-set, since the proof of the same statement over the 3rd iteration is no shorter. To do so we have to introduce a special curve, consisting of points resulted in the nth iteration of $X \in \gamma$. The Deltoid Theorem gives a good insight to that introduction.

Given a curve γ let a point $X \in \gamma$ and a constant $\alpha \in \mathbb{R} \bmod \pi$. Then, by analogy to the 3rd iteration case, the locus of points $\{X_{\theta^{n-1}(\alpha-(n-1)\theta)}\}_{\theta=0}^{\pi}$ will be denoted by $\tilde{\Gamma}_n^{\alpha}$. Clearly, it is a curve, depending on parameter θ.

Definition 6.3.1. *Let $\alpha \in \mathbb{R} \bmod \pi$ be some constant. We will call the image-set of $X_{\theta_1 \ldots \theta_n}$, where $(\theta_1 + \ldots + \theta_n) \bmod \pi = \alpha$, a constant sum image-set or a parallel tangent image-set in general and α-image-set in particular.*

The fact, that $\tilde{\Gamma}_n^{\alpha}$ bounds the α-image-set in some important cases will be proven later, and for now, we will manipulate with the notion of $\tilde{\Gamma}_n^{\alpha}$ without using this property. Further, we have not used the boundary property of Γ_n so far. For now, we just point out that tangents to curves $\gamma_{\theta^{n-1}(\alpha-(n-1)\theta)}$ at $X_{\theta^{n-1}(\alpha-(n-1)\theta)}$ are parallel.

Let us introduce two more objects for further research:

(1) Let us take and fix $\alpha \in [0, \pi]$ and consider $(n-1)$ evolutoidal transformations of the point $X_{\alpha} \in \gamma_{\alpha}$. Denote the set $\{X_{\alpha\theta^{n-1}}\}_{\theta=0}^{\pi}$ by Γ_n^{α}. Clearly, it is a closed curve parametrized by θ.

(2) Let us take and fix $\theta \in [0, \pi]$ and denote the set $\{X_{\theta^{n-1}\alpha}\}_{\alpha=0}^{\pi}$ by $\hat{\Gamma}_n^{\alpha}$. Clearly, $\hat{\Gamma}_n^{\alpha}$ is a circle, representing the image-set of one evolutoidal transformation of a point $X_{\theta^{n-1}} \in \gamma_{\theta^{n-1}}$.

Consider the equations of a family of curves in the form

$$\begin{cases} x = x(\theta, \alpha) \\ y = y(\theta, \alpha), \end{cases} \tag{6.3.1}$$

where the parameters $\theta, \alpha \in [0, \pi]$. Holding the parameter α fixed, we obtain parametric equations of a curve, and different values of α define different members of the family (6.3.1).

In this setting, a point is in the envelope of the family if

$$\begin{vmatrix} \dfrac{\partial x}{\partial \theta} & \dfrac{\partial x}{\partial \alpha} \\ \dfrac{\partial y}{\partial \theta} & \dfrac{\partial y}{\partial \alpha} \end{vmatrix} = 0. \tag{6.3.2}$$

Theorem 6.3.2. (Triple Envelope Theorem) *The envelopes of families of curves*

(a) $\{\Gamma_n^\alpha\}_{\alpha=0}^{\pi}$,

(b) $\{\hat{\Gamma}_n^\alpha\}_{\alpha=0}^{\pi}$,

(c) $\{\tilde{\Gamma}_n^\alpha\}_{\alpha=0}^{\pi}$,

coincide. If Γ_n has singular points, each of the curves Γ_n^α and $\tilde{\Gamma}_n^\alpha$ passes through them.

Proof. We will prove the statement for $n+1$ iterations instead of n to make formulas simpler.

Denote:

$$\begin{cases} x_\theta = Rs^2 + R_\theta s s_2 + \ldots + R_{\theta^{n-1}} s s_n \\ y_\theta = Rsc + R_\theta s c_2 + \ldots + R_{\theta^{n-1}} s c_n, \end{cases} \tag{6.3.3}$$

Consider the equations of each of the three families of curves, where α is a fixed parameter, defining a member of a family:

(a) Γ_{n+1}^α:

$$\begin{cases} x_1 = x_\theta + R_{\theta^n} \sin\alpha \sin(\alpha + n\theta) \\ y_1 = y_\theta + R_{\theta^n} \sin\alpha \cos(\alpha + n\theta). \end{cases} \tag{6.3.4}$$

(b) The circles (the image-sets of one iteration of X_{θ^n}), $\hat{\Gamma}^{\alpha}_{n+1}$:

$$\begin{cases} x_2 = x_\alpha + R_{\alpha^n} \sin\theta \sin(\theta + n\alpha) \\ y_2 = y_\alpha + R_{\alpha^n} \sin\theta \cos(\theta + n\alpha). \end{cases} \tag{6.3.5}$$

(c) $\tilde{\Gamma}^{\alpha}_{n+1}$:

$$\begin{cases} x_3 = x_\theta + R_{\theta^n} \sin\alpha \sin(\alpha - n\theta) \\ y_3 = y_\theta + R_{\theta^n} \cos\alpha \sin(\alpha - n\theta). \end{cases} \tag{6.3.6}$$

Let us show that the first two families of curves have the same envelope(s). Notice, that the parameters α and θ just swap the places in the equations (6.3.5) and (6.3.4). If a pair (α_*, θ_*) is a solution of equation (6.3.2) for the family (a), a pair (θ_*, α_*) is a solution of this equation for the faimily (b), and visa versa.

Plugging the equations (6.3.4) in (6.3.2) and denoting $\frac{\partial x_\theta}{\partial \theta}$ and$\frac{\partial y_\theta}{\partial \theta}$ by x'_θ and y'_θ respectively, we get

$\frac{\partial x_1}{\partial \theta}\frac{\partial y_1}{\partial \alpha} - \frac{\partial y_1}{\partial \theta}\frac{\partial x_1}{\partial \alpha} = R_{\theta^n}((x'_\theta + (\frac{\partial R_{\theta^n}}{\partial \theta}\sin(n\theta+\alpha) + nR_{\theta^n}\cos(n\theta+\alpha))\sin\alpha)\cos(n\theta+2\alpha) -$
$(y'_\theta + (\frac{\partial R_{\theta^n}}{\partial \theta}\cos(n\theta+\alpha) - nR_{\theta^n}\sin(n\theta+\alpha))\sin\alpha)\sin(n\theta+2\alpha)) = 0,$

or after combining the like-terms,

$$R_{\theta^n}(x'_\theta \cos(n\theta + 2\alpha) - y'_\theta \sin(n\theta + 2\alpha) - \frac{\partial R_{\theta^n}}{\partial \theta}\sin^2\alpha + nR_{\theta^n}\sin\alpha\cos\alpha) = 0. \tag{6.3.7}$$

If we use the identities $R_{\theta^n} = \cos\theta R_{\theta^{n-1}} - \sin\theta\frac{\partial R_{\theta^{n-1}}}{\partial \psi}$ (by (4.2.1)) and $\frac{\partial R_{\theta^n}}{\partial \theta} = -n\sin\theta R_{\theta^{n-1}} - n\cos\theta\frac{\partial R_{\theta^{n-1}}}{\partial \psi}$ (by (4.2.9)), we can combine the last two terms in (6.3.7):

$$R_{\theta^n}(x'_\theta \cos(n\theta + 2\alpha) - y'_\theta \sin(n\theta + 2\alpha) + n\sin\alpha R_{\theta^{n-1}(\theta-\alpha)}) = 0. \tag{6.3.8}$$

The equation (6.3.8) presents an implicit relationship between α and θ, which can be resolved locally by either

$$\theta = \Psi(\alpha) \tag{6.3.9}$$

or

$$\alpha = \Phi(\theta). \tag{6.3.10}$$

Without loss of generality. assume (6.3.9) is possible. Then plugging it in (6.3.7), we get parametric equations on the envelope of the family (a)

$$\begin{cases} x_1 = x_1(\Psi(\alpha), \alpha) \\ y_1 = y_1(\Psi(\alpha), \alpha). \end{cases} \tag{6.3.11}$$

Then we obtain the same relationship for the family (b)

$$\begin{cases} x_2 = x_2(\Psi(\theta), \theta) \\ y_2 = y_2(\Psi(\theta), \theta). \end{cases} \tag{6.3.12}$$

Hence, the two families have the same envelope(s). Moreover, it follows from (6.3.11) and (6.3.12) that a pair (α_*, θ_*) which satisfies (6.3.8) represents the same point as the pair (θ_*, α_*), solving the equation for the envelope(s) of the family (b). In other words, $X_{\theta_*^{n-1}\alpha_*}$ and $X_{\alpha_*^{n-1}\theta_*}$ coincide. Hence, the envelope(s) are the locus of such points.

Following the same procedure by plugging the equations (6.3.6) in (6.3.2), and combining the like terms in the way we just did above, we obtain:

$$R_{\theta^n}(x'_\theta \cos(2\alpha - n\theta) - y'_\theta \sin(2\alpha - n\theta) + n\sin(\alpha - n\theta)R_{\theta^{n-1}((n+1)\theta-\alpha)}) = 0. \tag{6.3.13}$$

Suppose a pair (α_*, θ_*) is a solution of (6.3.13). Then setting $\alpha_* - n\theta_* = \beta_*$, and plugging β_* for α_* in the equation, we get:

$$R_{\theta_*^n}(x'_{\theta_*}\cos(2\beta_* + n\theta_*) - y'_{\theta_*}\sin(2\beta_* + n\theta_*) + n\sin(\beta_*)R_{\theta_*^{n-1}(\theta_*-\beta_*)}) = 0, \quad (6.3.14)$$

which means that the envelope of $\tilde{\Gamma}_{n+1}^{\alpha}$ is a part of the envelope of Γ_{n+1}^{α}. On the other hand, for any (α_*, θ_*) solving (6.3.8), the point $X_{\theta_*^n\alpha_*}$ belongs to $\tilde{\Gamma}_{n+1}^{\alpha_*+n\theta_*}$. Setting $\beta_* = \alpha_* + n\theta_*$ and plugging it in the equation (6.3.8), we obtain, that the envelope of Γ_{n+1}^{α} is a part of the envelope $\tilde{\Gamma}_{n+1}^{\alpha}$. Hence, the envelopes coincide.

Suppose Γ_{n+1} has a singularity at $X_{\theta_*^{n+1}}$. That means, that $R_{\theta^n} = 0$, or, in other words, $X_{\alpha\theta_*^n}$ coincides with $X_{\theta_*^{n-1}}$ for any $\alpha \in [0, \pi]$. Therefore, any curve $\tilde{\Gamma}_{n+1}^{\alpha}$ and any curve Γ_{n+1}^{α} pass through all those points. $\square$

6.4 The envelopes of the deltoid's projections

In this Section, we will consider families of the boundaries of k-image-sets, $k \in [0, \pi)$, for the third iteration of a point $X \in \gamma$. Namely, we will focus on their envelopes and the envelopes of cusps of special families of cardioids, the image-sets of the second iteration of $X_\alpha \in \gamma_\alpha$, $\alpha \in [0, \pi)$. We will call them *cardioids of the last two iterations.* Clearly, the last two iteration cardioids are curves Γ_3^α, $\alpha \in [0, \pi]$.

Lemma 6.4.1. *If a point of the 3rd iteration $X_{\theta^2\alpha}$, $\alpha \neq \theta$, lies on the part of the envelope of the cardioids of the last two iterations, other then Γ_3, then it is the cusp of Γ_3^α, where $\alpha \in [0, \pi]$ is some fixed number.*

Proof. From The Triple Envelope Theorem, we know that if $X_{\theta^2\alpha}$, $\alpha \neq \theta$, belongs to the cardioidal envelope, it coincides with $X_{\alpha^2\theta}$.
We have $X_{\alpha^2\theta} = X_{\theta\alpha\alpha}$ and $X_{\theta^2\alpha} = X_{\theta\alpha\theta}$. In other words, $X_{\theta\alpha\alpha} = X_{\theta\alpha\theta}$. That implies that $R_{\theta\alpha} = 0$. Therefore, $\gamma_{\theta\alpha}$ has a singularity at $X_{\theta\alpha}$. It follows from Theorem 4.2.6, that $X_{\theta\alpha}$ is the cusp of the cardioid bounding the image-set of the second iteration of $X_\theta \in \gamma_\theta$. □

Theorem 6.4.2. (Cayley sextic construction). *Let Ω be a circle and $X \in \Omega$ be a fixed point. Let $[XX^*]$ be a chord of Ω, Ω^* be a circle based on $[XX^*]$ as its diameter and C^* be a cardioid obtained by tracing a fixed point on a circle of the size of Ω^*, rolling upon Ω^* starting from X. Then the envelope of such cardioids is a Cayley sextic.*

Proof. The procedure described in the statement of this Lemma resembles that of the construction of $\Gamma_3(1, 0, 0)$. The latter was the following:
Let $X \in \gamma$ be a point on a curve, passing through the origin with y-axis tangent to it. Let γ be parametrized by the Gaussian map parameter ψ. Let the radius of curvature and its first two derivatives with respect to ψ of γ at X be 1,0,0 respectively. Draw

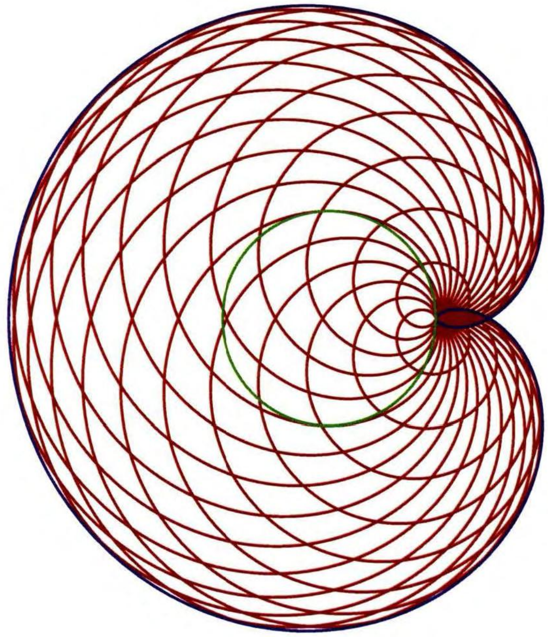

Figure 6.11: To Theorem 6.4.2.

a unit circle given by parametric equations

$$\begin{cases} x = \sin^2\theta \\ y = \sin\theta\cos\theta \end{cases}, \theta \in [0, \pi] \tag{6.4.1}$$

Then the range of the last two iterations of a point X_θ will be a cardioid with the cusp at $(1, 0)$ and the main chord (from the cusp to the opposite point) $[XX_\theta]$. The locus of midpoints of chords $[XX_\theta]$ when θ runs from 0 to π is a circle given by parametric equations

$$\begin{cases} x = \frac{1}{4}\cos\theta + \frac{3}{4} \\ y = \frac{1}{4}\sin\theta \end{cases}, \theta \in [0, \pi] \tag{6.4.2}$$

$\square$

Lemma 6.4.3. *Let* $(R, R', R'') = (1, 0, r) \in L_3$, $r \in \mathbb{R}$. *Then the envelope of* $\tilde{\Gamma}_3^\alpha$, *other then Γ_3, is*

(a) a complete circle, if $r > 0$,

(b) a point, if $r = 0$,

(c) a circular arc connecting the cusps of Γ_3, if $r < 0$.

In particular, if $r = -1$, the envelope is a line segment, which can be viewed as an arc of a circle of zero curvature.

Proof. By The Triple Envelope Theorem, we know that the the envelopes of Γ_3^α and $\tilde{\Gamma}_3^\alpha$ coincide. Definitely, a part of this envelope is Γ_3. To observe the remaining part of the envelope, we consider the locus of cusps of cardioids of the last two iterations. Let $r > 0$. Let Ω_1 be a unit circle based on $[XE]$ as its diameter, $X = (0,0)$, $E = X_{\frac{\pi}{2}} = (1,0)$, $E_e = X_{(\frac{\pi}{2})^2} = (1 - r, 0)$, and Ω_3 be circle of diameter r tangent to Ω_1 at E from inside (Figure 6.12(a)). Let $\theta \in [0, \pi]$, and construct by usual procedure X_θ and $X_{\theta(\frac{\pi}{2})^2}$, denoting them by A and C respectively. Let EB be a height of the triangle $\triangle AEC$, and $O = CA \cap XE$.

By construction, $\widehat{AEC} = \frac{\pi}{2}$. Since $\widehat{EXA} = \widehat{EOC} = \frac{\pi}{2} - \theta$, the triangles $\triangle EXA$ and $\triangle EOC$ are similar. Therefore, $\frac{|EO|}{|XE|} = \frac{|CE|}{|XA|} = \frac{r \sin\theta}{1 \cdot \sin\theta} = r$.

That implies, that the position of $O \in [XE]$ does not depend on θ. Hence, B lies on the circle based on $[EO]$ as its diameter. Clearly, as θ runs from 0 to π, B describes the whole circle. The argument is still valid when $r = 0$, but then O coincides with E.

Since $r_2 = 0$, we have $E = X_{\frac{\pi}{2}} = X_{\theta\frac{\pi}{2}}$. Now, since E and C are respectively the points on the evolute and the evolute of the evolute of γ_θ, corresponding to $A = X_\theta$, the point B corresponds to the cusp of the cardioid representing the image-set of the second iteration of X_θ. Apparently, the circle described by those cusps lies entirely inside the image-set of the 3rd iteration, since any cardioid of the last two iterations contains E by The Cardioid Theorem (see Figure 3.5), and the rest of the circle falls

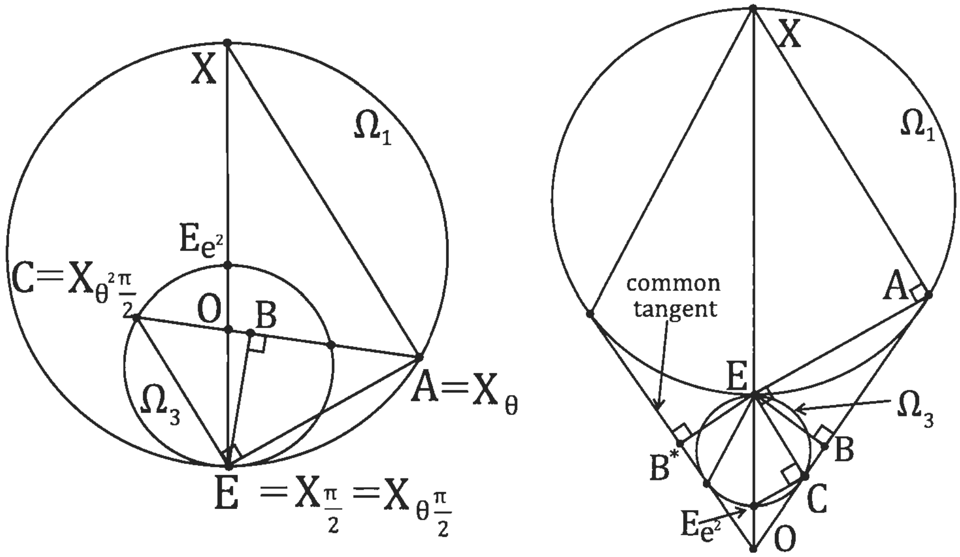

(a) (b)

Figure 6.12: To Lemma 6.4.3. (a) The case $r > 0$; (b) The case $r < 0$.

inside $\Gamma_2(r_1, 0)$. If $r_3 = 0$, then E is also an inner point of the image-set of the 3rd iteration (see Figure 6.11).

Now, let $r < 0$. Keeping the same notations, we notice the sketch will differ from the case $r > 0$ by the position of Ω_3, since now it is tangent to Ω_1 at E from outside. (Figure 6.12(b))

The position of the point $O = AC \cap XE$ is constant, since the triangles $\triangle OXA$ and $\triangle OEC$ are similar. We have: $\frac{|XO|}{|EO|} = \frac{|XA|}{|EC|}$. Using $|XO| = |EO| + 1$ and $\frac{|XA|}{|EC|} = -\frac{1}{r}$, we obtain $|EO| = \frac{r}{r+1}$. That implies that the foot of perpendicular dropped on AC from E (the cusp of the cardioid by Theorem (3.4.7)) lies on an arc of a circle of radius $\frac{r}{r+1}$ centered at O.

As we let θ run from 0 to π, the cardioidal cusps describe a circular arc, which endpoints lie on common tangents to Ω_1 and Ω_3. Denote one of the arc's endpoints (on the left) by B^*. Simple geometry suggests that $|EB^*| = -r\sin^2\theta = \cos^2\theta$. In other words, solving equation

$$r \sin^2 \theta + \cos^2 \theta = 0, \tag{6.4.3}$$

we find the "extremal" angles and the coordinates of the arc's endpoints, $\cot \theta = \pm\sqrt{-\frac{1}{r}}$. But the equation (6.4.3) is the condition for $R_{\theta^2} = 0$, therefore the endpoints of the arc are the points of singularity of Γ_3. $\square$

Lemma 6.4.4. *Let $(R, R', R'') = (r_1, r_2, r_3) \in L_3,\ r_2 \neq 0$. The locus of cusps of the cardioids representing the image-set of the second iteration of $X_\theta \in \gamma_\theta,\ \theta \in [0, \pi]$ is a circle or a circular arc.*

Proof. Apply the setting of Theorem 5.2.4, let circles $\Omega_i,\ i = 1, 2, 3$ be of radii r_1, r_2, r_3 respectively. Let $\theta_1 = \frac{\pi}{2},\ \theta_2 = \operatorname{arccot} \frac{r_1}{r_2},\ \theta_3 \in [0, \pi]$. Define $\theta_4 = \frac{\pi}{2} + \operatorname{arccot} \frac{r_3}{r_2}$, so that $X_{(\frac{\pi}{2})^2\theta_4} \in \Omega_2 \cap \Omega_3$, and denote $X_{(\frac{\pi}{2})^2\theta_4} = O$, see Figure 6.13.

It is clear that $X_{\theta_2}X_{\theta_1} \perp X_{\theta_2}X'_{\theta_1}$ and $OX_{\theta_1} \perp OX'_{\theta_1}$.

Assume first $r_1 + r_3 \neq 0$. Denote $X_{\theta_2}X''_{\theta_2} \cap X_{\theta_1}X''_{\theta_1} = Q_1$ and $X_{\theta_2}X_{\theta_1} \cap OP_{12}(X_{\theta_1}) = Q_2$. Note, that $\triangle Q_1X_{\theta_2}X_{\theta_1}$ and $\triangle Q_2X_{\theta_2}X_{\theta_1}$ are similar right triangles.

Now, denote $X_{\theta_2}X_{\theta_1} \cap X''_{\theta_1}X'_{\theta_1} = N$ and note, that $|X'_{\theta_1}N| = \frac{r_2^2}{r_1}$ (see Lemma 6.2.13). We have

$$|X_{\theta_2}X_{\theta_1}| = \frac{r_1 r_2}{\sqrt{r_1^2 + r_2^2}}, \tag{6.4.4}$$

$$|OX_{\theta_1}| = \frac{r_2^2}{\sqrt{r_3^2 + r_2^2}}. \tag{6.4.5}$$

The similarity of $\triangle Q_1X_{\theta_2}X_{\theta_1}$ and $\triangle Q_2OX_{\theta_1}$ implies

$$\frac{|X_{\theta_2}X_{\theta_1}|}{|OX_{\theta_1}|} = \frac{r_1}{r_2}\frac{\sqrt{r_3^2 + r_2^2}}{\sqrt{r_1^2 + r_2^2}}. \tag{6.4.6}$$

On the other hand,

$$\frac{|X_{\theta_1}X''_{\theta_1}|}{|NX_{\theta_1}|} = \frac{r_1}{r_2}\frac{\sqrt{r_3^2+r_2^2}}{\sqrt{r_1^2+r_2^2}}. \tag{6.4.7}$$

Therefore $NX''_{\theta_1} \parallel Q_1Q_2$.

Since $\triangle_1$ and $\triangle_3$ are similar and the sides are parallel the line $X''_{\theta_3}X_{\theta_3}$ passes

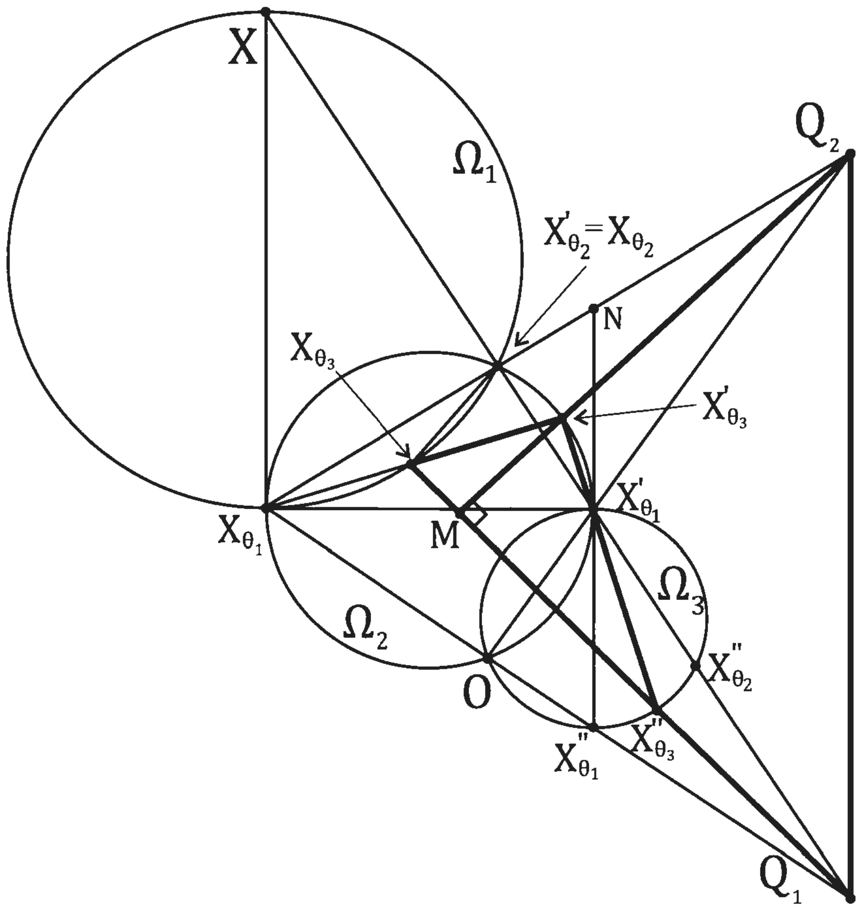

Figure 6.13: To Lemma 6.4.4.

through Q_1. Denote $M = Q_2X'_{\theta_3} \cap X''_{\theta_3}X_{\theta_3}$. Also note that $\triangle Q_1X''_{\theta_1}X''_{\theta_2}$ is similar to $\triangle Q_2X'_{\theta_1}X_{\theta_2}$ (the same angles). Applying rotational homothety with respect to O, mapping $\triangle_2$ onto $\triangle_3$, we map the line $Q_2X'_{\theta_3}$ onto $X''_{\theta_3}X_{\theta_3}$. Since angle of rotation is $\frac{\pi}{2}$, $Q_2X'_{\theta_3} \perp X''_{\theta_3}X_{\theta_3}$. Therefore, M lies on a circle based on Q_1Q_2 as its diameter.

But M is the foot of the height in $\triangle X_{\theta_3}X'_{\theta_3}X''_{\theta_3}$, and therefore the cusp of the cardioid representing the image-set of the second iteration of $X_{\theta_3} \in \gamma_{\theta_3}$.

The case $r_1 + r_3 = 0$ is treated by the similar argument, but in this case Q_1 and Q_2 are remote to "infinity", since the corresponding lines are parallel. So, applying the rotational homothety mapping $\triangle_2$ onto $\triangle_3$ we map the line parallel to $X_{\theta_2}X_{\theta_1}$ passing through X'_{θ_3} onto the line parallel to OX_{θ_1} passing through X''_{θ_3}. Clearly, the locus of intersections of of such lines is a segment, which can be viewed as an arc of a circle of zero curvature. $\square$

Theorem 6.4.5. (Deltoid Projection Envelope Theorem) *Let* $(R, R', R'') = (r_1, r_2, r_3) \in L_3$. *The envelope of* $\tilde{\Gamma}_3^{\alpha}$, *other then* Γ_3, *is a subset of a circle. Namely:*

(a) a complete circle, if the discriminant[4] $D > 0$, (Figure 6.14(a)),

(b) a point, if $D = 0$, (Figure 6.7),

(c) a circular arc connecting the cusps of Γ_3, *if* $D < 0$ (Figure 6.14(b)).

In particular, if (r_1, r_2, r_3) *belong to the nephroidal plane, the envelope is a line segment, which can be viewed as an arc of a circle of zero curvature* (Figure 6.14(c)).

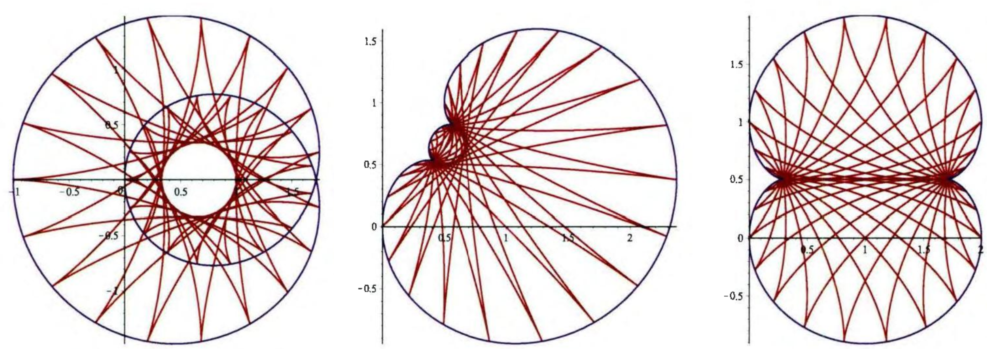

(a) (b) (c)

Figure 6.14: An illustration to Theorem 6.4.5: (a) $(R, R', R'') = (1, 0, 2)$, the envelope is a complete circle ; (b) $(R, R', R'') = (1, 1, 0.5)$, the envelope is a circular arc; (c) $(R, R', R'') = (1, 1, -1)$, the envelope is a line segment.

[4]Recall that the discriminant $D = RR'' - R'^2$ of the 3rd iteration was defined in Section 6.1

Proof. The statement of the Theorem holds when $r_2 = 0$ by Lemma 6.4.3. Assume $r_2 \neq 0$. Denote by Ω^* the circle based on Q_1Q_2 as its diameter[5].

Applying the setting and notations of Lemma 6.4.4, consider the position of the point X_{θ_2} with respect to the lines XX_{θ_1} and Q_1Q_2. There are three possible cases: (a) $D > 0$, (b) $D = 0$, (c) $D < 0$. Let us treat them separately.

(a) $D > 0$. Then it is clear that X_{θ_2} lies outside of the strip between XX_{θ_1} and Q_1Q_2. It was shown in Lemma 6.4.4, that $X_{\theta_2} \in \Omega^*$ and $O \in \Omega^*$. (Figure 6.15).

Note, that Ω^* is an incircle for Ω_1 and Ω_3, while X_{θ_2} and O being the corresponding

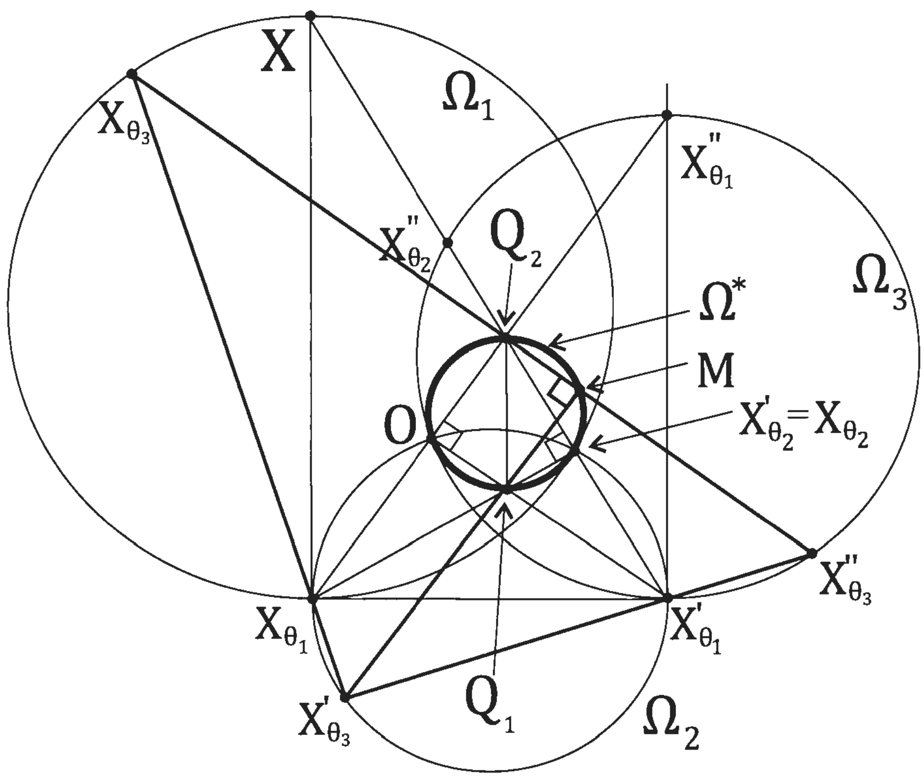

Figure 6.15: To Theorem 6.4.5. Case (a) $D > 0$.

tangency points: $X_{\theta_2} = \Omega^* \cap \Omega_1$, $O = \Omega^* \cap \Omega_3$. It follows from the fact, proven in Lemma 6.4.3, that $Q_1Q_2 \parallel XX_{\theta_1} \parallel X'_\theta X''_\theta$, so Ω^* is is homothetical to Ω_1 and Ω_3,

[5] All the points are defined as in Lemma 6.4.3

centers oh homotheties being X_{θ_2} and O respectively.

By Lemma 6.4.3, for any $\theta_3 \in [0, \pi]$, the foot of the height $X'_{\theta_3}M$ of triangle $\triangle X_{\theta_3}X'_{\theta_3}X''_{\theta_3}$, (point M), falls on Ω^*. Indeed, M, which is the cusp of the corresponding cardioid, is the second intersection point of line $X_{\theta_3}X''_{\theta_3}$ and circle Ω^*, so the cusps of cardioids of the last two iterations describe the whole circle as θ_3 runs from 0 to π.

(b) The case $D = 0$ follows from Theorem 6.4.2.

(c) Let now $D > 0$. Then obviously X_{θ_2} lies inside the strip between XX_{θ_1} and Q_1Q_2. If $r_1 = r_2 = 0$, then the radii of Ω_1 and Ω_3 are zero, and all the cusps of the cardioids representing the last two iterations of $X_\theta \in \gamma_\theta$ fall on the segment with the endpoints $(0, 0)$ and $(0, 1)$, which coincide with the cusps of the nephroid $\Gamma_3(0, 1, 0)$ by Lemma 6.1.6.

Assume now that $(r_1, r_2, r_3) \neq (0, r_2, 0)$. Since the case is a little bit more complicated, let us break it down into two separate cases:

Case 1. $r_1r_3 > 0$.

By the same argument presented in (a), Ω^* is the outcircle for Ω_1 and Ω_3, while X_{θ_2} and O being the corresponding tangency points: $X_{\theta_2} = \Omega^* \cap \Omega_1$, $O = \Omega^* \cap \Omega_3$, see Figure 6.16. Since $r_1 + r_3 < r_2$, we have $\Omega_3 \cap \Omega_1 = \varnothing$. We can also see that Ω^* is no longer covered fully by the feet of perpendiculars dropped from X'_θ to $X_\theta X''_\theta$ as θ runs from 0 to π. To determine the endpoints of the arc, draw two internal common tangents to Ω_1 and Ω_3. Denote their tangency points on Ω_1 by X_{θ^*} and $X_{\theta^{**}}$, where θ^*, θ^{**} are corresponding angles at the vertex X_{θ_1} of $\triangle XX_{\theta_1}X_{\theta^*}$ and $\triangle XX_{\theta_1}X_{\theta^{**}}$ respectively. Without loss of generality, let $\theta^* < \theta^{**}$, $\theta^*, \theta^{**} \in [0, \pi]$. Following the construction of X'_{θ^*}, $X'_{\theta^{**}}$, X''_{θ^*}, $X''_{\theta^{**}}$, according to definition 5.2.1, we conclude, that X''_{θ^*} and $X''_{\theta^{**}}$ coincide with the tangency points of common internal tangents, lying on Ω_3. It follows from the homothety with pole at Q_1, mapping Ω_1 onto Ω_3.

Denote by M^* and M^{**} the feet of heights in $\triangle X_{\theta^*}X'_{\theta^*}X''_{\theta^*}$ and $\triangle X_{\theta^{**}}X'_{\theta^{**}}X''_{\theta^{**}}$, corresponding to X'_{θ^*} and $X'_{\theta^{**}}$ respectively. So as the parameter θ runs from θ^* to θ^{**}, the corresponding foot of the height of $\triangle X_\theta X'_\theta X''_\theta$ describes the circular from M^* and M^{**}, and as the parameter runs from θ^{**} to $\theta^* + \pi$, the arc is spanned backwards. By the construction of the 2nd iteration, the point $X_{(\theta^*)^2}$ lies on the tangent to $\Gamma_1 = \Omega_1$ at X_{θ^*} and on the tangent to Ω_2 at X'_{θ^*}. But this is M^*!. Thus, $X_{(\theta^*)^2} = M^*$. Since M^* is the cusp of the cardioid of the second iteration of $X'_\theta \in \gamma_{\theta^*}$, we conclude, that $\gamma_{(\theta^*)^2}$ is singular. Therefore, by Lemma 6.1.15, M^* is a singularity point on Γ_3 (a cusp). By the same argument, M^{**} is another cusp of Γ_3.

<u>Case 2</u>. $r_1 r_3 > 0$.

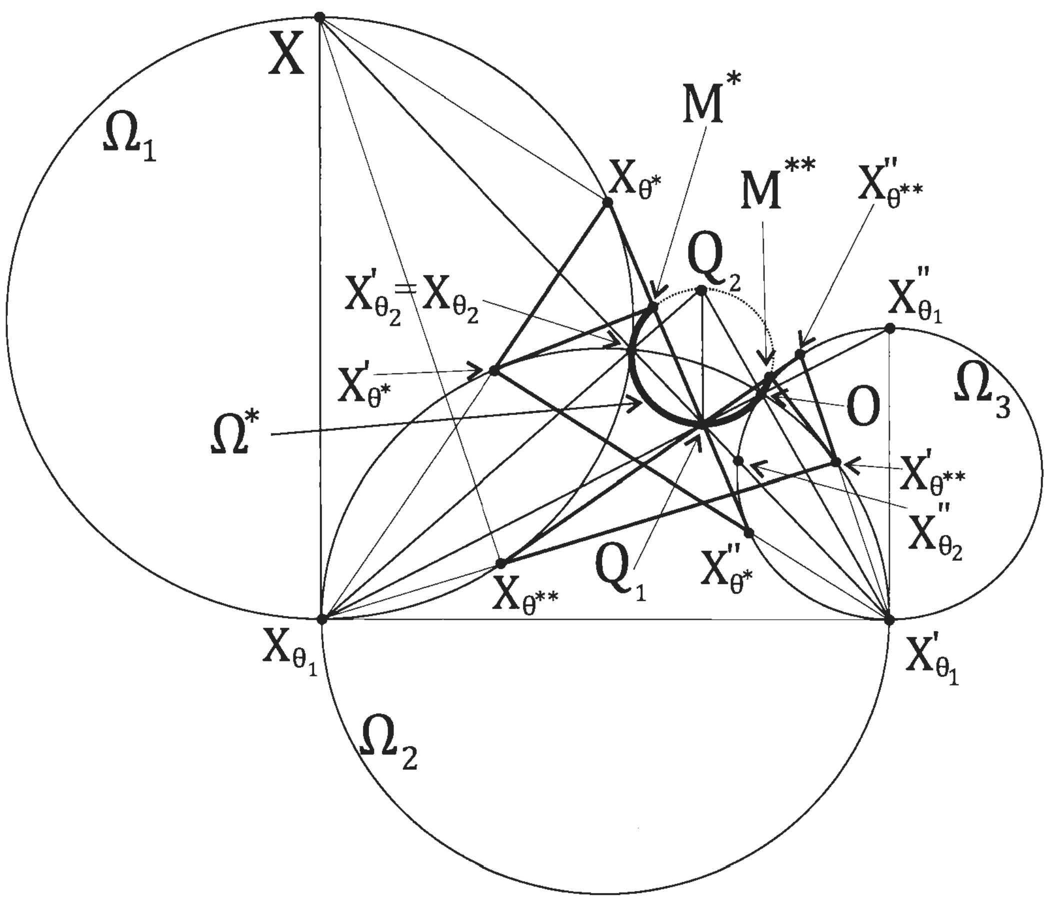

Figure 6.16: To Theorem 6.4.5. Case (a) $D < 0$, $r_1 r_3 > 0$.

We may use the picture to Lemma 6.4.4. In that case, Ω^* is an outcircle for Ω_1 and an incircle for Ω_3. It is clear that the arc of Ω^* between to external tangents to Ω_1 and Ω_3 is covered by the feet of perpendiculars dropped from X'_θ to $X_\theta X''_\theta$ as θ runs from 0 to π. The proof, that the endpoints of that arc are, in fact, the singularity points of Γ_3, is the same as presented above for the case $r_1 r_3 > 0$.

By Triple Envelope Theorem, the envelopes of the family of cardioids of the last two iterations and the boundaries of α-constant sum image-sets coincide. Then the statement of the theorem follows from Lemma 6.4.1. $\square$

Corollary 6.4.6. *If $\theta_1, \theta_2, \theta_3$ are pairwise different (by $\bmod \pi$), then $X_{\theta_1\theta_2\theta_3}$ is an inner point of the image-set of the 3rd iteration.*

Proof. Let $(\theta_1 + \theta_2 + \theta_3) \bmod \pi = \alpha \in [0, \pi)$. Then, the statement follows from the fact that the point $X_{\theta_1\theta_2\theta_3}$ is an inner point of $\tilde{\Gamma_3^\alpha}$, see Lemma 6.2.2. $\square$

Theorem 6.4.7. (The boundary of the 3rd iteration image-set) *The the 3rd iteration image-set is bounded by arcs of Γ_3.*

Proof. By Theorems 6.4.5 and 6.3.2, the image-set of the 3rd iteration is bounded by the envelope of cardioids of the last two iterations, which consists of Γ_3 and Ω^*. But all the points of the latter, except the arc's endpoints and X_{θ_2}, are inner points of the image-set of the 2nd iteration, not to mention the 3rd. In the case of Ω^* being a complete circle, it follows since all its points, except X_{θ_2} are inner points of the Γ_2 and X_{θ_2} is an inner point of $\Gamma_3^{\theta_1}$, see Figure 6.15. In case of Ω^* being a circular arc, it follows, since Ω^* lies within two circles triangle X_{θ_2} and based on $[X_{\theta^*} X'_{\theta^*}]$ and $[X_{\theta^{**}} X'_{\theta^{**}}]$ as their diameters, see Figures 6.16 and 6.13. The point X_{θ_2} is, obviously an inner point of $\Gamma_3^{\theta_1}$. In the case, when Γ_3 is a Cayley sextic, Ω^*, which is the pole of the Cayley sextic, is an inner point of the image-set of the third iteration by Theorem 6.4.2. $\square$

Corollary 6.4.8. *If $X_{\theta_1\theta_2\theta_3}$ lies on the boundary of the image-set of the 3rd iteration and is not a singular point of Γ_3, then $\theta_1 = \theta_2 = \theta_3$.*

Proof. Suppose, $X_{\theta_1\theta_2\theta_3}$ lies on the boundary of the image-set of the 3rd iteration and is not a singular point of Γ_3, and $\theta_1 = \theta_2 = \theta_3$ is not true. Then by Corollary 6.4.6, $\theta_1, \theta_2, \theta_3$ can not be pairwise different (by $\bmod \pi$), so without loss of generality $X_{\theta_1\theta_2\theta_3}$ is $X_{\alpha_1^2\alpha_2}$, $\alpha_1 \neq \alpha_2$.

Since $X_{\alpha_1^2\alpha_2}$ is not a cusp of Γ_3, then $\gamma_{\alpha_1^2}$ is not singular by Lemma 6.1.14. But then $X_{\alpha_1^2\alpha_2}$ is an inner point of the region bounded by the cardioid $\Gamma_3^{\alpha_2}$ and hence an inner point of the image-set of the 3rd iteration. Contradiction. □

Now, let us denote by $\Omega^n(R, R', ..., R^{n-1})$ the image-set of the nth iteration and by $\tilde{\Omega}^n_\alpha(R, R', ..., R^{n-1})$ the α-constant image-set. When it is irrelevant or clear, we will omit the specific notation $(R, R', ..., R^{n-1})$ and write simply Ω^n and $\tilde{\Omega}^n_\alpha$.

Theorem 6.4.7 gives a tool to prove the general statements about relationship between a curve $\Gamma_n(R, R', ..., R^{n-1})$ and $\Omega^n(R, R', ..., R^{n-1})$ on one hand, and between $\tilde{\Gamma}^\alpha_n(R, R', ..., R^{n-1})$ and $\tilde{\Omega}^n_\alpha(R, R', ..., R^{n-1})$ on the other, $n \in \mathbb{N}$, $\alpha \in \mathbb{R} \bmod \pi$. Analogously to $\tilde{\Omega}^n_\alpha$, we introduce also the image-set of the $(n-1)$th iteration of a point $X_\alpha \in \gamma_\alpha$, $\alpha \in [0, \pi)$ and denote it by Ω^n_α.

Denote also the boundaries of Ω^n, $\tilde{\Omega}^n_\alpha$ and Ω^n_α by $\partial\Omega^n$, $\partial\tilde{\Omega}^n_\alpha$ and $\partial\Omega^n_\alpha$ respectively.

We are going to present these relationships in the two following below theorems.

Theorem 6.4.9. (The boundary of the nth iteration image-set) *The boundary of Ω^n consists of arcs of the curve Γ_n.*

Proof. Let $\Gamma_n = \Gamma_n(R, R', ..., R^{n-1})$. Apply mathematical induction. The cases $n = 1, 2, 3$ are true by Theorems 2.4.6, 3.4.7 and 6.4.7.

Suppose the statement is true for all $k \leq n, n \geq 3$.

Clearly, $\Omega^{n+1} = \cup\Omega^{n+1}_\alpha$, $\alpha \in [0, \pi)$, hence[6] its boundary, $\partial\Omega^{n+1}$, is enveloped by the

[6]By the induction step, each of Ω^{n+1}_α, $\alpha \in [0, \pi)$ is bounded by arcs of Γ^α_{n+1}.

family $\{\Gamma^{\alpha}_{n+1}\}^{\pi}_{\alpha=0}$. Therefore, $\partial\Omega^{n+1}$ consists of arcs of envelope of $\{\Gamma^{\alpha}_{n+1}\}^{\pi}_{\alpha=0}$. By Triple Envelope Theorem, the latter consists of either points[7] $X_{\alpha\theta^n}$ or points[8] $X_{\theta^{n+1}}$. Let $X_{\theta^n} \in \Omega^n \in \Gamma_n$ be a regular point on γ_{θ^n}. Then by theorem 6.4.7, $X_{\theta^n\alpha}$, $\alpha \neq \theta$, is an inner point of the 3rd iteration of $X_{\theta^{n-2}} \in \gamma_{\theta^{n-2}}$ and therefore cannot belong to $\partial\Omega^{n+1}$.

On the other hand, if $X_{\theta^n} \in \Omega^n \in \Gamma_n$ is a singular point on γ_{θ^n}, the whole circle $\{X_{\theta^n\alpha}\}^{\pi}_{\alpha=0}$ degenerates into a point, and this point[9] belongs to Γ_{n+1}.

Therefore $\partial\Omega^{n+1} \in \Gamma_{n+1}$. $\square$

[7] not all the points $X_{\alpha\theta^n}$ lie on the envelope, see Theorem 6.3.2.

[8] these are Γ_{n+1}

[9] Γ_n has only finite number of singular points, those are the roots of the trigonometrical polynomial equation $R_{\theta_{n-1}} = 0$. So each singular point on Γ_n is isolated.

Chapter 7

Hypo- and Epicycloid Envelope Theorem

The frequent appearance of classical curves during our study of image-sets of the second and the third iterations prompts us to generalize the discovered facts, extending some of the statements in the previous Chapters onto the case of iterations of higher orders. We will begin with cycloidal curves. General decsription of them, the reader can find in [14]. Theorems 7.1.3 and 7.1.16 could be viewed as particular cases of Morley Theorem [15], but in this Section they appear in a different context and are proved in a different way.

7.1 The Epicycloid Envelope Theorem

Definition 7.1.1. *An epicycloid is a plane curve produced by tracing the path of a chosen point of a circle called a generating circle which rolls without slipping around a fixed circle.*

If the rolling circle has radius r*, and the fixed circle has radius* $R = kr$*, then the* *parametric equations for the curve can be given by:*

$$\begin{cases} x(\theta) = r(k+1)\cos\theta + r\cos((k+1)\theta) \\ y(\theta) = r(k+1)\sin\theta + r\sin((k+1)\theta). \end{cases} \tag{7.1.1}$$

Definition 7.1.2. *A hypocycloid is a plane curve produced by tracing the path of a chosen point of a circle called a generating circle which rolls without slipping within a fixed larger circle.*
If the rolling circle has radius r, and the fixed circle has radius $R = kr$, then the parametric equations for the curve can be given by:

$$\begin{cases} x(\theta) = r(k-1)\cos\theta + r\cos((k-1)\theta) \\ y(\theta) = r(k-1)\sin\theta - r\sin((k-1)\theta). \end{cases} \tag{7.1.2}$$

The theorems 6.4.5 and 6.3.2 give rise to nice generalizations in the realm of epicycloids, hypocycloids and sinusoidal spirals, a few of which we are going to prove in this section.

Theorem 7.1.3. (The Nephroid Envelope Theorem) *A nephroid, generated by a circle of radius R, is*
(a) an envelope of cusps of the family of deltoids, generated by circles of the same radius R, which envelope the segment, connecting the nephroid's cusps.
(b) an envelope of family of cardioids, generated by circles of the same radius R, whose cusps envelope the segment, connecting the nephroid's cusps.

Proof. The statement follows from Theorems 6.4.5 and 6.3.2, and Lemmas 6.1.6 and 6.2.8 and 6.2.12. □

Note that the segment connecting the cusps of a nephroid could be viewed as a two-cusped hypocycloid, generated by a circle of radius half the length of the segment, that is, generated by a circle the same size of the nephroid's generating circle. It is an amazing fact that the statement of Theorem 7.1.3 can be generalized to the case of an epicycloid of arbitrary many cusps.

Lemma 7.1.4. *If* $L_{n+1} \ni (R, R', ..., R^{(n)}) = (r_1, r_2, -r_1, -r_2, ...)$, *then* $R_{\theta^k} = r_1 \cos k\theta - r_2 \sin k\theta,\ \theta \in [0, \pi],\ k = 0, 1, ..., n.$

Proof. We can show it by mathematical induction.

1. $k = 0 \Leftrightarrow R_{\theta^0} = R = r_1$. Obviously, it is true.

2. Suppose $R_{\theta^k} = r_1 \cos k\theta - r_2 \sin k\theta$ for all $k \leq m \leq n$.

Then, we have:

$$R_{\theta^{k+1}} = \cos\theta R_{\theta^k} - \sin\theta \frac{\partial R_{\theta^k}}{\partial \psi}. \tag{7.1.3}$$

Taking into consideration another sequence $L_{n+1} \ni (\tilde{R}, \tilde{R}', ..., \tilde{R}^{(n)}) = (r_2, -r_1, -r_2, r_1, ...)$ and setting $(\cos\theta - \sin\theta\frac{\partial}{\partial\psi})^k \tilde{R} = \tilde{R}_{\theta^k}$, we notice that $\frac{\partial R_{\theta^k}}{\partial \psi} = \tilde{R}_{\theta^k}$, which by the induction step is equal to $r_2 \cos k\theta + r_1 \sin k\theta$, we have:

$R_{\theta^{k+1}} = \cos\theta(r_1 \cos k\theta - r_2 \sin k\theta) - \sin\theta(r_2 \cos k\theta + r_1 \sin k\theta) = r_1(\cos\theta \cos\ k\theta - \sin\theta \sin k\theta) - r_2(\sin\theta \cos\ k\theta + \cos\theta \sin k\theta)$.

Finally, we get

$$R_{\theta^{k+1}} = r_1 \cos(k+1)\theta - r_2 \sin(k+1)\theta. \tag{7.1.4}$$

□

Lemma 7.1.5. *If* $L_{n+1} \ni (R, R', ..., R^{(n)}) = (1, 0, -1, 0, ...)$, *then* Γ_{n+1} *is an n-cusped epicycloid.*

Proof. Let us consider a curve γ parametrized by the Gaussian map parameter ψ, whose radius of curvature and its first $n+1$ derivatives with respect to ψ at some point $X \in \gamma$ are respectively $1, 0, -1, 0, 1, 0, -1, 0, ...$[1]

[1]Such sequence could be acquired, for instance, if $R = \cos\psi$ and the point of consideration corresponds to $\psi = 0$.

Calculating $R_{\theta^k},\ k = 0, 1, ..., n$, we get $R_{\theta^k} = \cos k\theta$. So, the equations of Γ_{n+1} are:

$$\begin{cases} x = s(s + cs_2 + c_2 s_3 + ... + c_n s_{n+1}) \\ y = s(c + cc_2 + c_2 c_3 + ... + c_n c_{n+1}). \end{cases} \tag{7.1.5}$$

Using formulas $c_m s_{m+1} = \frac{1}{2}(s + s_{2m+1})$ and $c_m c_{m+1} = \frac{1}{2}(c + c_{2m+1})$, we get

$$\begin{cases} x = \frac{s}{2}((n+2)s + s_3 + s_5 + ... + s_{2n+1}) \\ y = \frac{s}{2}((n+2)c + c_3 + c_5 + ... + c_{2n+1}). \end{cases} \tag{7.1.6}$$

Then, expanding the products ss_{2k+1} and sc_{2k+1}, we obtain two telescoping sums

$$\begin{cases} x = \frac{1}{4}((n+2) - (n+2)c_2 + c_2 - c_4 + c_4 - c_6 + ... + c_{2n} - c_{2n+2}) \\ y = \frac{1}{4}((n+2)s_2 + s_4 - s_2 + s_6 - s_4 + ... + s_{2n+2} - s_{2n}). \end{cases} \tag{7.1.7}$$

Finally, after performing all the cancellations and introducing a new variable $\theta' = 2\theta$, we obtain a model equation of an n-cusped epicycloid

$$\begin{cases} x = \frac{1}{4}((n+2) - (n+1)\cos\theta' - \cos(n+1)\theta') \\ y = \frac{1}{4}((n+1)\sin\theta' + \sin(n+1)\theta'). \end{cases} \tag{7.1.8}$$

$\square$

Lemma 7.1.6. *If $L_{n+1} \ni (R, R', ..., R^{(n)}) = (r_1, r_2, -r_1, -r_2, ...)$, then Γ_{n+1} is an n-cusped epicycloid.*

Proof. By Lemma 7.1.5, $R_{\theta^k} = r_1 c_k - r_2 s_k = \sqrt{r_1^2 + r_2^2}\cos(\beta + k\theta)$, where $\beta = \arccos(\frac{r_1}{\sqrt{r_1^2+r_2^2}})$. Denote $\rho = \sqrt{r_1^2 + r_2^2}$ and write down the parametric equations of

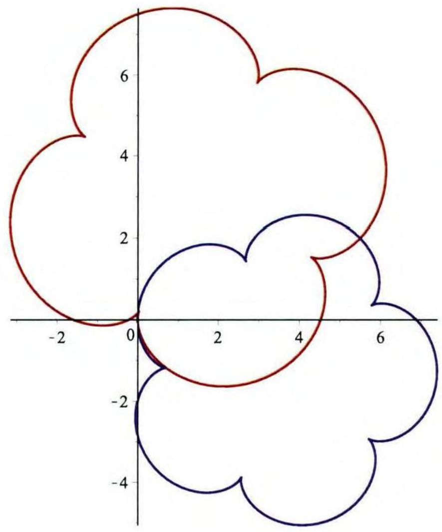

Figure 7.1: To Lemma 7.1.6. Two epicycloids: a 4-cusped, $\Gamma_5(1, 3, -1, -3, 1)$, and a 5-cusped, $\Gamma_6(2, -1, -2, 1, 2, -1)$.

Γ_{n+1}:

$$\begin{cases} x = \rho s(c_{(\beta+0\theta)}s + c_{(\beta+\theta)}s_2 + c_{(\beta+2\theta)}s_3 + \ldots + c_{(\beta+n\theta)}s_{n+1}) \\ y = \rho s(c_{(\beta+0\theta)}c + c_{(\beta+\theta)}c_2 + c_{(\beta+2\theta)}c_3 + \ldots + c_{(\beta+n\theta)}c_{n+1}). \end{cases} \tag{7.1.9}$$

As we can see, the equations (7.1.9) represents a curve similar to that represented by the equations (7.1.6), which is an n-cusped epicycloid. □

Corollary 7.1.7. *The epicycloids* $\Gamma_n(r_1, r_2, -r_1, -r_2, \ldots)$ *and* $\Gamma_n(r_1^*, r_2^*, -r_1^*, -r_2^*, \ldots)$ *are congruent if* $r_1^2 + r_2^2 = r_1^{*2} + r_2^{*2}$.

Proof. The congruence follows from the equation (7.1.9), since each of them is ρ times the same curve $\Gamma_n(1, 0, -1, 0, \ldots)$. □

Lemma 7.1.8. *If* $L_{n+1} \ni (R, R', \ldots, R^{(n)}) = (1, 0, -1, 0, \ldots)$, *then curves* $\{\Gamma_{n+1}^{\alpha}\}_{\alpha=0}^{\pi}$, *are a family of* $(n-1)$*-cusped congruent epicycloids.*

Proof. Let us take a fixed $\alpha \in [0, \pi]$ and write down the equation of Γ_{n+1}^{α}:

$$\begin{cases} x = s(s + cs_2 + c_2 s_3 + ... + c_n s_n) + c_n s_\alpha s_{(\alpha+n\theta)} \\ y = s(c + cc_2 + c_2 c_3 + ... + c_n c_n) + c_n s_\alpha c_{(\alpha+n\theta)}. \end{cases} \tag{7.1.10}$$

Expanding the last terms in the equations for x and y coordinates of Γ_{n+1}^{α}, we get:

$c_n s_\alpha s_{(\alpha+n\theta)} = \frac{1}{4}(1 + c_{2n} - c_{2\alpha} - c_{(2n+2\alpha)})$;

$c_n c_\alpha s_{(\alpha+n\theta)} = \frac{1}{4}(-s_{2n} - s_{2\alpha} + s_{(2n+2\alpha)})$.

Using the results proved in Lemma 7.1.5 and the expansion of the last terms, the equations of Γ_{n+1}^{α} takes the form

$$\begin{cases} x = \frac{1}{4}((n+2) - c_{2\alpha} - nc_2 - c_{(2n+2\alpha)}) \\ y = \frac{1}{4}(s_{2\alpha} + ns_2 + s_{(2n+2\alpha)}). \end{cases} \tag{7.1.11}$$

Changing he coordinates by $(x', y') = (-x, y)$ and the parameter in (7.1.11) by $\theta = \frac{\mu}{2} - \frac{\alpha}{n-1}$, we obtain a model equation of an $(n-1)$-cusped epicycloid. $\square$

Corollary 7.1.9. *If $L_{n+1} \ni (R, R', ..., R^{(n)}) = (r_1, r_2, -r_1, -r_2, ...)$, then the curves $\{\Gamma_{n+1}^{\alpha}\}_{\alpha=0}^{\pi}$, are a family of $(n-1)$-cusped congruent epicycloids.*

Proof. The proof is identical to that of Lemma 7.1.6. $\square$

Lemma 7.1.10. *Given $(1, 0, -1, 0, ...) \in L_{n+1}$. Then for a fixed $\alpha \in [0, \pi]$, the curve $\tilde{\Gamma}_{n+1}^{\alpha}$ is an $(n+1)$-cusped hypocycloid with generating circle of the same radius as that of the epicycloid Γ_{n+1}.*

Proof. Let us take a fixed $\alpha \in [0, \pi]$ and write down the equation of $\tilde{\Gamma}_{n+1}^{\alpha}$:

$$\begin{cases} x = s(s + cs_2 + c_2 s_3 + ... + c_n s_n) + c_n s_{\alpha-n\theta} s_\alpha \\ y = s(c + cc_2 + c_2 c_3 + ... + c_n c_n) + c_n s_{\alpha-n\theta} c_\alpha. \end{cases} \tag{7.1.12}$$

Expanding the last terms in the equations for x and y coordinates of $\tilde{\Gamma}^{\alpha}_{n+1}$, we get:

$c_n s_{(\alpha-n\theta)} s_\alpha = \frac{1}{4}(1 + c_{2n} - c_{2\alpha} - c_{(2n-2\alpha)})$;

$c_n s_{(\alpha-n\theta)} c_\alpha = \frac{1}{4}(-s_{2n} + s_{2\alpha} - s_{(2n-2\alpha)})$.

The expansions above and the results obtaining in Lemma 7.1.5, we get

$$\begin{cases} x = \frac{1}{4}((n+2) - c_{2\alpha} - nc_2 - c_{(2n-2\alpha)}) \\ y = \frac{1}{4}(s_{2\alpha} + ns_2 - s_{(2n-2\alpha)}). \end{cases} \tag{7.1.13}$$

Changing the coordinates by $(x', y') = (-x, y)$ and the parameter in (7.1.13) by $\theta = \frac{\mu}{2} + \frac{\alpha}{n-1}$, we obtain a model equation of an $(n+1)$-cusped hypocycloid. □

Corollary 7.1.11. *If $L_{n+1} \ni (R, R', ..., R^{(n)}) = (r_1, r_2, -r_1, -r_2, ...)$, then the curves $\{\tilde{\Gamma}^{\alpha}_{n+1}\}^{\pi}_{\alpha=0}$, are a family of $(n+1)$-cusped congruent hypocycloids. The radius of generating circles of these hypocycloids is the same as that of the epicycloids, $\{\Gamma^{\alpha}_{n+1}\}^{\pi}_{\alpha=0}$ for the same point $(r_1, r_2, -r_1, -r_2, ...) \in L_{n+1}$.*

Proof. The proof of the first part of the statement is identical to that of Lemma 7.1.6. By the same Lemma, it follows that the of radii of generating circles of the epi- and hypocycloids are the same and equal to $\frac{\sqrt{r_1^2+r_2^2}}{4}$. □

Lemma 7.1.12. *Given $(1, 0, -1, 0, ...) \in L_{n+1}$. Then the cusps of the $(n+1)$-cusped hypocycloids, representing the curves $\{\tilde{\Gamma}^{\alpha}_{n+1}\}^{\pi}_{\alpha=0}$, lie on the n-cusped epicycloid Γ_{n+1}.*

Proof. All the points of a hypocycloid $\tilde{\Gamma}^{\alpha}_{n+1}$, such that

$$\alpha - n\theta = \theta \bmod \pi, \tag{7.1.14}$$

lie on the epicycloid. Solving this equation with respect to θ, given a fixed $\alpha \in [0, \pi]$, we obtain $(n+1)$ distinct (by $\bmod \pi$) roots:

$$\theta = \left\{ \frac{\alpha + k\pi}{n+1} \right\}_{k=0}^{n}. \tag{7.1.15}$$

On the other hand, by Theorem 6.3.2, each of the hypocycloids passes through the cusps of the epicycloid Γ_{n+1}, which can be determined by solving

$$R_{\theta^n} = 0. \tag{7.1.16}$$

Since $R_{\theta^n} = \cos n\theta$, we immediately have

$$\theta = \frac{\pi}{2n}. \tag{7.1.17}$$

Since we have $(n+1)$ points of contacts of an $(n+1)$-cusped hypocycloid and the n-cusped epicycloid, and the hypocycloid passes through the cusps of the epicycloid, one point of contact at least will be not a cusp of the epicycloid. This point of contact is a cusp of the hypocycloid, since there could not be any tangency point between the two curves, when a hypocycliod lie entirely inside an epicycloid. Due to the symmetry of distribution of the points (7.1.15) over the interval $[0, \pi]$, all of them are the cusps of the hypocycloid. So, the two curves get their cusps resting on each other. $\square$

Lemma 7.1.13. *Given* $(1, 0, -1, 0, ...) \in L_{n+1}$. *Then the envelope of the hypocycloids, representing* $\{\tilde{\Gamma}_{n+1}^{\alpha}\}_{\alpha=0}^{\pi}$*, consists of the outer and inner parts, which are the n-cusped epicycloid* Γ_{n+1}*, and the n-cusped hypocycliod respectively. The cusps of the epicycloid and the hypocycloid coincide.*

Proof. Let us write the equation of envelope of the family of curves, each member of which is described by equations (7.1.11) with a fixed value of the parameter $\alpha \in [0, \pi]$ and θ running from 0 to π. To do so, we have to calculate partial derivatives of coordinates with respect to θ and α:

$\frac{\partial x}{\partial \theta} = \frac{n}{4}(2\sin(2\alpha + 2n\theta) + 2\sin 2\theta) = n\cos(\alpha + (n-1)\theta)\sin(\alpha + (n+1)\theta)$,

$\frac{\partial x}{\partial \alpha} = \frac{1}{4}(2\sin 2\alpha + 2\sin(2\alpha + 2n\theta)) = \cos n\theta \sin(2\alpha + n\theta)$,

$\frac{\partial y}{\partial \theta} = \frac{n}{4}(2\cos(2\alpha + 2n\theta) + 2\cos 2\theta) = n\cos(\alpha + (n-1)\theta)\cos(\alpha + (n+1)\theta)$,

$\frac{\partial y}{\partial \alpha} = \frac{1}{4}(2\cos 2\alpha + 2\cos(2\alpha + 2n\theta)) = \cos n\theta \cos(2\alpha + n\theta)$.

$$\frac{\partial x}{\partial \theta}\frac{\partial y}{\partial \alpha} - \frac{\partial y}{\partial \theta}\frac{\partial x}{\partial \alpha} = n\cos(\alpha + (n-1)\theta)\cos n \sin(\theta - \alpha) = 0. \tag{7.1.18}$$

Thus, a point $(x(\theta, \alpha), y(\theta, \alpha))$ satisfies the equation(7.1.18) if

1. $\alpha = \theta \bmod \pi$. In that case, we obtain Γ_{n+1}, an n-cusped epicycloid.
2. $\alpha = [(1-n)\theta \pm \frac{\pi}{2}] \bmod 2\pi$. Let us plug this expression into (7.1.11):

$$\begin{cases} x = \frac{1}{4}((n+2) - \cos(2(1-n)\theta \pm \pi) - n\cos 2\theta - \cos(2(1-n)\theta \pm \pi + 2n\theta)) \\ y = \frac{1}{4}(\sin(2(1-n)\theta \pm \pi) + n\sin 2\theta + \sin(2(1-n)\theta \pm \pi + 2n\theta)). \end{cases} \tag{7.1.19}$$

After combining the like terms, we obtain a model equation of an n-cusped hypocycloid:

$$\begin{cases} x = \frac{1}{4}((n+2) + \cos(2(n-1)\theta) - (n-1)\cos 2\theta) \\ y = \frac{1}{4}(\sin(2(n-1)\theta) + (n-1)\sin 2\theta). \end{cases} \tag{7.1.20}$$

Examining the equations of the epicycloid (7.1.8) and the hypocycloid (7.1.20), we see that their cusps coincide. □

Corollary 7.1.14. *The statement of Lemma* 7.1.13 *is valid for any* $(r_1, r_2, -r_1, -r_2, \ldots) \in L_{n+1}$.

Proof. Consider a general setting $(r_1, r_2, -r_1, -r_2, \ldots) \in L_{n+1}$. By Corollaries to Lemmas 7.1.6 and 7.1.10, it differs from the particular setting $(1, 0, -1, 0, \ldots) \in L_{n+1}$

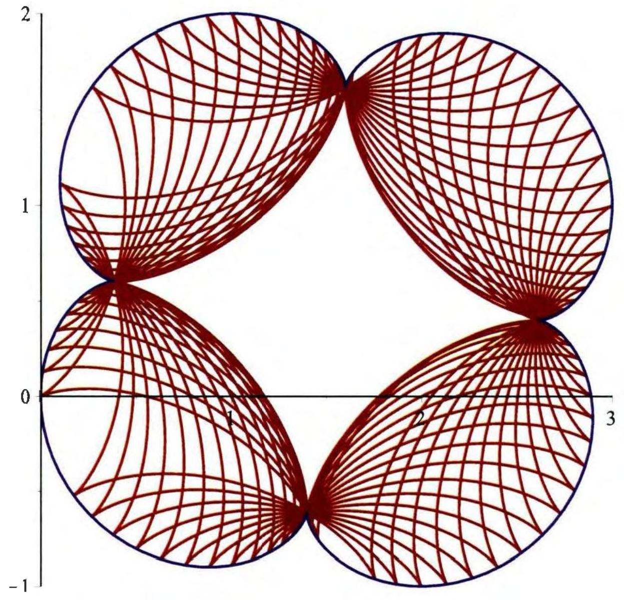

Figure 7.2: A family of curves $\tilde{\Gamma}_5^\alpha(1, 0.5, -1, -0.5, 1)$.

only by transition, rotation and homothety with respect to the origin and does not affect the property of parity, tangency, normality and inclusion. See an example in Figure 7.2. □

Denote the inner and outer envelopes of the hypocycloids $\{\tilde{\Gamma}_{n+1}^\alpha\}_{\alpha=0}^\pi$ by Γ_* and Γ^* respectively.

Lemma 7.1.15. *Given* $(1, 0, -1, 0, ...) \in L_{n+1}$. *The cusps of the family of epicycloids* $\{\Gamma_{n+1}^\alpha\}_{\alpha=0}^\pi$ *lie on the hypocycloid* Γ_* *and envelope it.*

Proof. The proof is similar to that of Lemma 7.1.12.

Take a fixed $\alpha \in [0, \pi]$ and consider Γ_{n+1}^α. Definitely, the point $X_{\alpha^{n+1}} \in \Gamma_{n+1}^\alpha$ lies on Γ^*. By the equation (7.1.18) it is the only point of Γ_{n+1}^α, lying on Γ^*.

Now, let us find out the points, which are the cusps of Γ_{n+1}^α. It is clear, they are such points $X_{\theta^n\alpha}$ that $R_{\theta^{n-1}\alpha} = 0$. We have

$R_{\theta^{n-1}\alpha} = (\cos\alpha - \sin\alpha\frac{\partial}{\partial\psi})R = \cos\alpha R_{\theta^{n-1}} - \sin\alpha\frac{\partial R_{\theta^{n-1}}}{\partial\psi}$.

By Lemma 7.1.4, we have

$$R_{\theta^{n-1}} = \cos(n-1)\theta, \quad \frac{\partial R_{\theta^{n-1}}}{\partial \psi} = \sin(n-1)\theta. \tag{7.1.21}$$

Therefore,

$$R_{\theta^{n-1}\alpha} = 0 \Leftrightarrow \cos\alpha\cos(n-1)\theta - \sin\alpha\sin(n-1)\theta = \cos(\alpha + (n-1)\theta) = 0, \tag{7.1.22}$$

But this is exactly the condition for a point to lie on Γ_*! Thus, all cusps of the epicycloid Γ^{α}_{n+1} lie on Γ_*. $\square$

Theorem 7.1.16. (The Epicycloid Envelope Theorem) *Given an $(n+1)$-cusped epicycloid, Γ^*, generated by a circle of radius R, and the hypocycloid, Γ_*, whose cusps coincide with those of Γ^*. Denote by Ω the circle of radius R, centered at the centroid of Γ_** [2]. *Then*

(a) Γ^* is the envelope of cusps of the family of $(n+2)$-cusped of hypocycloids, generated by circles of the same radius R, which envelope Γ_* and pass through its cusps. The centroids of those hypocycloids describe a circle Ω.

(b) Γ_* is the envelope of cusps of the family of n-cusped of epicycloids, generated by circles of the same radius R, which envelope Γ^* and pass through its cusps. If $n > 1$, then the centroids of those epicycloids describe the circle Ω.

Proof. In other words, the space between Γ^* and Γ_* is filled by two families of curves, passing through the common cusps of Γ^* and Γ_*:

(a) $(n+2)$-cusped congruent hypocycloids,

(b) n-cusped congruent epicycloids,

whose generating circles are of radius R.

[2] the centroids of Γ^* and Γ_* coincide for all $n = 1, 2, \ldots$.

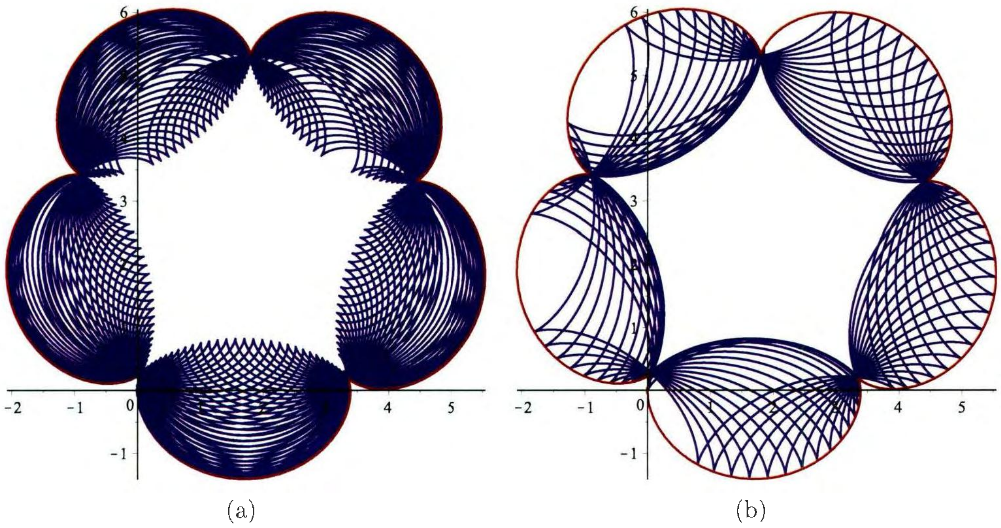

Figure 7.3: The 5-cusped epicycloid and hypocycloid are enveloped by two families: (a) $\{\Gamma_6^{\alpha}(1,2,-1,-2,1,2)\}_{\alpha=0}^{\pi}$ and (b) $\{\tilde{\Gamma}_6^{\alpha}(1,2,-1,-2,1,2)\}_{\alpha=0}^{\pi}$.

The statement of the theorem, except the centroid part, follows from Lemmas 7.1.12, 7.1.13, 7.1.15.

Let $n > 1$ and consider the epicycloids $\Gamma_{n+1}^{\alpha}(1,0,-1,0,...)$. Take any $\alpha_0 \in [0,\pi]$. Looking at the formulas of the family of the epicycloids (7.1.11), we notice that the centroid of the epicycloid, corresponding to $\alpha = \alpha_0$ is positioned at the point $(n+2-\cos 2\alpha_0, \sin 2\alpha_0)$. So, as α runs from 0 to π, the centroids describe the circle of radius $\frac{1}{4}$, which is the radius of a generating circle of the epicycloids, centered at the point $(n+2,0)$, which corresponds to the centroid of Γ_*.

The proof of the centroid part of (a) is analogous. $\square$

7.2 The Sinusoidal Spiral Theorem

Finally, before we prove a general statement about sinusoidal spirals, we would like to prove a few more generalization, inspired by Epicycloid Envelope Theorem.

Definition 7.2.1. *We will call the ordered sequence of points* $\{XX_{\frac{\pi}{2}}X_{(\frac{\pi}{2})^2}...X_{(\frac{\pi}{2})^{n-1}}\}$ *evolutal sequence of lenght* n. *Then the polygonal line based on such sequence will be called an evolutal chain.*

Lemma 7.2.2. *For any* $(r_1, r_2, ..., r_n) \in L_n$, *the curves*

(a) $\Gamma_n(r_1, -r_2, r_3, -r_4, r_5, ...)$,

(b) $\Gamma_n(-r_1, r_2, -r_3, r_4, -r_5, r_6, ...)$,

(c) $\Gamma_n(r_1, r_2, ..., r_n)$.

are congruent.

Proof. The curves (a) and (b) are obviously congruent, since they are symmetrical with respect to the origin[3].

Now, construct the evolutal chains of the curves (b) and (c). Denote curves, defining the point $(-r_1, r_2, -r_3, r_4, -r_5, ...) \in L_n$ and $(r_1, r_2, ..., r_n) \in L_n$ by γ^b and γ^c respectively. Their centers of curvature are in points $(-r_1, 0)$ and $(r_1, 0)$ respectively. Since the tangents to the two curves at X coincide, we conclude that they have opposite orientations. That means, that θ-secant to one of the curves is $\pi - \theta$-secant to another (at X). Hence, the corresponding to X points on a θ-evolutoid of one of the curves and on $(\pi - \theta)$-evolutoid on another are symmetrical with respect to y-axis. The following construction of the evolutal chains of length n of the two curves are symmetrical with respect to y-axis, too. Hence, given any sequence of angles $\{\theta_1, ..., \theta_n\}$, the corresponding points on $\gamma^c_{\theta_1...\theta_n}$ and $\gamma^b_{(\pi-\theta_1)...(\pi-\theta_n)}$ are symmetric with respect to

[3]As usual, we place the point of consideration, $X \in \gamma$ in the origin so that the direction of the tangent vector to γ at X is opposite to that of y-axis.

y-axis. Hence, the curves (b) and (c) are congruent, and hence so are all three curves[4]. An example is shown in Figure 7.4. $\square$

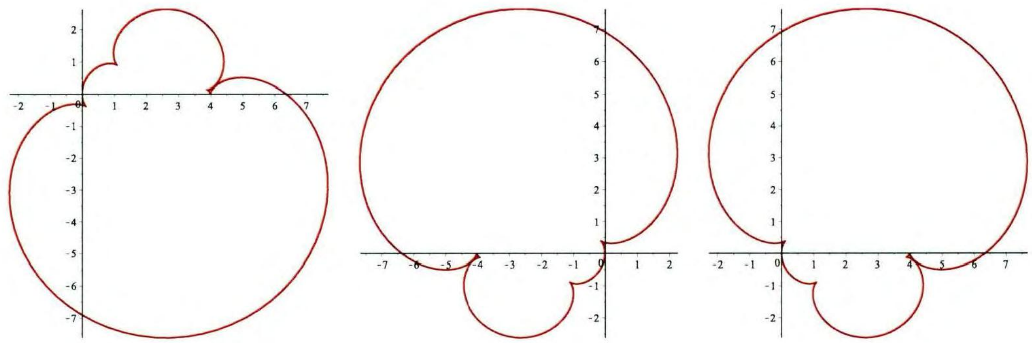

(a) (b) (c)

Figure 7.4: To Lemma 7.2.2. Three congruent curves: (a) $\Gamma_5(1, -1, -3, -1, 0)$; (b) $\Gamma_5(-1, 1, 3, 1, 0)$; (c) $\Gamma_5(1, 1, -3, 1, 0)$.

Lemma 7.2.3. *Two curves $\Gamma_n(r_1, r_2, ..., r_n)$ and $\Gamma_n(r_n, r_{n-1}, ..., r_1)$ are congruent.*

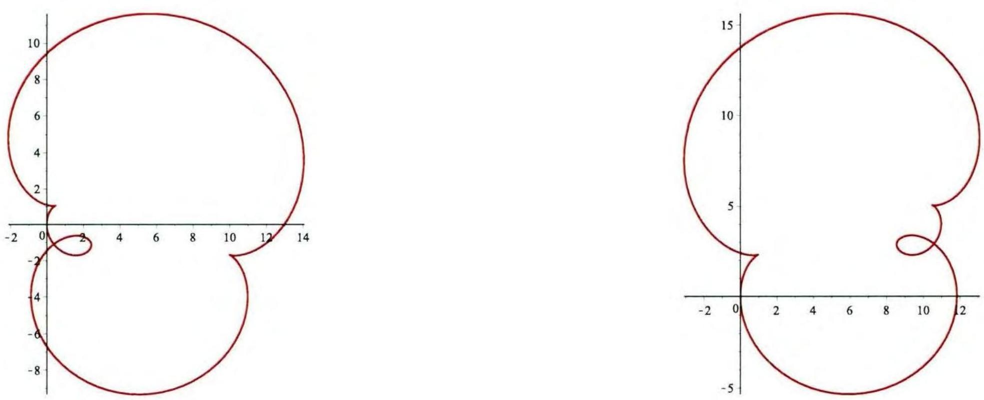

(a) (b)

Figure 7.5: To Lemma 7.2.3. Two congruent curves: (a) $\Gamma_5(2, 1, -4, 5, 5)$; (b) $\Gamma_5(5, 5, -4, 1, 2)$.

Proof. Let a curve γ be such that at a point $X \in \gamma$, the radius of curvature and its first $n-1$ derivatives with respect to Gaussian map parameter, ψ, are

[4]It follows, by the way, that curves (a) and (c) are symmetrical with respect to x-axis

$(R, R', R'', ..., R^{(n-1)}) = (r_1, r_2, ..., r_n, r_n)$. Then construct n circles Ω_1, $\Omega_2, ...,$ Ω_n built on $[X_{(\frac{\pi}{2})^i} X_{(\frac{\pi}{2})^{i+1}}]$ as their diameters, $i = 0, 1, 2, ..., n-1$.

Let us take any $\theta \in [0, \pi]$ and construct a polygonal line $X_\theta X_{\theta\frac{\pi}{2}} X_{\theta(\frac{\pi}{2})^2} ... X_{\theta(\frac{\pi}{2})^{n-1}}$, that is the evolutal chain of $X_\theta \in \gamma_\theta$. Denote it by P_θ. (See the first and the last few chains of the evolutal chain in Figure 7.6).

Let $\tilde{\gamma}$ be another curve that passes through $X_{(\frac{\pi}{2})^{n-1}}$ perpendicular to the line

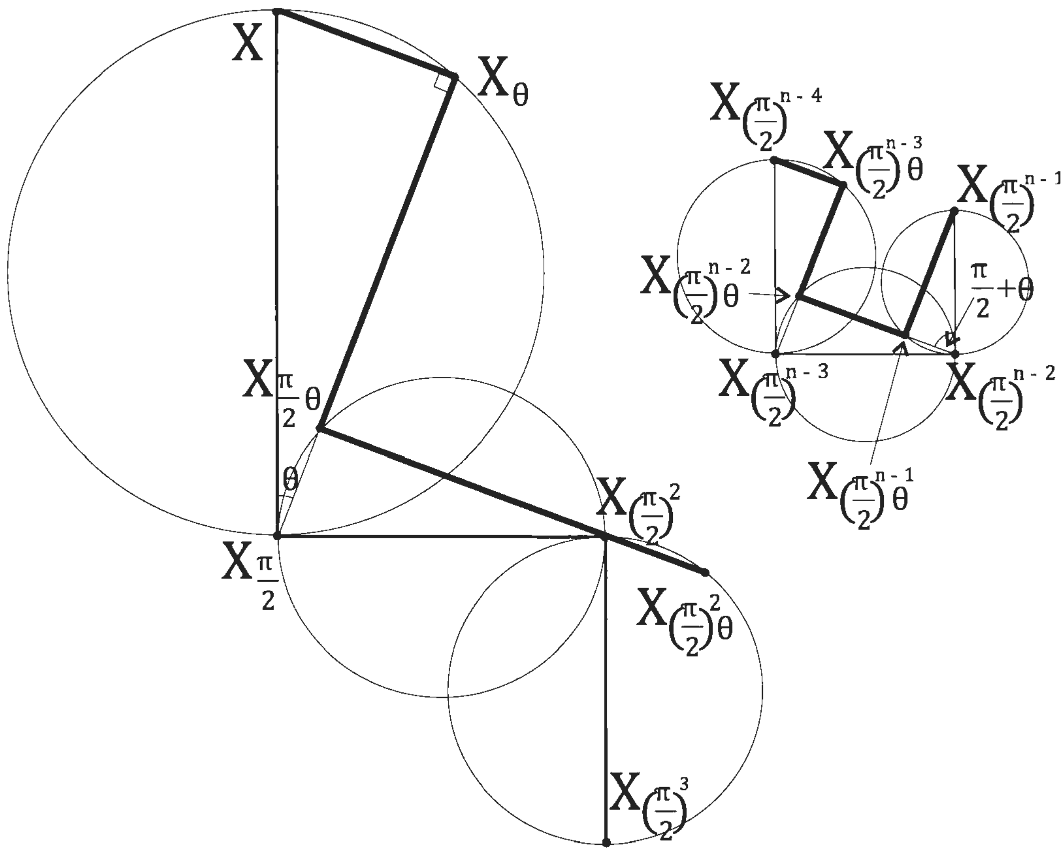

Figure 7.6: To Lemma 7.2.3. The beginning and the end of a polygonal line $XX_\theta X_{\theta\frac{\pi}{2}} ... X_{\theta(\frac{\pi}{2})^{n-1}}$.

$X_{(\frac{\pi}{2})^{n-1}} X_{(\frac{\pi}{2})^{n-2}}$. Suppose also that the direction of $\tilde{\gamma}$ and the radius of curvature and its first $(n-1)$ derivatives are such that the chain of corresponding points on its evolute, evolute of evolute and so on coincide in reverse order with those[5] of γ. That implies $(\tilde{R}, \tilde{R}', ..., \tilde{R}^{(n-1)}) = (r_n, -r_{n-1}, ..., (-1)^{n-j}r_j, ..., (-1)^n r_1)$.

According to our construction, the arrival point of P_θ will be $\tilde{X}_{\frac{\pi}{2}+\theta}$. If we construct the polygonal line $\tilde{X}_{(\frac{\pi}{2}+\theta)}\tilde{X}_{(\frac{\pi}{2}+\theta)\frac{\pi}{2}}\tilde{X}_{(\frac{\pi}{2}+\theta)(\frac{\pi}{2})^2}...\tilde{X}_{(\frac{\pi}{2}+\theta)(\frac{\pi}{2})^{n-1}}$, we arrive, of course, at X_θ. Continuing that process further with evolutal chains of $X_\theta \in \gamma\theta$ and $\tilde{X}_{\frac{\pi}{2}+\theta} \in \tilde{\gamma}_{\frac{\pi}{2}+\theta}$, we will get that the points $X_{\theta^2(\frac{\pi}{2})^{n-2}}$ and $\tilde{X}_{(\frac{\pi}{2}+\theta)^2(\frac{\pi}{2})^{n-2}}$ coincide with $\tilde{X}_{(\frac{\pi}{2}+\theta)^2}$ and X_{θ^2} respectively, and so on. Finally X_{θ^n} coincides with $\tilde{X}_{(\frac{\pi}{2}+\theta)^n}$. Therefore, $\Gamma_n(r_1, r_2, ..., r_n)$ and $\Gamma_n(r_n, -r_{n-1}, ..., (-1)^{n-j}r_j, ..., (-1)^n r_1)$ are congruent. By Lemma 7.2.2, so are $\Gamma_n(r_1, r_2, ..., r_n)$ and $\Gamma_n(r_n, r_{n-1}, ..., r_1)$. (see examples in Figure 7.5). $\square$

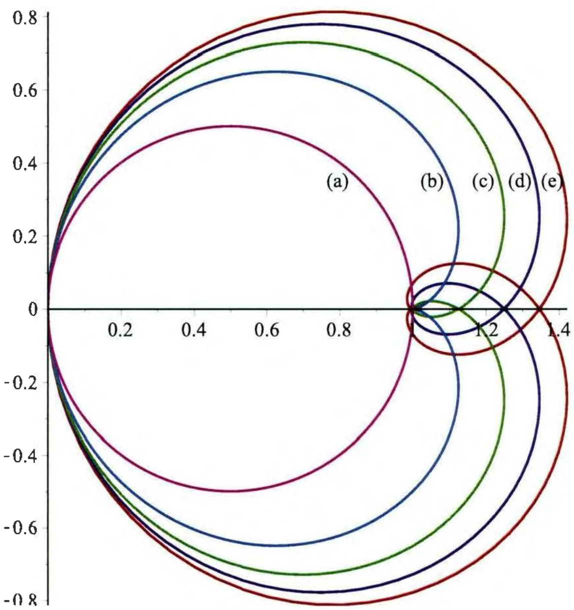

Figure 7.7: To Lemma 7.2.4. Sinusoidal spirals of orders $1, \frac{1}{2}, \frac{1}{3}, \frac{1}{4}, \frac{1}{5}$: (a) $\Gamma_1(1)$; (b) $\Gamma_2(1, 0)$; (c) $\Gamma_3(1, 0, 0)$; (d) $\Gamma_4(1, 0, 0, 0)$; (e) $\Gamma_5(1, 0, 0, 0, 0)$. Each of the curves if pedal to preceding with respect to the pole (point $(1, 0)$).

Lemma 7.2.4. *Two curves $\Gamma_{\theta^n}(0, 0, ..., 0, 1)$ and $\Gamma_{\theta^n}(1, 0, 0, ..., 0)$ are congruent sinusoidal spirals of order $\frac{1}{n}$.*

[5] If $r_n < 0$, then $\tilde{\gamma}$ is oriented clockwise.

Proof. Consider first the curve $\Gamma_{\theta^n}(0, 0, ..., 0, 1)$. The routine procedure of calculating $R, R_\theta, ..., R_{\theta^{n-1}}$ yields: $R = R_\theta = ... = R_{\theta^{n-2}} = 0$ and $R_{\theta^{n-1}} = \sin^n \theta$. Then the equations of $\Gamma_{\theta^n}(0, 0, ..., 0, 1)$:

$$\begin{cases} x = \sin n\theta \sin^n \theta \\ y = \cos n\theta \sin^n \theta. \end{cases} \tag{7.2.1}$$

after changing the parameter $\theta = \frac{\theta'}{n}$ become, according to (6.1.1), the equations of a sinusoidal spiral of order $\frac{1}{n}$. (See Figure 7.7). The congruence of the curves follows from Lemma 7.2.3. $\square$

From here follows a well-known property of sinusoidal spirals.

Corollary 7.2.5. *A sinusoidal spiral of order $\frac{1}{n}$ is pedal to a sinusoidal spiral of order $\frac{1}{n-1}$ with respect to the pole.*

Proof. The proof is identical to that of Lemma 6.1.3. $\square$

This pedality property give rise to a nice generalization over sinusoidal spirals of order $\frac{1}{n}$ in the following Theorem.

Theorem 7.2.6. *A curve $\Gamma_n(R, R', R'', ..., R^{(n-1)})$ is a sinusoidal spiral of order $\frac{1}{n}$ if the ordered sequences $\{R, R', R'', ..., R^{(n-1)}\}$ or $\{R^{(n-1)}, R^{(n-2)}, ..., R\}$ form a geometric series*[6].

Proof. Without loss of generality, we will prove the statement for $\Gamma_n(1, b, b^2, ..., b^{n-1})$, $b > 0$, see Figure 7.8. (The case $b < 0$ is symmetrical, and the case $b = 0$ has already been proven (see Lemma 7.2.4)).

[6]The mentioning of the reverse order makes sense when $(R, R', R'', ..., R^{(n-1)}) = (0, 0, ..., 0, 1)$.

Let us calculate, by the regular routine, $R_{\theta^k},\ k = 1, ..., n-1$:

$$R_{\theta^k} = \sum_{i=0}^{k} C_{n-1}^{i} b^i \cos^{n-1-i}\theta \sin^i\theta = (\cos\theta - b\sin\theta)^i. \tag{7.2.2}$$

Let us construct the chain $XX_{\frac{\pi}{2}}...X_{(\frac{\pi}{2})^n}$ and circles $\Omega_i,\ i = 1, ..., n$, built on segments $[X_{(\frac{\pi}{2})^{i-1}}X_{(\frac{\pi}{2})^i}]$ as their diameters. By the same argument used in Lemma 6.2.13, the circles are concurrent. Denote the concurrency point by O and $\widehat{OXX_{\frac{\pi}{2}}} = \beta$. From $XX_{\frac{\pi}{2}}X_{(\frac{\pi}{2})^2}$, $\beta = \arccos\frac{1}{\sqrt{b^2+1}}$. Denote $\sqrt{b^2+1} = \rho$. Now, we may rewrite equation (7.2.2):

$$R_{\theta^k} = \rho^k \cos^k(\theta + \beta). \tag{7.2.3}$$

Fix a $\theta \in [0, \pi]$. Construct the chains $X_\theta X_{\theta\frac{\pi}{2}}...X_{\theta(\frac{\pi}{2})^{n-1}}$, then $X_{\theta^2}X_{\theta^2\frac{\pi}{2}}...X_{\theta^2(\frac{\pi}{2})^{n-2}}$,

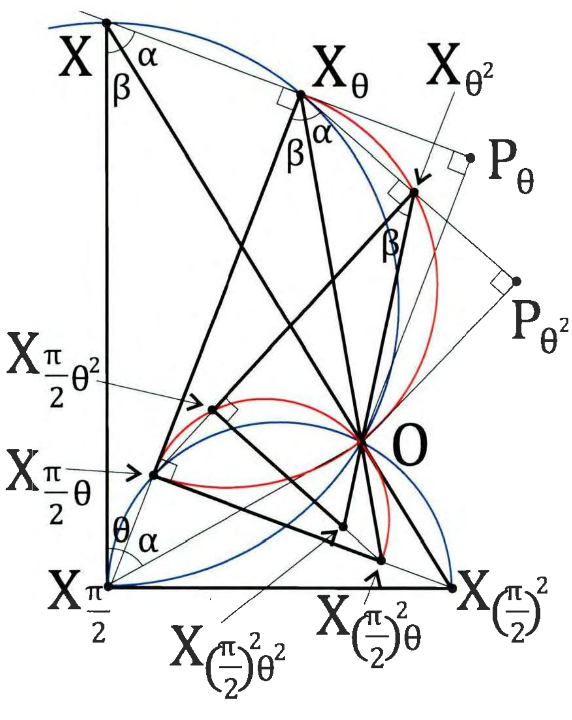

Figure 7.8: To Theorem 7.2.6.

and so on. Draw the corresponding circles built on segments of these polygonal lines.

By the same argument, the new rows circles intersect in the same concurrency point, O, as it is shown in the picture (Figure 7.8) for the first two iterations.

Next, drop perpendicular from O to XX_θ and denote the foot of the perpendicular by P_θ: $OP_\theta \perp XX_\theta$. Clearly, the locus $\{P_\theta\}$ is a circle based on XO as its diameter.

From the triangles $\triangle OX_\theta P_\theta$, $\triangle OX_\theta X_{\theta\frac{\pi}{2}}$, $\triangle OX_\theta P_\theta$ and $\triangle OXP_\theta$, we have:

$\widehat{OXX_{\frac{\pi}{2}}} = \widehat{OX_\theta X_{\frac{\pi}{2}}} = \beta$, since they are angles inscribed in Ω_1.

$\widehat{OXP_\theta} = \widehat{X_\theta X_{\frac{\pi}{2}} P_\theta} = \frac{\pi}{2} - \theta - \beta$, denoted by α in the picture.

$|OP_\theta| = |XO|\cos(\theta+\beta) = \cos\beta\cos(\theta+\beta)$.

$|OX_\theta| = |X_\theta X_{\theta\frac{\pi}{2}}|\cos\beta$.

On the other hand, $|X_\theta X_{\theta\frac{\pi}{2}}| = R_\theta \Leftrightarrow |OX_\theta| = \rho\cos(\theta+\beta)\cos\beta$. Therefore

$\frac{|OX_\theta|}{|OP_\theta|} = \rho \Leftrightarrow \widehat{X_\theta OP_\theta} = \beta$.

Since all triangles $\triangle OX_{\theta^k}P_{\theta^k}$ are similar, we conclude:

$$\frac{|OX_{\theta^k}|}{|OP_{\theta^k}|} = \rho \quad \text{and} \quad \widehat{X_{\theta^k}OP_{\theta^k}} = \beta. \tag{7.2.4}$$

Let us finally apply mathematical induction to complete the statement of the theorem.

The basic case, $n = 1$. Obviously, Γ_1, that is a circle, is a sinusoidal spiral of order 1.

Suppose, the statement if true for all $n \leq k$.

Then consider the triangle $\triangle OX_{\theta^k}P_{\theta^k}$. By Lemma 4.2.9 and Theorem 6.3.2, $X_{\theta^{k+1}} \in [X_{\theta^k}P_{\theta^k}]$ and $X_{\theta^k}P_{\theta^k}$ is tangent to Γ_k at X_{θ^k}. Hence, the locus of points $\Gamma'_{k+1} = \{P_{\theta^{k+1}}\}_{\theta=0}^{\pi}$ is pedal to Γ_k with respect to the pole, O. Therefore, by Corollary 7.2.5, Γ'_{k+1} is a sinusoidal spiral of order $\frac{1}{k+1}$.

Since all $[OX_{\theta^{k+1}}]$ are the result of rotation the corresponding $[OP_{\theta^{k+1}}]$ around O by the same angle β and their extension by ρ, Γ_{k+1} is a sinusoidal spiral of order $\frac{1}{k+1}$, too. $\square$

Below, we present an illustration to Theorem 7.2.6. Clearly, the sequaences R, R', R'', ... of all the curves in the Figure 7.9 form geometric series, and the curves are sinusoidal spirals of the corresponding order.

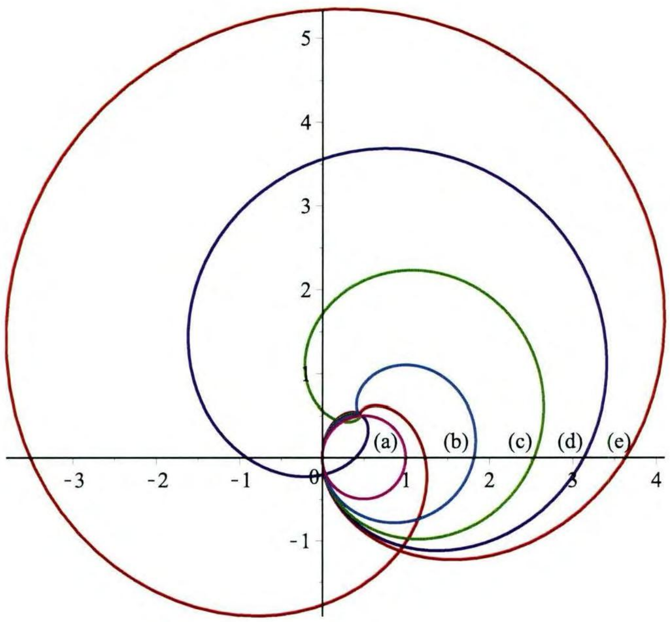

Figure 7.9: To Theorem 7.2.6. Curves: (a) $\Gamma_1(1)$, (b) $\Gamma_2(1, 1.1)$, (c) $\Gamma_3(1, 1.1, 1.21)$, (d) $\Gamma_4(1.1, 1.21, 1.331)$, (e) $\Gamma_5(1, 1.1, 1.21, 1.331, 1.4641)$ are sinusoidal spirals of order 1, $\frac{1}{2}$, $\frac{1}{3}$, $\frac{1}{4}$, $\frac{1}{5}$ respectively.

In the light of the Theorems and Lemmas, proved in this Chapter, many statements in the previous Chapters become their particular cases. However, we needed to prove those particular cases to better understand different image-sets under lower iterations. For instance, The Cardioid Theorem (Theorem 3.4.7) may be viewed as a particular case of either Theorem 7.2.6 or Lemma 7.1.6.

Chapter 8

Further research directions

Lack of time did not allow me to complete certain proofs. Some sketches and ideas for these are outlined in this Chapter.

The results obtained in Section 7.1 pave the way to generalizations of The Epicycloid Envelope Theorem (Theorem 7.1.16). They can be derived by the same technique if we try to represent the image-set of the nth iteration as a set of image-sets of an mth iteration of images of a point of consideration under k iterations, where $n = m + k$. The case when either m or k equals to 1 has been closely studied in Section 7.1.

Let us consider $k + m = n > 3,\ k > 1,\ m > 1$, and a fixed $\alpha \in [0, \pi)$. Define a curve $\Gamma^{\alpha}_{n,k}$ as the locus of points $\{X_{\theta^k \alpha^m}\}^{\pi}_{\theta=0}$. By the same technique used in proving The Triple Envelope Theorem it should be possible to show that the envelope of family of these curves coincides with the envelopes of family of curves $\Gamma^{\alpha}_{n,m}$. Moreover, these envelopes are epi- and hypocycloids; see Figures 8.1, where (a) depicting a family of nephroids and (b) depicting a family of 3-cusped epicycloids.

Analogously, we may define a curve $\tilde{\Gamma}^{\alpha}_{n,k}$ as the locus of points $\{X_{\theta^k (\frac{\alpha - k\theta}{m})^m}\}^{\pi}_{\theta=0}$. Definitely, the sums of angles, constituting the nth iteration, along curves $\tilde{\Gamma}^{\alpha}_{n,k}$ is constant, α. So the family of curves $\{\tilde{\Gamma}^{\alpha}_{n,k}\}^{\pi}_{\alpha=0}$ will play role of generalized α-constant sum

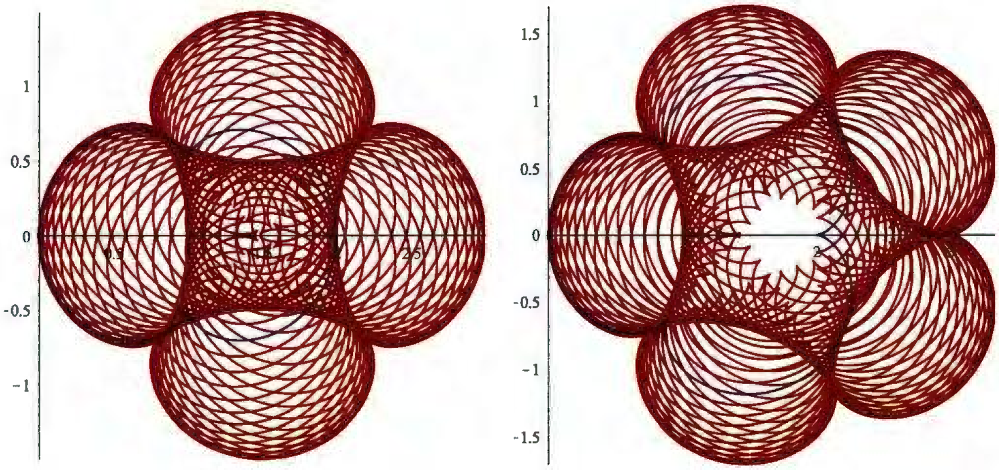

(a) (b)

Figure 8.1: (a) The tangential envelopes of the family $\{\Gamma^{\alpha}_{5,3}(1,0,-1,0,1)\}^{\pi}_{\alpha=0}$ are the 4-cusped epi- and hypocycloids, and the cuspidal envelopes are the segments connecting the cusps of the tangential envelopes; (b) The tangential envelopes of the family $\{\Gamma^{\alpha}_{6,4}(1,0,-1,0,1,0)\}^{\pi}_{\alpha=0}$ are the 5-cusped epi- and hypocycloids, and the cuspidal envelope is the 5-cusped "star-like" hypocycloid.

curves. By the technique used in the proof of Triple Envelope Theorem, we should be able to show that if $n = m + k$, then the envelopes of the four families:

(a)$\{\Gamma^{\alpha}_{n,k}\}^{\pi}_{\alpha=0}$,

(b)$\{\Gamma^{\alpha}_{n,m}\}^{\pi}_{\alpha=0}$,

(c)$\{\tilde{\Gamma}^{\alpha}_{n,k}\}^{\pi}_{\alpha=0}$,

(d)$\{\tilde{\Gamma}^{\alpha}_{n,m}\}^{\pi}_{\alpha=0}$

coincide. This statement completes the cycloidal part of the Morley Theorem and can likely be proved by induction.

Observation of the curves $\tilde{\Gamma}^{\alpha}_{n,k}$ for different $k = 1, ..., n-1$ should give a answers to further questions concerning areas and shapes of boundaries of constant sum image-sets.

In the end, we remark that curves Γ_n may be of shape of epicycloids whose ratio (see the footnote on page 4) is not an integer. For example, $\Gamma_4(1, 0, \frac{1}{3}, 0)$ is such an epicycloid with one cusp, a *double cardioid* (Figure 8.2). Conditions for Γ_n to be an epicycloid in the general sense (with not necessarily an integer ratio) are subject to further research.

A cardioid itself is called sometimes an apple without a stalk. But the envelope

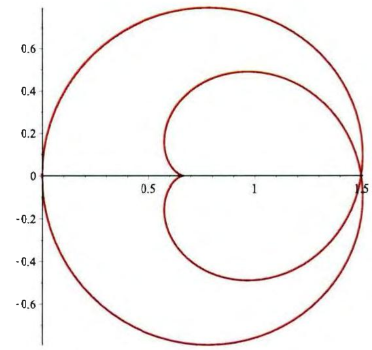

Figure 8.2: A double cardioid, $\Gamma_4(1, 0, \frac{1}{3}, 0)$. This is an epicycloid with ratio 1/2.

of $\{\tilde{\Gamma}_4^{\alpha}(1, 0, \frac{1}{3}, 0)\}_{\alpha=0}^{\pi}$ consists of $\Gamma_4(1, 0, \frac{1}{3}, 0)$ (of course) and a cardioid with a 'stalk' lying entirely inside the cardioid-like inner loop of the double cardioid. (Figure 8.3). Thus the image-set envelope approach is an interesting way to generate new curves.

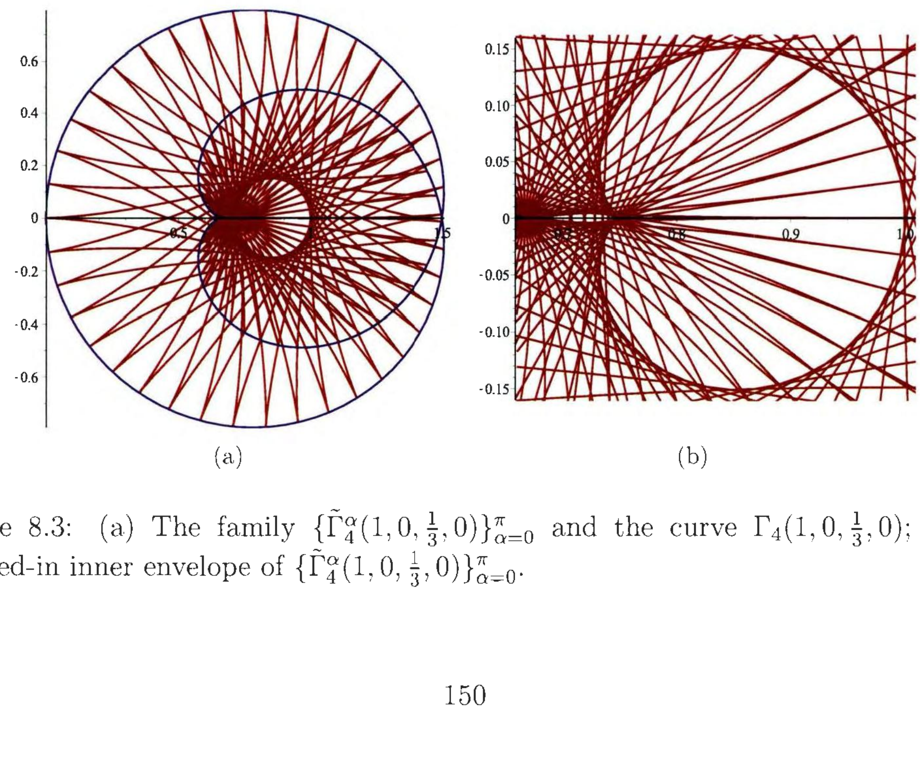

Figure 8.3: (a) The family $\{\tilde{\Gamma}_4^{\alpha}(1, 0, \frac{1}{3}, 0)\}_{\alpha=0}^{\pi}$ and the curve $\Gamma_4(1, 0, \frac{1}{3}, 0)$; (b) a zoomed-in inner envelope of $\{\tilde{\Gamma}_4^{\alpha}(1, 0, \frac{1}{3}, 0)\}_{\alpha=0}^{\pi}$.

Bibliography

[1] Abolghassem, A.A., *Sur quelques courbes liées au mouvement dune courbe plane dans son plan.* Thèse a la Faculté des Sciences de Montpellier, 1938, 132 pp. Source: Thèses françaises de l'entre-deux-guerres, `http://www.numdam.org`

[2] Bruce, J. W., Giblin, P. J. *Curves and singularities*, 2nd ed., Cambridge University Press, Cambridge, 1992.

[3] Butchart, J. H., *Some Properties of the Limaçon and Cardioid.* Amer. Math. Monthly, 1945, vol. 52, no. 7, 384–387.

[4] Evolute, *Wikipedia*, `http://en.wikipedia.org/wiki/Evolute`, version Feb. 23, 2013.

[5] Fuchs, D., Tabachnikov, S., *Mathematical Omnibus: Thirty Lectures on Classic Mathematics.* AMS, 2007.

[6] Guggenheimer, H.W. *Differential Geometry.* Dover Publications, Inc. New York, 1977.

[7] Haton de la Goupillière, J.-N. *Recherches sur les développoïdes.* Annales de la Société scientifique de Bruxelles, t. 2, 1877–1878, 2nd partie, 1–24. Bruxelles, F. Hayez, Imprimeur de l'Academie Royale de Belgique, 1878.

[8] Review of the paper [7], Jahrbuch über die Fortschritte der Matematik, Bd. 9 (Jahrgang 1877), 477–479, Druck und Verlag von G.Reimer, Berlin, 1880.

[9] Jeronimo-Castro, J. *On evolutoids of planar convex curves*, Aequationes Mathematicae, Springer Basel 2013, DOI 10.1007/s00010-013-0213-y.

[10] John, E., *An ancient elliptic locus*, Amer. Math. Monthly, 2010, vol. 117, no. 2, 161–167.

[11] Kondratieva, M. F., Sadov, S. Yu., *Symbol of the Dirichlet-to-Neumann operator in 2D diffraction problems with large wavenumber*, Day on Diffraction 2003 (Proceedings Int. Seminar, St. Petersburg, Russia, 24–27 June 2003), 88–98; also `arXiv:physics/0310048`.

[12] Kondratieva, M., Sadov, S., *Numerical study of high frequency asymptotics of the symbol of the Dirichlet-to-Neumann operator in 2D diffraction problems*, `arXiv:physics/0505054`.

[13] Lockwood, E.H., *A book of curves*, Cambridge University Press, Cambridge, 1961.

[14] Lawrence, J.D., *A catalog of special curves*, Dover Publications, Inc. New York, 1972.

[15] Morley, F., *On Adjustable Cycloidal and Trochoidal Curves*, Amer. J. Math., 1894, vol. 16, no. 2, 188–204.

[16] Mozgawa, W., Skrzypiec, M., *Some properties of secantoptics of ovals*, Beitr. Algebra Geom., 2012, vol. 53, 261–272.

[17] Poston, T., Stewart, I.N., *Taylor expansions and catastrophes*, Pitman, London—San Francisco—Melbourne, 1976.

[18] Puiseux, V., *Rapport sur un Mémoire de M. Haton de la Goupillière, intitulé: "Des développoïdes directes et inverses d'ordres successifs."*, C.R. Acad. Sci. Paris, 1875, t. 81, no. 9, 396–397.

[19] Rudin, W., *Real and complex analysis*, 3rd ed., McGraw-Hill Book Co., New York, 1987.

[20] Shawyer, B., *Explorations in Geometry*, World Scientific Publishing Co. Pte. Ltd., 2010.

[21] Williamson, B., *The Differential Calculus*, 9th ed., Longmans, Green, and Co., London—New York—Bombay, 1899.

[22] Willson, F.N., *Theoretical and Practical Graphics.*, BiblioBazaar, LLC., 2009.

[23] Wood, F., *Similar-Perspective Triangles*, Amer. Math. Monthly, 1929, vol. 36, no. 2, 67–73.